Dissertation zur Erlangung des Doktorgrades
der Fakultät für Chemie und Pharmazie
der Ludwig-Maximilians-Universität München

Functional characterization of PINCH-1 in embryoid bodies and keratinocytes and identification of new interaction partners

Esra Karaköse
aus
Istanbul/Türkei

2012

Erklärung

Diese Dissertation wurde im Sinne von § 7 der Promotionsordnung vom 28. November 2011 von Herrn Prof. Dr. Reinhard Fässler betreut.

Eidesstattliche Versicherung

Diese Dissertation wurde eigenständig und ohne unerlaubte Hilfe erarbeitet.

München, am 03.05.2012

Esra Karaköse

Dissertation eingereicht am:

1. Gutachter: Prof. Dr. Reinhard Fässler

2. Gutachter: Prof. Dr. Michael Schleicher

Mündliche Prüfung am: 29.05.2012

To my family

(Aileme)

TABLE of CONTENTS

Abbreviations

AFP	α-feto protein
ANK	Ankyrin
AJ	adherens junction
Akt	RAC-alpha serine/threonine protein kinase
Arp2/3	actin-related protein 2/3 complex
ATP	adenosine triphosphate
Bak	Bcl-2 homologous antagonist
Bax	Bcl-2 associated X protein
Bcl-2	B-cell lymphoma 2
Bcl-X_L	B-cell lymphoma-extra large
Bid	BH3 interacting-domain death agonist
Bim	Bcl-2 interacting mediator of cell death
Bmf	Bcl-2-modifying factor
BMP	bone morphogenetic protein
Cdc42	cell division cycle 42
CH	calponin homology
Cre	cyclization recombinase
Dab2	disabled homolog 2
DAPI	4',6-diamidino-2-phenylindole
DP	desmoplakin
DSC	desmocollin
DSG	desmoglein
DTT	dithiothreitol
E	embryonic day
ECM	extracellular matrix
EGF	epidermal growth factor
ERK	extracellular signal-regulated kinase
FA	focal adhesion
F-actin	filamentous actin
FAK	focal adhesion kinase
FBS	fetal bovine serum
FERM	4.1, ezrin, radixin, moesin
FGF	fibroblast growth factor
GAP	GTPase-activating protein
GEF	guanine nucleotide exchange factor
Gsk-3β	glycogen synthase kinase-3β
GTP	guanosine triphosphate
HGF	hepatocyte growth factor
ICAM	intercellular adhesion molecule
ILK	integrin-linked kinase
IP3	inositol triphosphate
IPP	ILK/PINCH/parvin
IRS	inner root sheet
JAM	junctional adhesion molecule
JNK	c-jun N-terminal kinase

KGM	keratinocyte growth medium
LB	lysogeny broth
LC	Liquid chromotography
LDV	lysine-aspartate-valin
LFA-1	leukocyte-specific Function Antigen
LIM	Lin11, Isl-1 and Mec-3
Lima-1	Lim domain and actin binding 1
LN	Laminin
MAPK	mitogen-activated protein kinase
Mcl-1	Induced myeloid leukemia cell differentiation protein
MDCK	Madin Darby canine kidney cells
MIDAS	metal-ion-dependent adhesion site
MLC	myosin light chain
MOMP	mitochondrial outer membrane permeabilization
MS	Mass Spectrometry
Nck2	noncatalytic region of tyrosine kinase, adaptor protein 2
NF-κB	nuclear factor-κB
ORS	outer root sheet
PBS	phosphate buffer saline
PCR	polymerase chain reaction
PDK1	Pyruvate dehydrogenase lipoamide kinase isozyme 1
PG	plakoglobin
PH	pleckstrin homology
PI3K	phosphatidylinositol 3-kinase
PtdIns(3,4,5)P_3	Phosphatidylinositol (3,4,5)-triphosphate
PIPKIγ	phosphatidylinositol 4-phosphate 5-kinase γ
PINCH	particularly interesting new Cys-His rich protein
PKB	protein kinase B
PKC	protein kinase C
PKP	plakophilin
Rac1	Ras-related C3 botulinum toxin substrate 1
Rap-1	Ras related protein 1
RGD	arginine, glycine, aspartate
RhoA	Ras homology gene family, member A
RIAM	Rap-1-GTP interacting molecule
ROCK	Rho-associated protein kinase
RPM	revolutions per minute
RSU-1	Ras suppressor protein-1
RT	Real time
RTK	Receptor tyrosine kinase
SDS	Sodium dodecyl sulphate
SH2	src homology 2
Shh	sonic hedgehog
Src	Rous sarcoma oncogene
TBS	Tris buffered saline
TBS-T	Tris buffered saline and tween

TEM	Transmission electron microscope
TGFβ	transforming growth factor β
TJ	tight junction
TM	transmembrane
VCAM	vascular cell-adhesion molecule
vHNF	variant Hepatocyte Nuclear Factor
ZO	zonula occludens

Summary

Integrins are heterodimeric transmembrane receptors that mediate cell-ECM and cell-cell adhesion. Upon ECM binding integrins cluster and assemble focal adhesions (FAs). Since the short cytoplasmic tails of integrins lack enzymatic activity, they rely on downstream adaptor, signaling, and scaffolding proteins to exert their functions such as proliferation, survival, differentiation, and migration. One important complex that works downstream of integrin signaling is the ILK-PINCH-Parvin (IPP) complex. A core component of the IPP complex is PINCH, which consists of 5 LIM domains and a nuclear localization/export signal. It has two isoforms in mice and men, namely PINCH-1 and PINCH-2. PINCH-2 null mice have no overt phenotype whereas PINCH-1 null mice die at the peri-implantation stage due to several defects including apoptosis of endoderm cells. The molecular mechanism leading to this apoptotic event is not known and therefore we determined how PINCH-1 executes cell survival. An abnormal cell-cell adhesion of endoderm and epiblast is a second characteristic defect of PINCH-1-deficient embryos. The cause for this defect was addressed in the second part of this thesis work.

In the first part of the thesis we investigated how endoderm cell survival is regulated by PINCH-1. We derived embryoid bodies (EBs) from mouse embryonic stem cells and used them as an embryonic development model. We demonstrate that loss of PINCH-1 expression in EBs and isolated EB-derived endoderm cells results in increased activity of JNK and of the pro-apoptotic Bcl-2-associated X protein (Bax), which are known to trigger apoptosis. The sustained activation of JNK was due to diminished levels of the Ras suppressor protein-1 (RSU-1), whose stability depends on PINCH-1 binding. Importantly, chemical inhibition of JNK ablates apoptosis of endoderm cells, however, without diminishing Bax activity. The increased Bax activity was associated with reduced integrin signaling and diminished Bcl-2 levels, which has been shown to inhibit Bax. Altogether our findings show that primitive endoderm cells require PINCH-1 to regulate a pro-survival signaling pathway that functions via Bax through integrin-mediated Bcl-2 expression and to inhibit a pro-apoptotic pathway that functions via; JNK through the PINCH-1 binding partner RSU-1.

In a second study, we investigated the role of PINCH-1 in cell-cell adhesion formation and maintenance. To this end, we generated a mouse that conditionally lacks PINCH-1 in epidermis. We report that lack of PINCH-1 in epidermis leads to epidermal detachment from the basement membrane (BM), epidermal hyperthickening and progressive hair loss as well as increased intercellular spaces. In vitro studies with keratinocytes revealed that PINCH-1 is a mechanosensory molecule that is recruited to cell-cell junctions as soon as tension is applied to the cells. Mechanistically, recruitment of PINCH-1 to cell-cell adhesion sites occurs independently of its binding partner integrin-linked kinase but requires ROCK-dependent myosin light chain phosphorylation. Interestingly, PINCH-1 recruitment to cell-cell adhesion sites occurs in conjunction with a novel PINCH-1 binding partner, called Epithelial Protein Lost In Neoplasm (EPLIN). We also show that EPLIN is recruited to focal adhesions (FAs) in a PINCH-1-dependent manner. Our results suggest that PINCH-1 and EPLIN form a complex to maintain stable FAs and to regulate the maintenance of cell-cell junctions in a force dependent manner.

Introduction

1. Integrin receptor family

Integrins are heterodimeric transmembrane receptors that mediate cell-extracellular matrix (ECM) and cell-cell adhesion. They consist of α and β subunits. They were originally referred as integrins to underscore their ability to link the ECM to the cytoskeleton (Tamkun et al., 1986). Integrins are evolutionarily conserved. There are no homologs in the prokaryotes, or fungi. However, simple metazoan such as sponges and cnidaria as well as flies, nematodes and vertebrates possess integrin dimers (Hynes, 2002; Hynes and Zhao, 2000; Johnson et al., 2009). In mammals, there are 18 α subunits and 8 β subunits, generating 24 integrin heterodimers (Takada et al., 2007).

Integrins function in a bidirectional way. Inside-out signaling regulates ligand affinity and outside in signaling relays signals from the extracellular environment into the cell. These signals are crucial for different cellular processes such as proliferation, survival, adhesion, migration, polarity, haptotaxis, gene expression and cell shape (Takada et al., 2007). Integrins lack enzymatic activity and actin binding sites, and thus their ability to regulate and bind actin relies on downstream signaling molecules.

1.1 Integrin structure

Integrin subunits have large extracellular domains (approximately 800 amino acids (aa)) that contribute to ligand binding, single transmembrane domains (approximately 20 aa) and short cytoplasmic tails (13 to 70 aa, except that of β4) (Moser et al., 2009b). The α subunit is composed of a seven-bladed β-propeller, which is connected to a thigh, a calf-1 and a calf-2 domain, together forming the leg structure that supports the integrin head. The last three or four blades of the β-propeller contain EF hand domains that bind Ca^{2+} on the lower side of the blades facing away from the ligand binding surface (Barczyk et al., 2010; Humphries et al., 2003). Nine of the α chains contain an I domain (also referred as a von Willebrand factor A domain), which is a domain of approximately 200 aa, inserted between blades 2 and 3 in the β-propeller. The I domain is almost always the ligand binding site. The I domain contains a conserved metal ion-dependent adhesion site (MIDAS), which binds divalent cations required for ligand binding (Barczyk

et al., 2010; Moser et al., 2009b). The characteristics of α subunits are summarized in Table 1.

β subunits are composed of a βI domain, a hybrid domain, a plexin-semaphorin-integrin (PSI) domain, four epidermal growth factor (EGF) domains and a membrane proximal β tail domain (βTD) (Figure 1). In integrins lacking an I domain, ligands bind to a crevice between the αβ subunit interface where they interact with a metal ion-occupied MIDAS within the β subunit and the propeller domain of α subunit (Moser et al., 2009b).

Integrins can exist in low-, intermediate- and high-affinity states (Figure1). There are two models that have been proposed to explain the allosteric changes that occur when integrins move to the high affinity state: the 'switchblade' model (Luo et al., 2007) and the 'deadbolt' model (Arnaout et al., 2007). In both models, the low affinity state is defined by bent integrins, in which the head domain faces the plasma membrane. In the switchblade model, the α and β transmembrane and cytoplasmic regions separate (Kim et al., 2003) and lead to dislocation of an EGF-like repeat. This causes the head domain to extend outwards with a switchblade-like motion (Arnaout et al., 2005). In the deadbolt model activated integrins maintain their bent conformation. However, the extracellular stalks of α and β subunits slide due to the piston-like movements of the transmembrane regions. This sliding disrupts the interaction between headpiece and the β stalk.

Transmembrane (TM) domains are crucial for integrin activation. Separation of integrin TM domains, which is mediated either by tilting and thus shortening of the TM domains or the by piston-like movements leading to the disruption of interactions within the membrane, is a requirement for the high affinity state of integrins (Moser et al., 2009b).

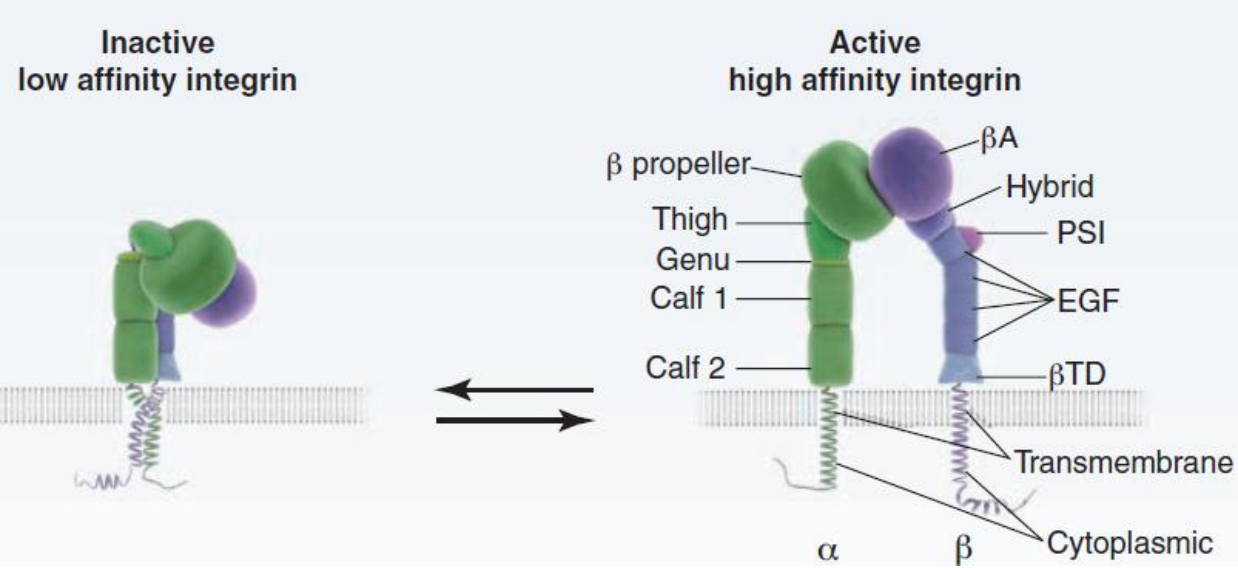

Figure 1: Integrin architecture and schematic representation of integrin activation. When integrins are activated integrin legs, TM and cytoplasmic tails are separated, resulting in an extended conformation (Moser et al., 2009b).

Integrin cytoplasmic tails regulate integrin affinity by carrying highly conserved NxxY motifs which serve as binding sites for talin and kindlins. Integrin activation via talin and/or kindlin binding has been extensively studied on leukocyte-specific β2 and platelet-specific αIIbβ3 integrins and also on β1 integrin in the case of kindlins (Calderwood et al., 2002; Calderwood et al., 1999; Montanez et al., 2008; Moser et al., 2008; Tadokoro et al., 2003; Wegener et al., 2007).

Table 1: Characteristics of human integrin α subunits (Barczyk et al., 2010).

Integrin	Human α chain characteristics	Cleavage	αI	Prototypic ligands/ recognition sequences	Additional ligands
α1β1 (CD49a, VLA1)	1151 aa		X	collagens (collagen IV > collagen I (GFOGER); collagen IX)	semaphorin 7A
α2β1 (CD49b, VLA2)	1181 aa		X	collagens (collagen I >collagen IV (GFOGER); collagen IX)	E-cadherin, endorepellin
α3β1 (CD49c, VLA3)	1051 aa, splice variants α3 A and α3B	X		laminins (LN-511>LN-332>LN-211)	
α4β1 (CD49d, VLA4)	1038 aa			fibronectin VCAM-1	
α5β1 (CD49e, VLA5)	1049 aa	X		fibronectin (RGD)	endostatin
α6β1 (CD49f, VLA6)	1073 aa, splice variants α6A and α6B	X		laminins (LN-511>LN-332>LN-111>LN-411)	
α7β1	1137 aa, splice variants X1, X2, α7A, α7B	X		α7X1β1: laminins (LN-511>LN-211>LN-411>LN-111) α7X2β1: laminins (LN-111>LN-211>LN-511)	
α8β1	1025 aa	X		fibronectin, vitronectin, nephronectin (RGD)	
α9β1	1035 aa			tenascin-C, VEGF-C, VEGF-D	
α10β1	1167 aa		X	collagens (collagen IV> collagen VI >collagen II (GFOGER); collagen IX)	
α11β1	1188 aa, inserted domain 21 aa		X	collagens (collagen I>collagen IV (GFOGER); collagen IX)	
αLβ2 (CD11a)	1170 aa		X	ICAM-1, -2, -3, -5	
αMβ2 (CD11b)	1153 aa		X	iC3b, fibrinogen + more	
αXβ2 (CD11c)	1163 aa		X	iC3b, fibrinogen + more	
αDβ2 (CD11d)	1162 aa		X	ICAM-3, VCAM-1	
αIIBβ3 (CD41, GpIIb)	1039 aa	X		fibrinogen, fibronectin (RGD)	
α6β4		X		laminins (LN-332, LN-511)	
αvβ1 (CD51)	1048 aa	X		fibronectin, vitronectin (RGD)	
αvβ3		X		vitronectin, fibronectin, fibrinogen (RGD)	tumstatin
αvβ5		X		vitronectin (RGD)	
αvβ6		X		fibronectin, TGF-β-LAP (RGD)	
αvβ8		X		vitronectin, TGF-β-LAP (RGD)	
αEβ7 (CD103, HML-1)	1178 aa	X	X	E-cadherin	
α4β7				MadCAM-1, fibronectin, VCAM-1	

1.2 Integrin ligands

In vertebrates, 18 different αsubunits can couple with 8 different β subunits to produce 24 different heterodimers (Figure 2). Based on their ligand binding properties, integrins can be categorized into 4 major classes: the laminin-binding integrins, the collagen-binding integrins, arginine-glycine-aspartate (RGD)-binding integrins as well as leukocyte-specific integrins (Barczyk et al., 2010; Humphries et al., 2006). Leukocyte-specific integrins bind to endothelium by interacting with other adhesion molecules such as intercellular adhesion molecules (ICAMs) and vascular cell adhesion molecules (VCAMs).

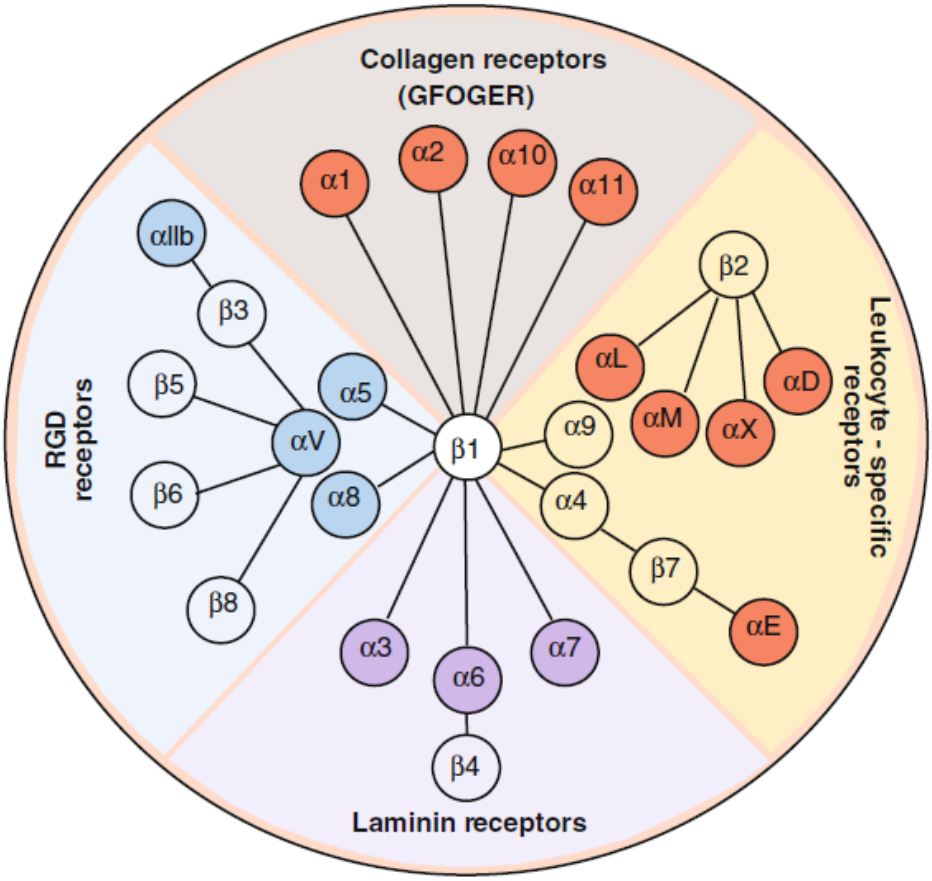

Figure 2: Representation of the integrin family in vertebrates (Barczyk et al., 2010). In vertebrates, integrins consist of 24 heterodimers.

Five αV integrins, two β1 (α5β1 and α8β1) and the αIIbβ3 integrins recognize and bind to RGD peptide, which is present eg. in fibronectin, vitronectin, tenascin, osteopontin

and fibrinogen. α4β1, α4β7 and α9β1 bind to an acidic motif called 'LDV' (lysine-aspartate-valin), which is functionally related to RGD. However, osteopontin interacts with α4β1, α4β7 and α9β1 via different peptide, SVVYGLR. The binding sites of ligands that bind to β2 are structurally similar to the LDV motif. The main difference is that β1/β7 ligands have an aspartate residue for cation coordination whereas β2 integrins have a glutamate. The consensus sequence for LDV motif is therefore L/I-D/E-V/S/T-P/S (Humphries et al., 2006).

α1, α2, α10 and α11 subunits heterodimerize with β1 subunit and constitute the collagen binding integrin subfamily. GFOGER is the triple, helical collagenous sequence that all these heterodimers interact with (Knight et al., 1998). The common property for these α subunits is that all of them contain an αA domain. Certain variants of GFOGER sequence might show preference to different collagen-binding integrins. For instance, GLPGER sequence binds preferentially to α11β1 over α2β1 (Barczyk et al., 2010).

α3β1, α6β1, α7β1 and α6β4 heterodimers are the laminin-binding integrins. The common property of α subunits is that they do not contain an αA domain (Humphries et al., 2006).

Additional integrin ligands are generated by proteolysis of ECM components, which include endostatin (derived from collagen XVIII), endorepellin (derived from perlecan) and tumbstatin (derived from collagen α3 (IV)). Moreover, integrins can also bind snake toxins, certain viruses and bacteria (Barczyk et al., 2010). Other integrin ligands are milk fat globule-EGF factor 8 (MFGE) and complement factor iC3b, which mediate phagocytosis of apoptotic cells and pathogens, respectively, and the latency-associated peptide of the transforming growth factor β (TGFβ) that regulates TGFβ signaling (Legate and Fassler, 2009).

Each individual integrin has specific biological functions, which are apparent from genetic studies in mice for single integrin unit. The phenotypes observed after ablation of single integrin subunits vary from embryonic lethality in the case of β1 integrins, to perinatal lethality as in the case of α3, α6, α8, αV, β4, β8 integrins, defects in leukocyte function (αL, αM, αE, β2, β7) and others (Hynes, 2002).

1.3 Bidirectional regulation of integrin signaling

Integrins signal in a bidirectional way. Intracellular changes can induce a conformational alteration in the integrin, which induces binding affinity for different ligands. This process is named either ‘inside-out signaling’ or ‘integrin activation’. After integrins are activated, they cluster due to the complex nature of ECM, and this in turn leads to concentration of cytoplasmic regulators.

Upon ligand binding, downstream adaptor and signaling proteins are recruited to the cytoplasmic tail of integrins. These proteins are important in terms of linking integrin signaling to actin cytoskeleton as well as to different signaling pathways. This process is called ‘outside-in’ signaling.

1.3.1 Inside-out signaling

Integrins are localized to cell surface in an inactive conformation. Upon binding of cytoplasmic ligands to specific binding sites, conformational changes are transmitted to extracellular ligand binding domain via the TM and stalk region. Talin and kindlins are the only known integrin binding proteins capable to active integrins.

Inside-out signaling has been extensively studied in platelets and leukocytes. These cells contain mainly αIIbβ3 and β2 integrins at their cell surface. These integrins are only activated under certain physiological conditions such as extravasation through the blood vessel wall and migration to the site of inflammation and thrombus formation during primary homeostasis (Coller and Shattil, 2008). The molecular mechanism of integrin activation has not been precisely elucidated; however it is known that the small GTPase Rap1 and its effector RIAM are involved in the process. Activated Rap1 binds to RIAM, which in turn binds to talin and this ternary complex is recruited to plasma membrane to target β2 and β3 integrins (Lee et al., 2009). Furthermore, cytohesin-1 and cytohesin-2 were reported to bind with the sec7 domain the membrane proximal region of the β2 integrin chain of Leukocyte-specific Function Antigen (LFA-1) (Geiger et al., 2000; Kolanus et al., 1996). This interaction leads to increased substrate binding of integrin (Kolanus, 2007).

Talin has two isoforms in vertebrates, talin1 and talin2. They differ in their expression pattern. Talin1 is expressed ubiquitously, whereas talin2 is the primary isoform of brain

and striated muscle (Monkley et al., 2001; Senetar et al., 2007). They are 270 kD proteins consisting of an N-terminal 47 kD head domain and a C-terminal flexible rod domain. The talin head is composed of a FERM (4.1, ezrin, radixin, moesin) domain consisting of 3 subdomains (F1-F3) and an F0 subdomain (Moser et al., 2009b)(Figure 3). The F3 subdomain binds to the conserved membrane proximal NPxY motif in the β1 integrin tail (Calderwood et al., 2002), phosphatidylinositol 4-phosphate 5-kinase γ (PIPKIγ). The rod domain contains binding sites for the F-actin binding protein vinculin and a second integrin-binding site. It is thought that talin binding to integrin leads to recruitment of vinculin and actin filaments, which links the cytoskeleton with the ECM (Critchley and Gingras, 2008).

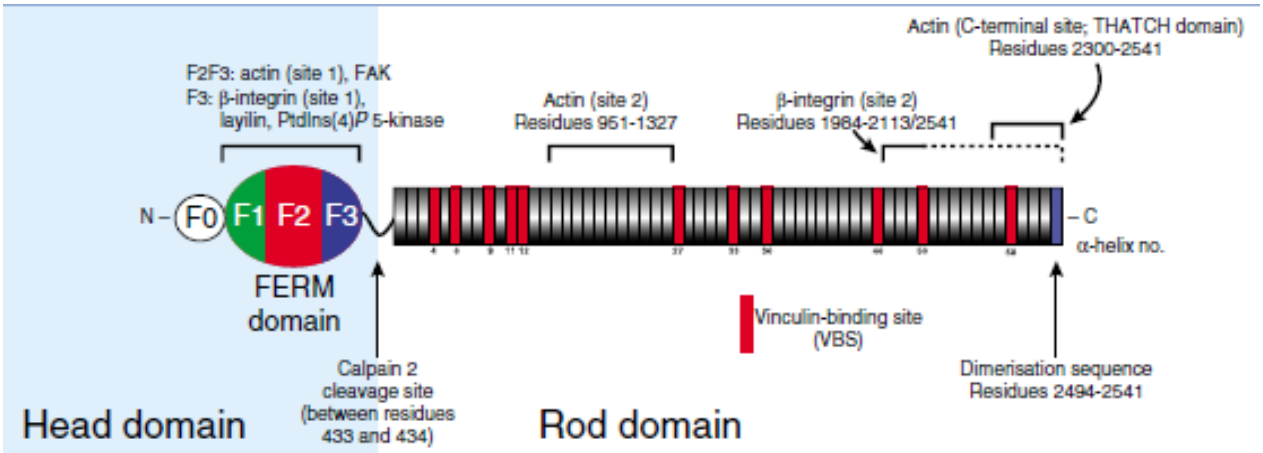

Figure 3: Domain structure and binding partners of talin (Critchley and Gingras, 2008).

Kindlins are the second known integrin activating molecules. It has recently been shown that talin alone is not sufficient to activate integrins and that kindlins are also required (Ma et al., 2008; Montanez et al., 2008; Moser et al., 2009a; Moser et al., 2008; Ussar et al., 2008). Kindlins belong to a family of FERM-domain containing proteins which bind to the membrane distal NxxY motif of β1, β2 and β3 integrins (Meves et al., 2009). Since talin and kindlins bind different regions of integrin tails, they may regulate integrin affinity in a cooperative manner. Kindlins alone are not sufficient to activate the integrins. They require talin function. On the other hand, talin depends on kindlins to promote integrin affinity because it has been demonstrated that overexpression of talin

head is not sufficient to induce the activation of αIIbβ3 integrin in kindlin-depleted CHO cells. Therefore, kindlins require talin and talin requires kindlin to increase integrin affinity (Moser et al., 2009b). For more information on kindlins, please refer to Karaköse et. al., 2010.

1.3.2 Outside-in signaling

After integrins are activated and clustered, they transmit an array of intracellular changes, which are collectively referred as 'outside-in signaling'. Integrin activation requires large conformational changes including the outward swing of the hybrid domain in the extracellular region, and in turn separation of α and β cytoplasmic tails, which leads to the binding of intracellular signaling molecules (Arnaout et al., 2005). Over the years, 156 signaling, structural and adaptor molecules that comprise the 'integrin adhesome' have been described (Zaidel-Bar et al., 2007).

The intracellular effects after integrin activation can be divided in 3 temporal stages; (1) the immediate effects that occur within 0-10 minutes after integrin activation and include tyrosine phosphorylation of specific substrates and an increase in the lipid second messenger concentration, (2) the short term effects which take place within 10-60 minutes after integrin activation and include cytoskeletal changes that allow cells to spread and migrate and (3) the long term effects that take place after 60 minutes of ECM-integrin interaction and require changes in gene expression (Legate et al., 2009) (Figure 4).

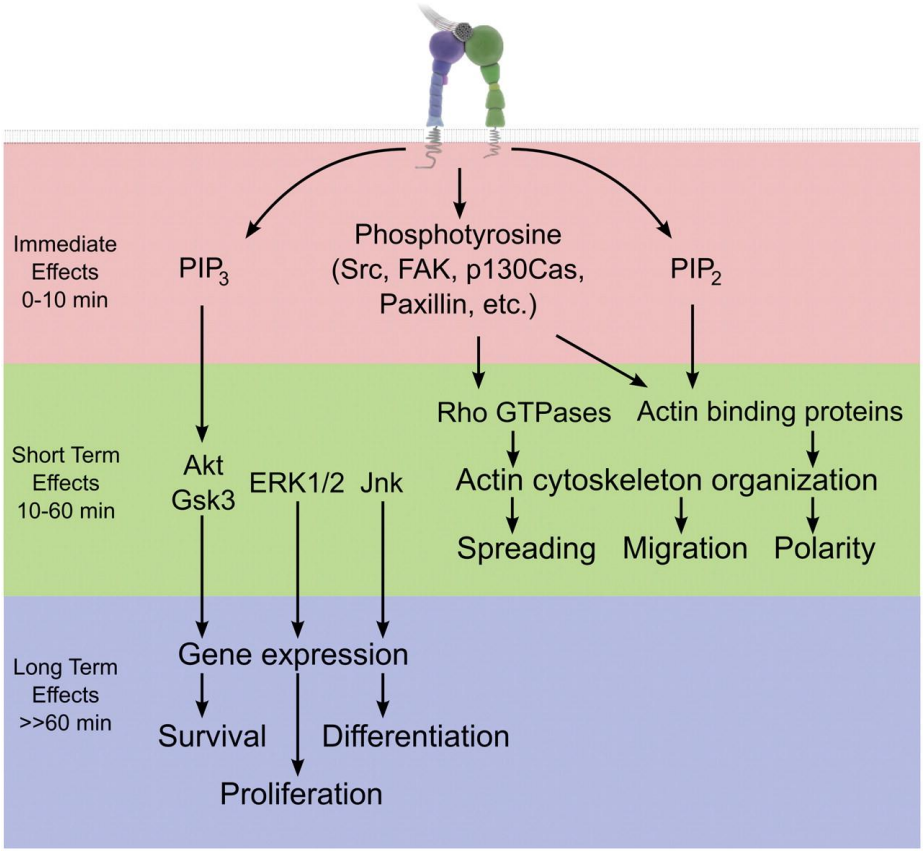

Figure 4: Consequences of integrin activation (Legate et al., 2009).

1.4 Assembly of integrin dependent adhesion structures

Cell-matrix attachment sites are dynamic places containing active integrin clusters. These sites include nascent focal adhesions, focal complexes, focal adhesions (FA), fibrillar adhesions and podosomes. Collectively, these sites are called integrin adhesions (Zaidel-Bar et al., 2007). The molecular composition of earliest integrin adhesion complex is not clear, but it contains two molecules of talin that connect two α-β integrin dimers. The earliest microscopically visible integrin-containing structures are focal complexes or nascent adhesions which are ~100nm in diameter (Geiger et al., 2009). When stabilized, they mature into FCs and FAs, which are cell-substrate adhesion structures with a size of 1-5 μm that anchor the ends of stress fibers. Stress fibers consist of actin filament bundles that contain an array of proteins, including myosin II and actin crosslinkers such as α-actinin and filamin. Myosin II regulates the contractility of stress fibers (Geiger et al., 2009; Kumar et al., 2006).

FAs are mechanosensitive cellular complexes. It has recently been shown that certain binding sites for vinculin that reside in the talin rod are only accessible after force application, suggesting that vinculin recruitment to FAs is enhanced by local tensile force (Lee et al., 2007). Therefore, it seems that FA maturation requires F-actin-generated mechanical force.

Fibrillar adhesions are streak-like structures with different integrin composition in comparison to FAs. While αvβ3 integrin is enriched at the FA sites, fibrillar adhesions contain α5β1 integrin. It seems that different integrins recruit different cytoplasmic factors, which give rise to different signaling responses. Fibrillar adhesions also contain abundant tensin and low levels of protein tyrosine phosphorylation (Berrier and Yamada, 2007) (Figure 5).

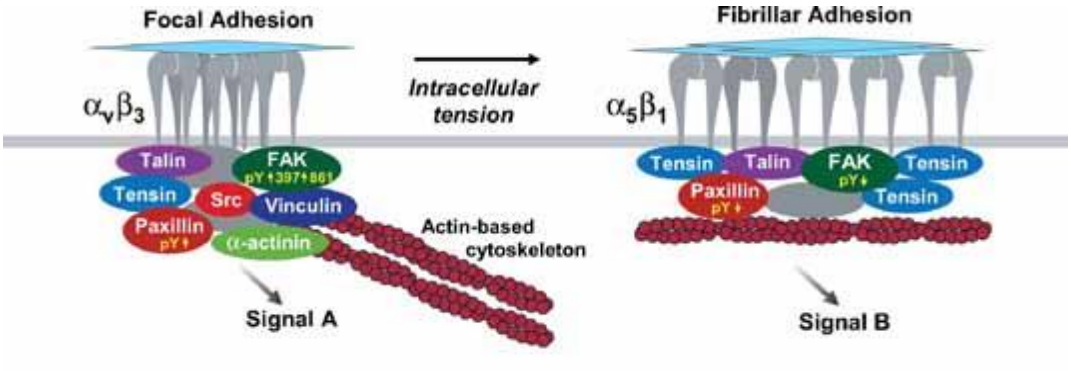

Figure 5: Comparison of focal adhesions and fibrillar adhesions (Berrier and Yamada, 2007). Different cytoplasmic proteins are recruited to distinct adhesion types. For example, FAKpY397 levels are high at FAs, but lower at fibrillar adhesions.

Podosomes are found on the ventral side of osteoclasts, hematopoietic and endothelial cells (Albiges-Rizo et al., 2009). They are similar to FAs in terms of size and half-life. However they have a ring-like composition of adhesion components and surround an F-actin core (Gimona et al., 2008).

1.4.2 The integrin-actin connection

Integrin outside-in signaling induces the interaction between integrins and the actin cytoskeleton, which is required for cell spreading and cell migration. FA proteins that establish and maintain the integrin-actin linkage can be divided into four groups: (1)

integrin-bound proteins that directly bind actin, such as talin, α-actinin and filamin; (2) integrin-bound proteins that indirectly associate with cytoskeleton such as kindlin, ILK, paxillin and focal adhesion kinase (FAK); (3) non-integrin bound actin binding proteins, such as vinculin and (4) adaptor and signaling molecules that regulate interactions of the above mentioned groups (Legate et al., 2009).

The talin head domain is sufficient for integrin activation, however is not able to rescue the cytoskeletal linkage in talin deficient cells indicating that the rod domain of talin is responsible for the actin binding activity of talin and that talin is a direct mechanical link between actin and integrins (Tanentzapf and Brown, 2006; Zhang et al., 2008). The role of talin in connecting integrins to actin cytoskeleton is also underlined with *in vivo* studies in different organisms. Mice lacking talin-1 die during gastrulation due to cytoskeletal defects and cell migration (Monkley et al., 2000). *Drosophila* embryos lacking talin (*rhea* gene) display germ band retraction and muscle detachment that are similar to integrin-deficient (βPS) flies (Brown et al., 2002).

Upon talin binding, other proteins such as vinculin are recruited to nascent adhesions. Expression of the talin head, which is unable to bind vinculin, in talin-null cells activates integrins but fails to induce the formation of focal contacts (Zhang et al., 2008). This finding suggests that talin makes the initial contacts between integrins and actin, however, is unable to maintain them. Vinculin is required to strengthen the integrin-actin linkage by acting as a cross-linker and by binding directly to both proteins (Legate et al., 2009).

Recently, α-actinin has been shown to be a binding partner for both talin and vinculin. The force dependent strengthening of integrin-actin linkage correlates with α-actinin incorporation into integrin adhesion sites (Laukaitis et al., 2001). α-actinin, in collaboration with myosin II also plays a critical role in FA growth and maturation (Choi et al., 2008).

The physical link between integrins and actin allows both local and global control of cytoskeletal dynamics. Local actin polymerization is also regulated by Rho GTPases. The mammalian Rho GTPase family is composed of 20 proteins, which cycle between

an active GTP-bound form and an inactive GDP-bound form. The switch between different forms is regulated by three different sets of proteins: guanine nucleotide exchange factors (GEFs), GTPase-activating proteins (GAPs) and guanine nucleotide dissociation inhibitors (GDIs). The most studied GTPases for the regulation of actin dynamics at FAs are Rac1, Cdc42 and RhoA (Legate et al., 2009). RhoA activation leads to actin-myosin filament contraction, whereas Rac1 and Cdc42 activation leads to the protrusive lamellipodia and filopodia, respectively (Etienne-Manneville and Hall, 2002). Both Rac1 and Cdc42 stimulate actin polymerization via the Arp2/3 complex, and RhoA initiates actin polymerization via formins (Jaffe and Hall, 2005). Recent studies have revealed that Cdc42-induced filopodia act as precursors for Rac-induced lamellipodia (Guillou et al., 2008).

As a central molecular machine for the actin polymerization, Arp2/3 is recruited to nascent adhesions via interacting with FAK as well as vinculin. FAK-deficient cells display impaired lamellipodium formation and cell spreading defects (Serrels et al., 2007), whereas vinculin binding is more transient and is not required for cell motility or spreading, but it might be necessary for relocating the Arp2/3 complex to nascent adhesions (DeMali et al., 2002; Legate et al., 2009).

1.5 The ILK/PINCH/parvin (IPP) complex

ILK, PINCH and parvin have emerged as key regulators of integrin functions. These molecules form a heterotrimeric complex (IPP complex) that regulates several cellular processes.

1.5.1 Molecular composition of the IPP complex

ILK was first identified in a yeast two hybrid screen (Hannigan et al., 1996). It links the IPP complex to cytoplasmic tails of β1 and β3 integrins (Li et al., 1999; Pasquet et al., 2002). The N-terminal domain contains five ankyrin repeats, which mediate protein-protein interactions. The C-terminus shares sequence homology to Ser/Thr protein kinases. A putative pleckstrin homology (PH) domain is inserted in between these two domains (Legate et al., 2006). The PH domain of ILK has been shown to bind phosphatidylinositol-3,4,5-triphosphate (Delcommenne et al., 1998; Persad et al., 2001).

The ankyrin repeats 2-5 of ILK bind to PINCH, a family of LIM-only domain proteins composed by PINCH-1 and PINCH-2 (Chiswell et al., 2008). PINCH-1 was identified in 1994 as a marker for senescent erythrocytes and was shown to bind ILK in 1999 (Rearden, 1994; Tu et al., 1999). PINCH-2 was identified by a sequence-database mining based prediction (Braun et al., 2003; Hobert et al., 1999; Zhang et al., 2002a). Both PINCH-1 and PINCH-2 contain 5 LIM domains, and the first LIM domain is responsible to interact with ILK (Chiswell et al., 2008; Tu et al., 2001; Tu et al., 1999) (Figure 6). The main difference of these two proteins is that PINCH-2 contains 11 additional amino acids at the C-terminal tail (Chiswell et al., 2008).

The linkage of ILK to the F-actin cytoskeleton is mediated either via parvin or paxillin. Paxillin was shown to bind to parvin and vinculin (Legate et al., 2009). Parvin protein family consist of three members; (1) the ubiquitously expressed α-parvin (also known as actopaxin or CH-ILKBP), (2) the heart and skeletal muscle enriched β-parvin (also known as affixin) and (3) the γ-parvin, which is exclusive to the hematopoietic system (Chu et al., 2006; Nikolopoulos and Turner, 2000; Olski et al., 2001; Tu et al., 2001; Yamaji et al., 2001). Parvins consist of two calponin homology (CH) domains. The second CH domain of parvin mediates the interaction with ILK (Grashoff et al., 2004).

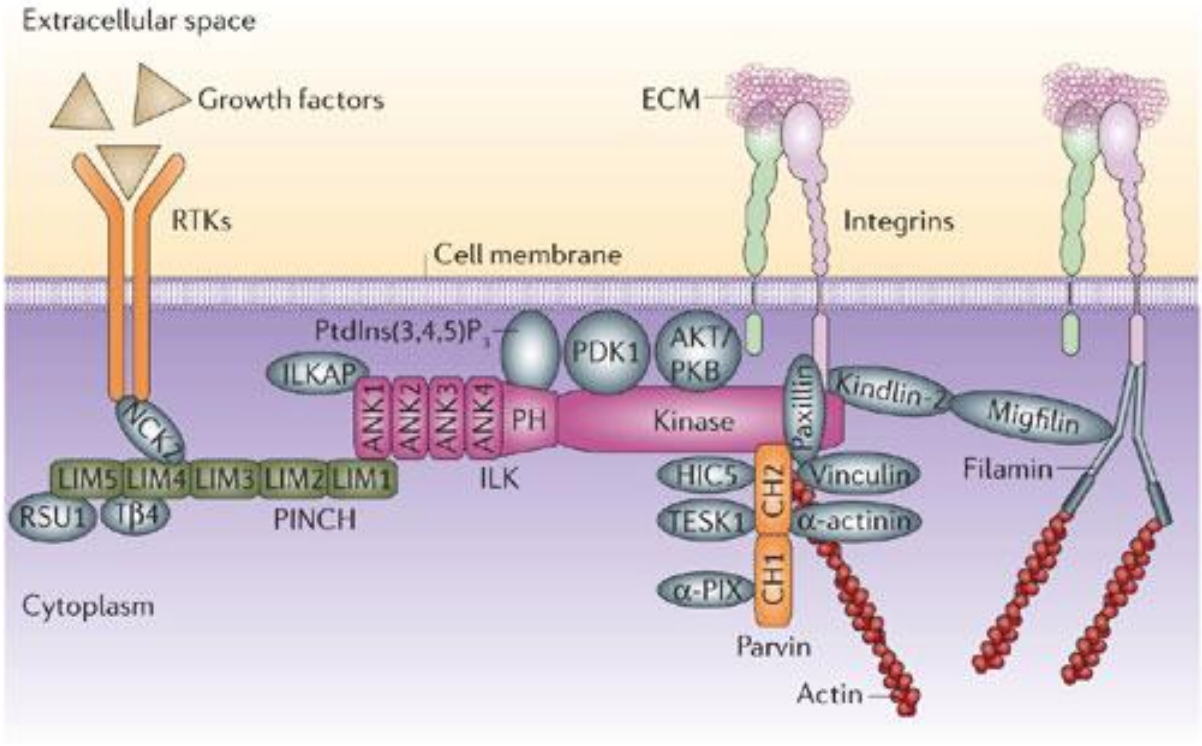

Figure 6: Anatomy of the IPP complex and its binding partners (Legate et al., 2006).

ILK binds to PINCH via the ANK 2-5 domains and to parvins, paxillin, kindlin-2, cytoplasmic tails of integrins and the RAC-alpha serine/threonine protein kinase/protein kinase B (AKT/PKB) and Pyruvate dehydrogenase lipoamide kinase isozyme 1 (PDK1) via the kinase domain. The LIM4 domain of PINCH binds to RTKs through the SH2-SH3 containing adaptor Nck2. PINCH also binds to RSU1 and thymosin-β4 (Tβ4). α- and β-parvins bind to F-actin directly and indirectly through paxillin or HIC5 (only α-parvin) or α-actinin (only β-parvin).

1.5.2 Biological functions of the IPP complex

Several organisms have been used to study the biological functions of the IPP complex. ILK-deficient fibroblasts fail to adhere, spread and migrate (Sakai et al., 2003; Stanchi et al., 2009). Deletion of ILK in *Caenorhabtidis elegans (C. elegans)*, *Drosophila* or zebrafish leads to muscle detachment from the body wall due to the detachment of actin from the plasma membrane (Mackinnon et al., 2002; Postel et al., 2008; Zervas et al.,

2001). Genetic deletion of ILK in mice leads to lethality at the peri-implantation stage due to a failure in the epiblast polarization (Sakai et al., 2003). Moreover, conditional deletion of ILK in the epidermis leads to epidermal defects and hair loss (Lorenz et al., 2007).

The role of parvins in cell spreading and migration is more complex. Mice lacking β- or γ-parvin show no overt phenotype, whereas mice lacking α-parvin die between E11.5 and E14.5 due to vascular defects (Chu et al., 2006; Montanez et al., 2009). α-parvin depletion in HeLa cells leads to activation of Rac and lamellipodium formation, suggesting that α-parvin can function as a negative regulator of Rac in α- and β-parvin expressing cells (Zhang et al., 2004). α-parvin binds to F-actin directly and also indirectly through paxillin. However, it is not clear whether ILK and α-parvin bind the same paxillin molecule or two paxillin molecules bind the same IPP complex. A paxillin related protein Hic5 also binds α-parvin (Nikolopoulos and Turner, 2000).

PINCH-1 is expressed ubiquitously during development and adult life, whereas PINCH-2 expression starts at the second half of embryonic development (Braun et al., 2003). PINCH-2 ablation in mice does not alter the embryonic development. However, loss of PINCH-1 in mice leads to embryonic lethality due to abnormal epiblast polarity, impaired cavitation, detachment of endoderm and epiblast from BMs, endoderm survival defects and cell-cell adhesion defects of endoderm and epiblast (Li et al., 2005).

PINCH-1 has several interaction partners. For instance, a link between the IPP-complex and the actin cytoskeleton is maintained via the interaction of PINCH and ILK with thymosin β4, a small, G-actin monomer sequestering peptide (Bock-Marquette et al., 2004). Furthermore, the fourth LIM domain of PINCH binds to Nck2, which in turn links PINCH-1 to growth factor receptor and GTPase signaling (Tu et al., 1998). Nck2 regulates actin dynamics through several pathways: (1) the WASP family members and the Arp2/3 complex, (2) small GTPases and (3) PAK or DOCK180 (Buday et al., 2002).

Moreover, PINCH-1 interacts with RSU-1 in both vertebrates (Dougherty et al., 2005a) and *D. melanogaster* (Kadrmas et al., 2004) which negatively regulates JNK activity. In addition, an Akt-1 regulating protein phosphatase1α (PP1α) has been shown to directly

bind PINCH-1. Upon binding, PP1α activity is inhibited and therefore the Akt phosphorylation is increased, which in turn leads to radio-resistance (Eke et al., 2010). Despite PINCH-1 play a role in cell survival of tumor cells, the molecular mechanism underlying the survival of primitive endoderm cells remains elusive.

The PINCH-interacting protein ILK has been suggested to play a role in epithelial sheet morphogenesis and to localize to cell-cell junctions (Vespa et al., 2005; Vespa et al., 2003). However, whether PINCH and parvin follow ILK to cell-cell junctions has not been addressed thus far.

2. Apoptosis

Apoptosis is programmed cell death that is involved in development and homeostasis and is characterized by cell contraction, membrane blebbing, chromatin condensation and DNA fragmentation (Meier et al., 2000; Tait and Green, 2010). In vertebrates, there are two main signaling pathways through which apoptosis is proceeding; (1) the intrinsic and (2) the extrinsic pathway. Both pathways converge on caspase-3 which executes the apoptosis (Degterev et al., 2003). The intrinsic pathway is triggered by intracellular stress signals such as DNA damage or ECM detachment and leads to mitochondrial outer membrane permeabilization (MOMP) which in turn triggers the release of pro-apoptotic proteins from the mitochondria. The extrinsic pathway is triggered by cell death receptor ligation which leads to the activation of the caspase-8 that initiates apoptosis (Tait and Green, 2010).

The members of the Bcl-2 family, which comprise anti-apoptotic or pro-apoptotic proteins, regulate the MOMP. Anti-apoptotic Bcl-2 family proteins (Bcl-2, Bcl-X_L, Mcl-1) antagonize the function of pro-apoptotic Bcl-2 family proteins that fall into two classes; the so-called BH3-only proteins such as Bim, Bid, Puma or Bmf, and multi-domain proteins such as Bax and Bak (Gilmore et al., 2009). The activity of these proteins can be regulated at different levels. For example, the activity of Bim, which can activate Bax, can be regulated at transcriptional, post-transcriptional and post-translational levels (Tait and Green, 2010).

Mitogen-activated protein kinases (MAPKs) are key regulators of cell survival and apoptosis (Dhanasekaran and Reddy, 2008). For instance, extracellular signal-regulated kinase (ERK) and Jun N-terminal kinase (JNK) signaling can regulate both cell survival and apoptosis during embryonic development (Lei and Davis, 2003). A transient activation of JNK pathway is associated with cell survival, whereas a sustained activation is associated with apoptosis (Ip and Davis, 1998). JNKs induce apoptosis by regulating the expression of pro-apoptotic genes or by controlling the activities of mitochondrial pro- and anti-apoptotic proteins through phosphorylation (Dhanasekaran and Reddy, 2008).

Integrin-mediated cell-ECM adhesion and signaling regulate cell survival and apoptosis during embryonic development and tumor progression (Frisch and Screaton, 2001; Liu et al., 2009; Martin and Vuori, 2004; Reddig and Juliano, 2005). It has been previously reported that α5β1 integrin can regulate apoptosis by regulating Bcl-2 expression levels (Lee and Ruoslahti, 2005). Whether PINCH-1 is involved in this signaling pathway is not known.

PINCH-1 is an important survival factor of endoderm cells during embryo development (Li et al., 2005). Moreover, PINCH-1 protects tumor cell from death by enhancing the activity of the pro-survival proteins ERK1/2 and AKT (Chen et al., 2008; Eke et al., 2010; Sandfort et al., 2010). How PINCH-1 regulates cell survival during peri-implantation, however, is not understood.

3. Intercellular adhesion complexes

Adhesion between epithelial cells is of crucial importance to maintain tissue homeostasis. In mammals, three different types of junctions mediate adhesion between epithelial cells: 1. adherens junctions (AJ), 2. desmosomes, and 3. tight junctions (TJ) (Perez-Moreno et al., 2003). AJ and TJ are associated with actin cytoskeleton, whereas desmosomes link to the intermediate filaments (Figure 7). Epidermis and other tissues also contain gap junctions that provide a direct connection between neighboring cells.

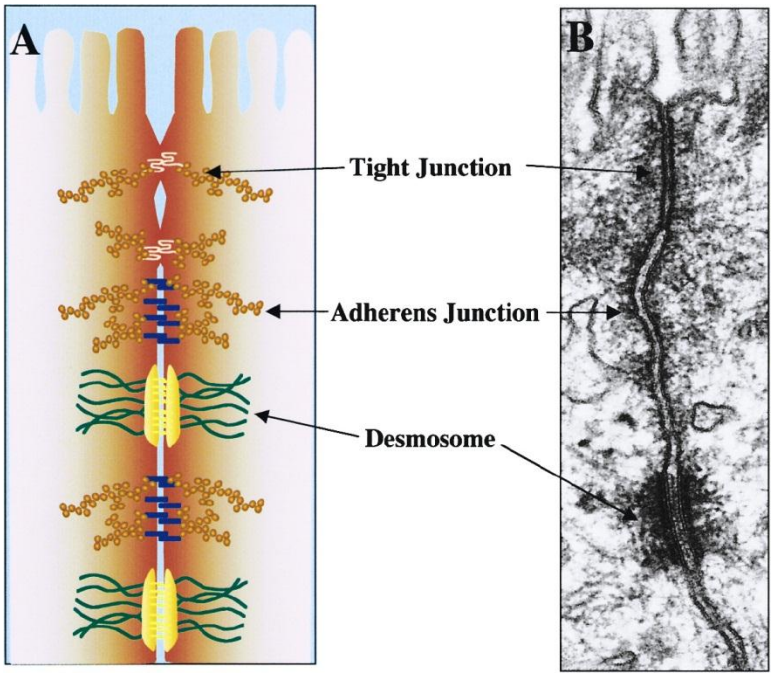

Figure 7: Composition of three types of intercellular junctions (Perez-Moreno et al., 2003). (A) Cartoon and (B) electron micrograph of three major types of intercellular junctions in epithelial cells.

In stratified epithelium such as epidermis, there are four main cell layers, namely basal layer (stratum basale), spinous layer (stratum spinosum), granular layer (stratum granulosum) and stratum corneum. These four layers comprise of specific cytoskeleton and cell junction types, including AJ, TJ, desmosomes and gap junctions (Figure 8) (Simpson et al., 2011).

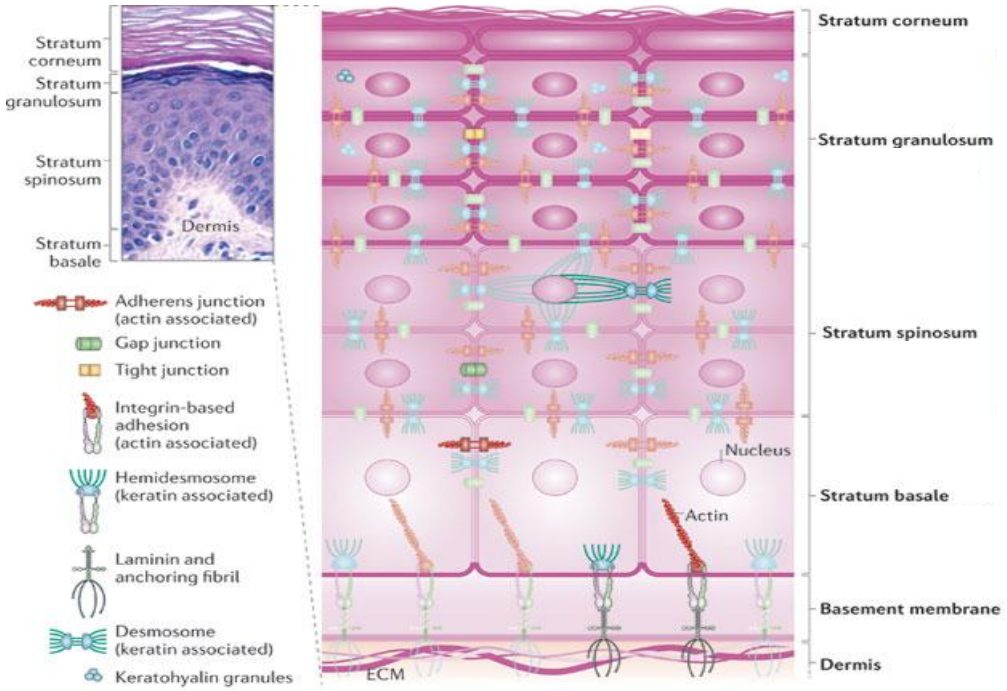

Figure 8: Epidermal architecture and intercellular junctions (Simpson et al., 2011). Cytoarchitectural organization of epidermis. Cytoskeleton and adherens junctions, tight junctions, desmosome and gap junctions are depicted.

3.1 Adherens junctions (AJs)

AJs are the intercellular connections that contain classic cadherins, namely epithelial (E)- and placental (P)-cadherin, also known as cadherin 3. Homophilic interactions between their extracellular domains provide mechanically strong adhesive links between cells (Baum and Georgiou, 2011). Binding of Ca^{2+} to their extracellular domain is required for their correct conformational organization (Hartsock and Nelson, 2008). The cytoplasmic tails of classical cadherins recruit p120 catenin and β-catenin by binding directly to their armadillo repeat domains, and α-catenin, which is linked to the cadherin complex via β-catenin (Simpson et al., 2011).

p120 catenin was first identified as a Src-tyrosine receptor kinase substrate and later as a member of the catenin family, mainly based on the sequence homology to an armadillo domain of β-catenin (Hartsock and Nelson, 2008). p120 catenin positively regulates cadherin function by counteracting cadherin endocytosis and degradation, thereby enhancing their surface levels (Ishiyama et al., 2010). p120 catenin also links

cadherin to microtubules through either a kinesin or the adaptor protein PH domain-containing family member 7 (PLEKHA7), which indirectly links p120 catenin to microtubule minus ends (Harris and Tepass, 2010).

Cytoplasmic tails of cadherins are resistant to proteolysis only when they are bound to β-catenin (Huber et al., 2001). The association starts at the endoplasmic reticulum (ER) and is required for cadherin exit from ER (Chen et al., 1999). At the plasma membrane, the cadherin-β-catenin complex recruits α-catenin (Bajpai et al., 2008), which is essential for AJ formation. Similarly like β-catenin, α-catenin can also bind actin filaments directly (Rimm et al., 1995). It has recently been suggested that α-catenin binds to actin preferentially as a dimer and the dimerization domain overlaps with the β-catenin binding site. Therefore α-catenin is not able to bind β-catenin and actin at the same time (Yamada et al., 2005). Recent models suggest that α-catenin dimerizes after detaching from β-catenin and the dimers then compete with the ARP2/3 complex which nucleates actin. This in turn helps to convert lamellipodial actin networks into actin bundles associated with AJs (Drees et al., 2005; Yamada et al., 2005).

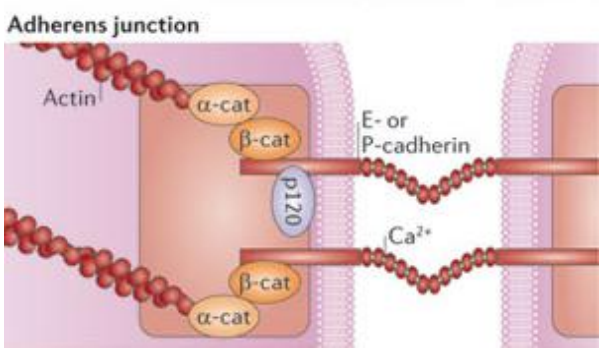

Figure 9: Adherens junctions (Simpson et al., 2011). E- or P- cadherin homophilic interactions are formed between the neighboring cells, by Ca^{2+} induction. Cytoplasmic molecules p120 catenin, β-catenin and α-catenin are recruited to the cytoplasmic tails of cadherins.

Rho family GTPases regulate AJ formation by driving actin-based protrusions (Ridley, 2006). Active GTP-bound Rac can stimulate the activity of phosphatidylinositol 3-kinase (which leads to formation of PIP2), Cdc42- and Arp2/3-mediated actin nucleation and the recruitment of adhesion proteins which increases the cell-cell contact zone (Baum

and Georgiou, 2011). In addition, RhoA helps to maintain AJs via mDia1 (Sahai and Marshall, 2002) and non-muscle myosin II (Shewan et al., 2005). RhoA signaling is also important for the disassembly of cell-cell contacts during epithelial-mesenchymal transition (Bhowmick et al., 2001).

As a core component of the IPP complex, ILK has also been shown to localize in the vicinity of AJs and associated F-actin fibers (Vespa et al., 2005). However, whether ILK recruitment to AJs occurs with other IPP complex members has not been addressed.

3.2 Desmosomes

Desmosomes are composed of proteins from three families: the cadherins, the armadillo proteins and the plakins.

Human desmosomal cadherins include four desmogleins (DSG1-4) and three desmocollins (DSC1-3). In contrast to classical cadherins of AJs, DSGs have extended cytoplasmic tails whose function has not been fully elucidated yet. Desmosomal cadherins interact directly with armadillo family members, which include plakoglobin (PG, also known as γ-catenin) and p120-catenin-related proteins, plakophilin (PKP) 1-3 and p0071 (also known as plakoglobin4) (Getsios et al., 2004). PG and PKPs are homologous to β-catenin and p120 catenin, respectively, and bind to desmosomal cadherins via armadillo repeat domains and N-terminal head domain, respectively (Simpson et al., 2011). The link to the keratin intermediate filament network is mediated by plakin family member desmoplakin (DP) (Bornslaeger et al., 1996; Gallicano et al., 1998) (Figure 10).

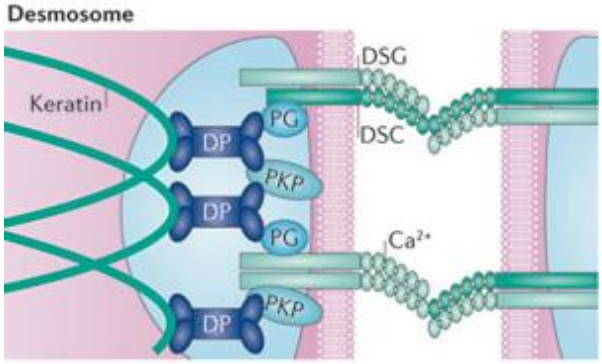

Figure 10: Desmosomes (Simpson et al., 2011). DSGs and DSCs are the cadherin family proteins mediating desmosomal interaction between two neighboring cells. PG and PKPs are recruited to the cytoplasmic tails of DSGs and DSCs. DP mediates the linkage to intermediate filament network.

PG is an armadillo protein that links desmosomes to the intermediate filament system by directly binding to desmosomal cadherins, DP, plakophilin-2, plakophilin-3 and p0071 (Bonne et al., 2003; Chen et al., 2002; Hatzfeld et al., 2003). PG depletion in mice leads to skin and heart defects and can result in embryonic lethality (Bierkamp et al., 1996; McKoy et al., 2000; Ruiz et al., 1996). Interestingly, in these mutant embryos desmosomes can form, which occurs through the related protein β-catenin that becomes redistributed to desmosomes (Bierkamp et al., 1999). On the other hand, PG has been suggested to cross talk between AJs and desmosomes by binding desmosomal and classical cadherins (Lewis et al., 1997).

Although DP, plectin, envoplakin and periplakin bind intermediate filaments and localize to desmosomes, genetic studies suggest that only DP is indispensable for desmosomes. The N-terminus of DP is responsible for targeting DP to junctions by mediating interactions with desmosomal armadillo proteins and potentially directly binding the DSG1 and DSC1 cytoplasmic tails (Getsios et al., 2004; Leung et al., 2002).

3.3 Tight junctions (TJs)

Desmosomes and AJs cooperate to hold epithelial sheets together, whereas TJs establish a diffusion barrier between apical and basolateral membrane domains. In skin, they form a belt at the apical side of keratinocytes of the stratum granulosum and

provide a barrier beneath the stratum corneum that controls fluid loss and protects against pathogens. TJs form a belt-like adhesion between cells, allowing the passage of only small molecules and ions (Simpson et al., 2011). TJs contain two types of transmembrane proteins, occludins and claudins, which link TJs to the actin cytoskeleton, AJs and junctional adhesion molecules (JAM-1-4). Other cytoplasmic scaffolding proteins play a role to associate with occludins, claudins and JAMs. They include the zonula occludens (ZO) proteins ZO1, ZO2 and ZO3 that can directly interact with occludin and claudins (Niessen, 2007) (Figure 11).

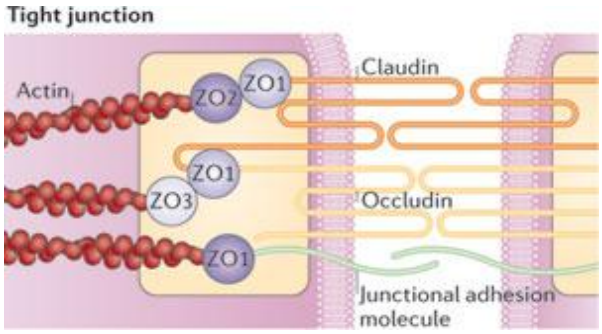

Figure 11: Tight junctions (Simpson et al., 2011). Claudins and occludins are the main TJ components. ZO proteins mediate the linkage to the actin cytoskeleton.

Occludin is a tetraspan protein with two extracellular loops (Furuse et al., 1993). Occludin localization to AJs and TJs is regulated by phosphorylation in both epithelial and endothelial cells (Sakakibara et al., 1997). The second extracellular loop of occludin interacts with claudin and JAMs (Nusrat et al., 2005).

The claudin family consists of at least 24 members. Although they do not share sequence similarity with occludins, they also comprise a tetra span with two extracellular loops (Hartsock and Nelson, 2008). Claudins are responsible to recruit occludins to TJs (Furuse et al., 1998).

Zonula occludens 1 (ZO1), ZO2 and ZO3 are members of MAGUK (membrane-associated guanylate kinase homologs) family with the capability of binding to AJs and

TJs. ZO1 and ZO2 can bind α-catenin (Itoh et al., 1999; Itoh et al., 1997) whereas the C-terminus of ZO3 has been shown to bind p120 catenin (Wittchen et al., 2003). This region overlaps with the binding region to N-terminal ZO3. It has been proposed that this binding switch could sequester p120 catenin from regulation of RhoA activity (Hartsock and Nelson, 2008; Wittchen et al., 2003).

3.4 Actin linkage to AJ

AJs are closely related to actin cytoskeleton in early and mature state. In Madin Darby canine kidney (MDCK) cells, the lamellipodial protrusions bring neighboring cells in close proximity. As protrusion form, cadherins and catenins form small clusters at the nascent cell-cell contact (Harris and Tepass, 2010). As cadherins and catenins aggregate, they connect with actin and actin is remodeled to promote AJ growth (Vasioukhin and Fuchs, 2001).

In primary keratinocytes, initial contact formation between cells is mediated by filopodia, which also leads to cadherin clustering at the ends of radial actin filaments (Vasioukhin et al., 2000). When the adhesions mature, radial arrays of actin filaments are replaced by circumferential actin belts (Yonemura et al., 1995).

To promote formation of early cell-cell contacts, cadherin-catenin clusters must recruit actin polymerizing proteins such as ARP2/3, formins and Ena/VASP family member proteins (Kobielak et al., 2004; Kovacs et al., 2002; Scott et al., 2006; Verma et al., 2004). This suggests that these proteins are active at cell protrusions even before the cell-cell adhesion is formed (Harris and Tepass, 2010).

How actin cytoskeleton and AJs are linked to each other is currently not well understood. Either actin de-polymerization or removal of α-catenin disrupts the movement of cadherin clusters with actin bundles (Kametani and Takeichi, 2007), suggesting a crucial role for α-catenin in cadherin tethering to actin. Recent studies suggest that α-catenin might interact with actin via other actin-binding proteins, such as vinculin, formin, ZO1 and afadin (Kobielak and Fuchs, 2004). EPLIN has also been shown to be involved in linking cadherin-catenin complex to actin cytoskeleton. However, EPLIN loss has no effect on the actin cables that enter the junction

perpendicularly (Abe and Takeichi, 2008). These actin bundles may be linked to AJs by the α-catenin-binding protein afadin (Sawyer et al., 2009). As α-catenin can interact with many actin-binding proteins, there may be redundancies between different interactions linking actin to α-catenin (Harris and Tepass, 2010).

EPLIN is also known as Lima-1 (Lim domain and actin binding 1). It was identified as a gene that displays different expression patterns in normal and transformed cells (Chang et al., 1998). There are two isoforms of EPLIN, EPLINα and EPLINβ. They are derived from the same gene by different promoter usage (Maul and Chang, 1999). EPLIN consists of one LIM (Lin11, Isl-1 and Mec-3) and two actin-binding domains (Maul and Chang, 1999; Zheng and Zhao, 2007). The ability to crosslink and bundle actin filaments suggest that EPLIN is involved in different actin-related processes such as cytokinesis, migration and intercellular junction formation (Abe and Takeichi, 2008; Chircop et al., 2009; Han et al., 2007). EPLIN has never been observed at FAs.

4. Mechanotransduction

The process by which cells sense and respond to their mechanical environment, eg. the ECM, adjacent cells or external stresses, is termed mechanotransduction (DuFort et al., 2011). There are more and more studies indicating that forces can regulate important biological processes such as cell proliferation, differentiation, tissue homeostasis and inflammatory cascades (Eyckmans et al., 2011). For instance, mechanical stress may cause alterations in endothelial and smooth muscle cell signaling (Chien et al., 1998; Tzima et al., 2005), expression of inflammatory markers (Yamawaki et al., 2005) and vascular cell proliferation (Davies et al., 1984; Sumpio et al., 1987). Moreover, diseases such as artherosclerosis, arthritis, deafness, osteoporosis, cancer and developmental disorders such as Kartagener's syndrome result from an abnormal response to extrinsic or intrinsic forces (DuFort et al., 2011; Jaalouk and Lammerding, 2009). Therefore, understanding the link between mechanical sensing and the subsequent biochemical response is of crucial importance.

4.1 Mechanotransduction machinery of cell-ECM interactions

Integrins have been implicated in a range of mechanotransduction events, such as responses to stretch, increased hydrostatic pressure, shear stress and osmotic forces (Katsumi et al., 2004). Integrins together with their downstream molecules form a major mechanical link between the actin cytoskeleton and the ECM (Figure 12).

Proteins within FAs including integrins (Friedland et al., 2009), talin (del Rio et al., 2009) and p130Cas (Sawada et al., 2006) can undergo conformational changes in response to force. The outcome of the force-dependent conformational change can either be that it stabilizes protein-protein interactions as in the case for fibronectin bound integrin or it may produce a cryptic binding site as in the case of talin. Moreover, p130Cas can activate Rap1 in response to force, which may induce conformational activation of integrin through its effector RIAM, which directly binds to talin (Han et al., 2006; Schwartz and DeSimone, 2008).

The major focus of mechanotransduction field has so far been on proteins with the ability to change conformation under tension; however, FAs also show force-dependent responses that do not only rely on protein switches (Bershadsky et al., 2006). For example, intermolecular distance may change upon force generation, which then leads to different cellular functions. In this model, FA assembly is linked to ECM compliance and force (DuFort et al., 2011; Paszek et al., 2009).

Cytoskeleton is the main structure to mediate force transmission (Wang et al., 1993). The cytoskeleton is composed of F-actin with a diameter of 6 nm, intermediate filaments with a diameter of 10 nm and microtubules with diameter of 23 nm. These three cytoskeletal components are not single proteins, but consist of many monomers (Eyckmans et al., 2011). F-actin together with myosin filaments constitutes the cellular contractile machinery. Inhibition of myosin II reduces cytoskeletal tension and leads to disassembly of FAs (Kirfel et al., 2004; Rid et al., 2005). Recent proteomics studies have suggested that the FAs formed after myosin II inhibition have a very distinct composition in comparison to native adhesion (Byron et al., 2011; Kuo et al., 2011; Schiller et al., 2011).

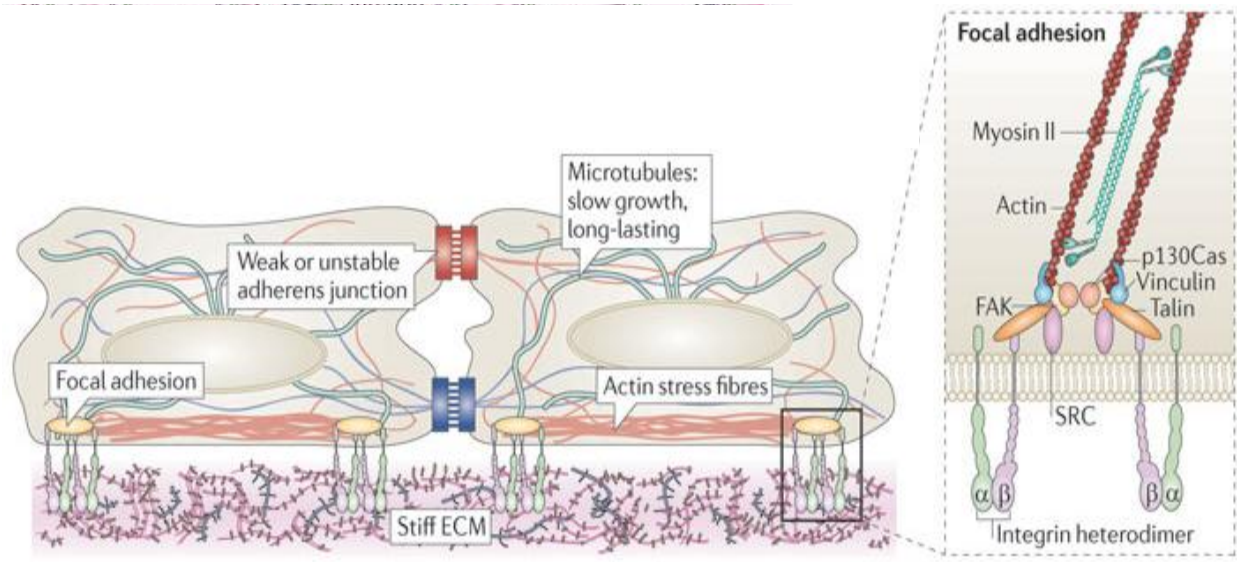

Figure 12: The mechanical network at FAs (DuFort et al., 2011).

Integrin-containing cell-matrix adhesions can sense physical properties of the ECM via proteins such as vinculin, talin, p130Cas and integrins which undergo conformational changes upon force application to trigger downstream cellular responses.

IPP-complex members have also been suggested to play a role in mechanotransduction in different cellular systems. For instance, ILK and α-parvin negatively regulate RhoA-ROCK signaling in vascular smooth muscle cells (Kogata et al., 2009; Montanez et al., 2009). ILK has also been shown to negatively regulate RhoA-ROCK signaling both *in vivo* and *in vitro* in Schwann cells (Pereira et al., 2009). Moreover, primary ILK-deficient fibroblasts have elevated RhoA levels, indicating that ILK regulates contractility in a wound-healing system (Blumbach et al., 2010). Whether PINCH-1 is involved in mechanotransduction, however, remains unclear.

4.2 Mechanotransduction machinery of cell-cell interactions

Although majority of the mechanotransduction studies focus on cell-ECM contacts, recently cell-cell adhesion complexes have also been elucidated as mechanosensors. Upon cell-cell adhesion, cells generate contractile forces that modulate the actin organization at the AJs. Actin bundles can have two different orientations, namely parallel and orthogonal bundles to the junctions. Parallel bundles can be found at the

apical actin belt next to the zonula adherens (ZA) of simple epithelium whereas orthogonal bundles are observed in the hypodermis of early *C.elegans* embryos (Gomez et al., 2011b). These bundles are rich in myosin II suggesting that they are contractile (Shewan et al., 2005; Smutny et al., 2010). Predictably, bundles that are parallel to the junctions would exert the tension along the junctions; however orthogonal bundles exert the tensile forces on junctions themselves (Figure 13). However, tension generated on cadherin adhesions is probably more complex, because many filaments terminate at the puncta of cadherin at the junctions (Shewan et al., 2005; Yonemura et al., 1995).

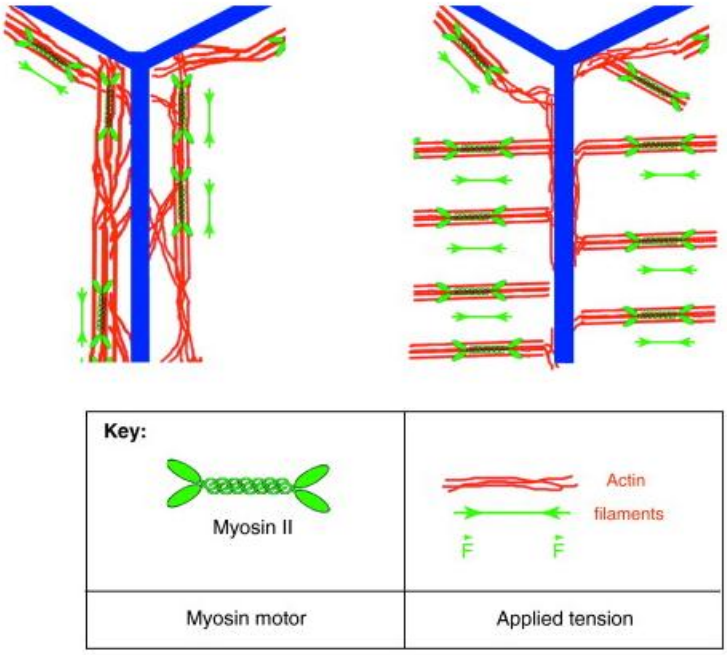

Figure 13: Relationship of actin bundles and cell-cell junctions (Gomez et al., 2011b). The orientation of actin bundles influences the tensile forces.

Experiments with soluble cadherin ligands demonstrated that cadherins are also force sensors. Similar to integrins, cadherins are able to sense the matrix rigidity. Increased substrate rigidity increases the force generated by cells plated on cadherins (Ladoux et al., 2010; le Duc et al., 2010). Mechanical stimuli can regulate cadherin receptors via several signal transduction modes, including small GTPases, PI3-kinases and Src

kinases (Niessen et al., 2011). Another way of regulating cadherins in response to force occurs via conformational changes of proteins, which reveal cryptic binding sites. It was known that α-catenin can recruit vinculin to cell-cell junctions (Watabe-Uchida et al., 1998; Weiss et al., 1998). However, it was only recently that it has been shown that recruitment of vinculin to cell-cell junctions requires force (Yonemura et al., 2010).

Vinculin interacts with a central motif (residues 325-402) of α-catenin. A region C-terminal to the vinculin binding motif inhibits vinculin binding by keeping α-catenin in a 'closed' conformation when no actomyosin tension is present. When tension is applied, α-catenin is unfolded and the vinculin binding site is exposed, which in turn leads to vinculin-mediated F-actin recruitment to E-cadherin sites (Lecuit, 2010) (Figure 14).

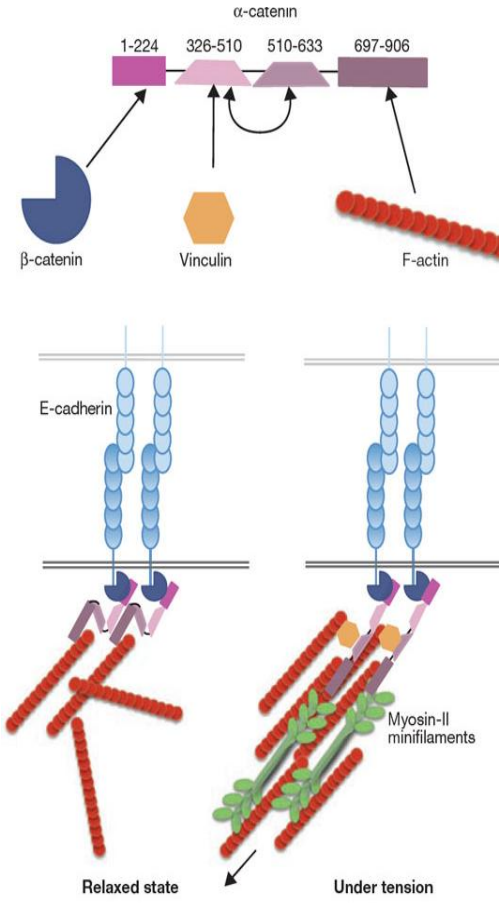

Figure 14: Actin cytoskeleton is mechanically coupled to adherens junctions via a force-dependent vinculin binding to α-catenin (Lecuit, 2010). The cartoon depicting α-catenin structure and domains responsible for β-catenin, vinculin and F-actin binding.

A central domain binds and masks the vinculin binding site when no force is applied. Upon myosin II-dependent contractility, vinculin can bind α-catenin and mediate the link between the F-actin cytoskeleton and cell-cell junctions.

A mechanosensitive role for EPLIN at the AJs has also recently been shown. EPLIN cooperates with vinculin to maintain the ZA and regulate epithelial reshaping (Taguchi et al., 2011). Furthermore, vinculin is missing from AJs when EPLIN is absent, suggesting a cooperation between EPLIN and vinculin to maintain AJs (Chervin-Petinot et al., 2012).

Beside vinculin no other FA protein has been reported to be recruited to cell-cell junctions upon force stimulation (le Duc et al., 2010). ILK has been shown to localize to AJs. However, this localization is not force-dependent (Vespa et al., 2005; Vespa et al., 2003).

5. Skin

Skin separates the body from the environment and thereby maintains homeostasis and protects against potential hazards, such as radiation, pathogens and mechanical damage.

Mammalian skin is a multilayered organ consisiting of an epithelial and a mesenchymal compartment called epidermis and dermis, respectively. These two compartments are separated by a BM. There are also appendages such as hair follicles (HFs) and sweat glands present in the skin.

5.1 Epidermal architecture and homeostasis

Epidermis is a stratified epithelium, which consists of several layers of keratinocytes (Figure 8). Stratum basale consists of the basal keratinocytes, which are the only cell type in epidermis with the capacity to proliferate. The following layers are the stratum spinosum and stratum granulosum. Spinous cells synthesize extensive network of keratin filaments which are connected to desmosomes, while granular cells produce lipid-rich lamellar granules (Fuchs and Horsley, 2008). Stratum corneum, which consists

of cornified cells lies on top of these layers. As granular cells move to stratum corneum, they lose their metabolic activity and cytoplasmic organelles. The cornified envelope serves as an epidermal barrier (Fuchs, 2007; Koster and Roop, 2007). The different layers can be distinguished by expression of specific markers. Keratin5 and Keratin14 are specific for the basal cell layer, whereas Keratin1 and 10 are characteristic for the spinous layer. Granular and cornified layers express lorigrin and fillagrin, respectively.
The epidermis originates from the ectoderm. After gastrulation, a layer of epidermal cells form between E9.5 and E12.5. Then the HF morphogenesis initiates with the signals received from the mesenchymal cells that populate the skin, meanwhile the same signals govern the epidermal stratification (Blanpain and Fuchs, 2006; Koster and Roop, 2007). During stratification, suprabasal cells occasionally divide, however at E17.5 epidermal stratification is completed and epidermis consists of a basal layer with the proliferative capacity and a suprabasal layer with terminally-differentiated cells.

Mammalian skin consists of a pilosebaceous unit, which is composed of a HF and its interfollicular epidermis (IFE) (Figure 15a). The tissue homeostasis and repair are ensured by stem cells present the bulge of the skin.

HFs undergo cycles of degeneration and regeneration throughout life (Figure 15b). After the first 2 weeks of morphogenesis are completed, the supply of matrix cells declines, HF growth stops and the follicle enters a degenerative phase called catagen. This phase takes 3-4 days in mice. During catagen, the lower two-thirds of the follicle regress and the HF is reduced to an epithelial strand by apoptosis; however the bulge region containing the HF stem cells remains intact (Blanpain and Fuchs, 2009; Fuchs, 2007). Catagen is followed by a quiescent stage called telogen. After the telogen phase, activating factors stimulate the stem cells to regrow the hair (Paus and Cotsarelis, 1999).

The molecular mechanisms regulating the HF morphogenesis and cycle are poorly understood. However, the signaling pathways important for these processes involve Notch, Wnts, bone morphogenic proteins (BMPs), sonic hedgehog (shh), fibroblast

growth factor (FGF), EGF, MAPK, and nuclear factor-κB (NF-κB) signaling pathways (Blanpain and Fuchs, 2009; Schmidt-Ullrich and Paus, 2005).

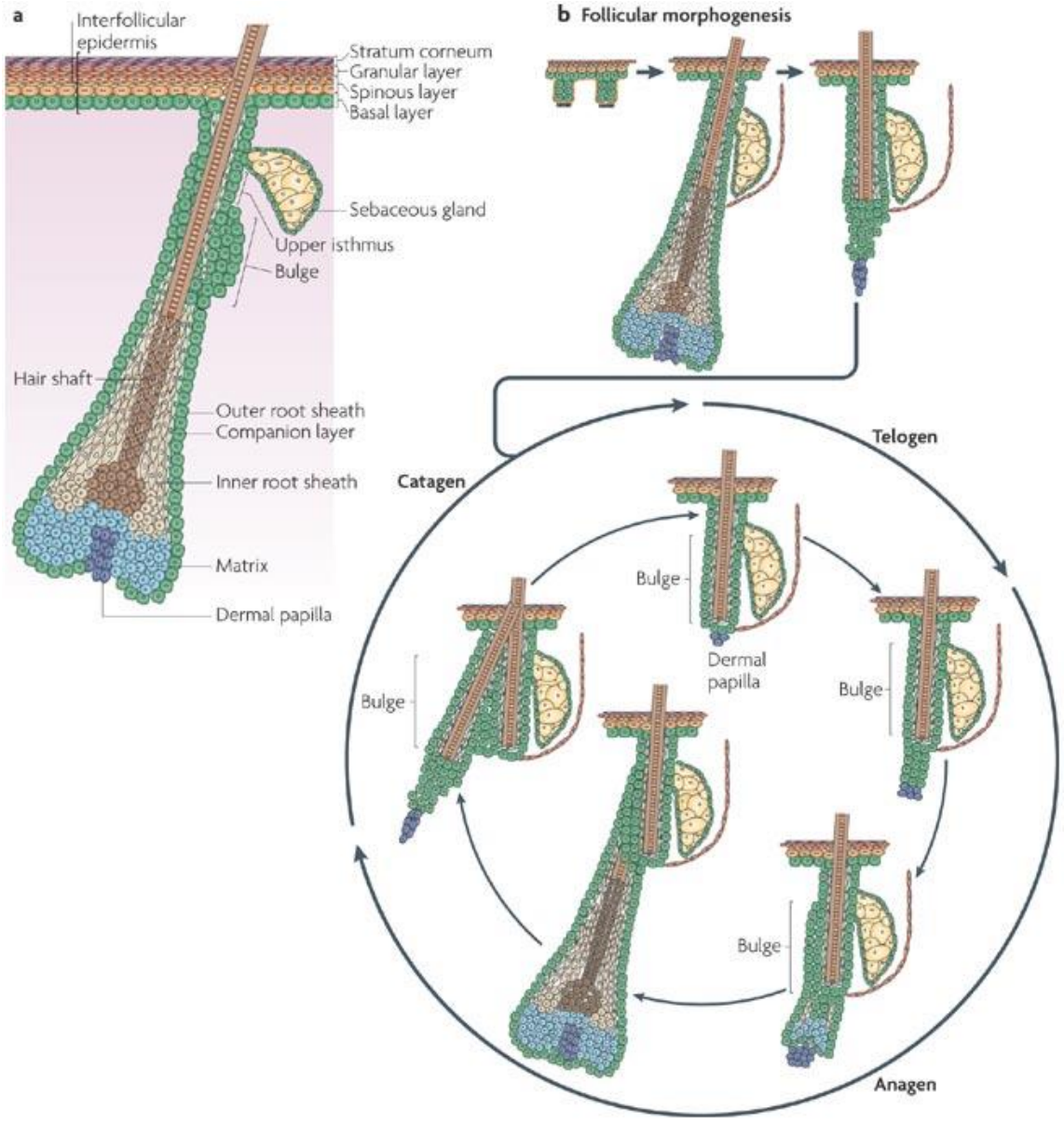

Figure 15: Homeostasis in the epidermis and hair follicle (Blanpain and Fuchs, 2009). Mammalian skin is composed of hair follicles (HF) and its surrounding interfollicular epidermis (IFE). (a) Bulge region contains the stem cells that are necessary to ensure the turnover of skin epidermis. (b) As matrix cells lose their proliferative capacity, the hair growth stops and follicle enters the destructive phase

called catagen that is followed by a resting phase called telogen. Following telogen, HF stem cells are activated and a new growth phase (anagen) starts.

5.2 Role of integrins in epidermis and HF homeostasis

Integrins are found at the BM attachment sites of the basal or ORS cells. The main integrin heterodimers that are present in keratinocytes are α2β1 (collagen receptor), α6β4 (laminin receptor), α3β1 (laminin receptor), α9β1 (tenascin receptor) and at lower levels αvβ5 (vitronectin receptor). In pathological conditions, fibronectin receptors (α5β1, αvβ6 and α9β1) become upregulated (Watt, 2002).

The importance of integrins in epidermis and HF homeostasis is mainly based on the integrin knock-out mice experiments. The Cre-LoxP system has been commonly used to delete genes in keratinocytes. To this end the Cre recombinase was expressed under the control of Keratin-5 (K5) or Keratin-14 (K14) promoters that are specifically expressed in basal keratinocytes.

Constitutive deletion of α6 or β4 integrin leads to neonatal lethality due to severe BM impairment (Dowling et al., 1996; Georges-Labouesse et al., 1996; van der Neut et al., 1996). Constitutive α3-knock-out mice die shortly after birth due to renal and/or lung failure (Kreidberg et al., 1996). When skin is analyzed, BM defects are observed, suggesting a role for α3β1 in epidermal homeostasis (DiPersio et al., 1997).

When β1 integrin is conditionally deleted in epidermis by using K14-Cre, it leads to early lethality due to severe blistering and dehydration and when K5-Cre is used (Raghavan et al., 2000), they die later and show progressive hair loss, infiltrating macrophages surrounding the HFs, upregulated pro-inflammatory cytokines and dermal fibrosis (Brakebusch et al., 2000; Grose et al., 2002; Lopez-Rovira et al., 2005; Raghavan et al., 2000).

Keratinocyte-specific ILK depletion in skin in a K5- or K14-Cre background, gives rise to epidermal defects, HF disruption and hair loss. Moreover primary ILK-deficient keratinocytes display adhesion, spreading and migration defects (Lorenz et al., 2007;

Nakrieko et al., 2008). However, the role of PINCH-1 in skin homeostasis has not been studied so far.

5.3 Role of intercellular adhesions in epidermal homeostasis

Intercellular adhesions are crucially important for epidermal homeostasis. For instance, targeted ablation of E-cadherin in skin leads to hyperproliferation, aberrant differentiation and impaired barrier formation (Tinkle et al., 2004; Tunggal et al., 2005; Young et al., 2003), whereas depletion of both E- and P-cadherin results in lethal blistering (Tinkle et al., 2008). On the other hand, epidermal deletion of p120 catenin does not have an effect on adhesion (Perez-Moreno et al., 2006). However, it impairs cytokinesis leading to binucleated cells in the suprabasal layers of epidermis (Perez-Moreno et al., 2008).

In addition to the roles in adhesion and cytokinesis, adhesion molecules can also regulate inflammatory signaling in epidermis (Perez-Moreno and Fuchs, 2006). Epidermal deletion of α-catenin leads to hyperproliferation through elevated mitogenic MAPK signaling (Kobielak and Fuchs, 2006). p120 catenin also affects inflammatory signaling in the epidermis (Perez-Moreno et al., 2006) by regulating NF-κB signaling.

Aim of the Thesis

PINCH-1 is a core component of IPP-complex that acts downstream of integrin signaling and functions in concert with the other complex members. Similar to ILK and β1 integrin deficient mice, constitutive PINCH-1 gene deletion leads to early embryonic lethality due to abnormal epiblast polarity, impaired cavitation and detachment of endoderm and epiblast from BMs. However, PINCH-1 deletion in mice is also leading to phenotypes that are differ from ILK and β1 integrin deficient mice. They include endoderm survival defects and cell-cell adhesion defects of the primitive endoderm and epiblast. This suggests that PINCH-1 may also act independently from the IPP-complex. Whether IPP-complex-independent functions operate *in vivo* and *in vitro* was the major aim of my thesis work.

The aims of the thesis were:

1. to determine how PINCH-1 molecularly regulates cell survival by using EBs and EB-derived endoderm cells as a model.
2. to investigate how PINCH-1 regulates cell-cell adhesions in the epidermis *in vivo*.

Materials and Methods

1. Common Chemicals

All the chemicals used in this study were purchased from Carl Roth GmbH (Karlsruhe, Germany), Merck (Darmstadt, Germany), Peprotech (Hamburg, Germany), Reidel de Haen (Seelze, Germany), Roche Diagnostics GmbH (Mannheim, Germany), Serva (Heidelberg, Germany), Sigma Aldrich (Munich, Germany) unless otherwise specified.

2. Animals

All mouse strains used in this study were kept and bred in the animal facility of the Max-Planck-Institute of Biochemistry (Martinsried, Germany). The mice had standard rodent diet and water. The light cycle was set to 12 hours. 8 week-old mice were used for breeding. 3 weeks after birth, mice were separated according to the sex, marked with ear tags and maintained in separated cages. For genotyping, mice tails were clipped, and used for DNA isolation immediately (2.7.2). All experiments were carried out according to the German Animal Protection Law.

2.1 Breeding scheme

To generate a conditional PINCH-1 knockout in the epidermis, we crossed mice with a *loxP*-flanked *PINCH-1* gene (PINCH-1$^{fl/fl}$) (Li et al., 2005) and mice expressing the *Cre* recombinase under control of the *K5* promoter (*K5-Cre*) (Ramirez et al., 2004).

3. Histological analyses of conditional PINCH-1 knockout mice

3.1 Histology material

Embedding machine: Shandon, HistoCentre 2

Microtomes: Microm, Vacutome HM5000M, HM355S

Cryomold: Sakura, Tissue-Tek, #4566

Cryomatrix: Thermo Scientific, Shandon Cryomatrix™, #6769006

Microscope slides: Thermo Scientific, Menzel-Gläser Superfrost®Plus, #J1800AMNZ

Entellan mounting medium: Merck, #1.07960

Meyers hemalaun: Merck, #1.09249

Eosin G: Merck, #1.09844

3.2 Histological methods

The most important aspect of histological methods was to preserve on one hand the morphology of the biological specimen and on the other hand to its biological activity in the best possible way. This is crucially affected by the selection of fixation and embedding, therefore a variety of fixation and embedding protocol is used for each particular experiment. The most commonly-used fixatives are paraformaldehyde (PFA) and alcohols (ethanol and methanol). PFA better preserves the morphology of the specimen, but can compromise the biological activity. Paraffin is used as embedding material. If the specimen is not affected from PFA treatment, the best combination is to fix the sample with PFA and to embed in paraffin, which allows cutting of thin sections (6µm). Another commonly-used embedding method is freezing un-fixed specimen in a cryomatrix. This method is preferred when the biological activity of the specimen should not be compromised.

3.2.1 Preparation of paraffin sections

To analyze epidermis and HF morphology, skin was isolated at selected time points. The back skin of mice was shaved and a fragment was cut. This fragment was fixed in freshly-prepared 4% PFA/PBS solution overnight at 4°C. The following day, samples were dehydrated in consecutive baths with a gradually increasing concentration of ethanol: 50%, 70% and 80% for 60 minutes, 90% for O/N and 100% – 3 × 60 minutes. Then, skin fragments were treated with xylol for 2 × 15 minutes and subsequently transferred to a container with liquid paraffin (kept at 56°C). To remove all traces of xylol, paraffin solution was changed twice during the incubation time (60 + 60 + 90 minutes). In the end, skin fragments were set in paraffin blocks using an embedding device. Samples were stored at 4°C. Before cutting, they were cooled down on ice or in a -20°C freezer. Paraffin embedded tissue was cut using a microtome into 6 µm thick sections. They were collected on glass slides and stored at RT or 4°C.

3.2.2 Preparation of cryosections

To analyze epidermis and HF morphology, skin was isolated at selected time points. The back skin of mice was shaved and a fragment was cut. This fragment was directly

embedded in cryomatrix placed in plastic cryo-molds in a vertical position to the base of the mold.

To analyze morphology of EBs, they were transferred from culture into 15 ml conical tubes and allowed to settle by gravity and the supernatant was removed. Then they were re-suspended in 10 ml PBS, allowed to settle by gravity and then the supernatant was again removed. They were kept in the fixation solution (4% PFA in PBS, freshly-prepared) for 30 minutes, transferred into 7,5% sucrose in PBS for 3 hours at RT, followed by overnight incubation at 4°C in 15% sucrose. Next day, sucrose solution was replaced by cryomatrix and the samples were frozen (Montanez et al., 2007).

Frozen samples were kept at -80°C. Before cutting, they were warmed to -20°C. Cryo-embedded specimen was cut using a cryotome into 8µm or 10µm thick sections and collected on glass slides. These slides were kept at -20°C. Before using for further applications, they were air-dried for 1 hour.

3.2.3 Hematoxylin/Eosin (H&E) staining

It is a widely-used histological method that allows visualizing several different tissue structures. The color properties of the section stained with hematoxylin depend on oxidation product Hematein. It stains basophilic molecules such as DNA and RNA and other acidic structures in blue. Eosin, on the other hand, stains cytoplasmic structures and connective tissue in pink.

To perform an H&E staining, paraffin sections were deparaffinized by xylol treatment for 2 x 5 minutes. Then, they were rehydrated in 100%, 95%, 90%, 80% and 70% ethanol series for 2 minutes, each. The slides were then treated with hematoxylin (Mayers hemalaun) for 1 minute and after that with tap water. Subsequently, samples were treated with Eosin for 1 minute and after that with tap water and dehydrated in 70%, 90%, 95% and 100% ethanol series for 2 minutes, each. Finally, they were washed in xylol for 2 x 5 minutes and mounted in Entellan.

4. Immunological methods

4.1 Material immunological analyses

NAME	COMPANY	CATALOG NO	SOURCE

PINCH	BD Transduction Lab	612711	Mouse
Actin	Sigma	A2066	Mouse
Phalloidin-Alexa488	Invitrogen	A12379	
Phalloidin-Alexa488	Invitrogen	A22287	
Beta Catenin	SIGMA	C7207	Mouse
Bromodeoxyuridine	Roche	1 202 693	Mouse
Cleaved Caspase3	Cell signaling	9661	Rabbit
EPLIN	Bethyl labs		
Nidogen	Chemicon	MAB1946	Rat
Keratin14	Covance	PRP-155P	Rabbit
plakoglobin	Santa Cruz	Sc-7900	Rabbit
GAPDH	Calbiochem	CB1001	Mouse
GATA-3	Santa Cruz	Sc268	Mouse
MAPK	SIGMA	M-5670	Rabbit
MAPK	SIGMA	M-8159	Mouse
ILK	Cell Signaling	3862	Rabbit
Integrin α6-FITC	Pharmingen	555735	Rat
Integrin β1	Chemicon	MAB1997	Rat
Akt	Cell Signaling	9272	Rabbit
P-Akt(Ser473)	Cell Signaling	9277	Rabbit
ERK1/2	Cell Signaling	9103	Rabbit
pERK1/2	Cell Signaling	4376	Rabbit
ILK	BD Transduction Lab	611802 6118031	Mouse
FAK	Upstate	#06-543	Rabbit
Paxillin	Sigma	V9131	Mouse
Secondary antibodies			
α-mouse HRP	Bio-Rad	170-6516	Mouse
α-rabbit HRP	Bio-Rad	170-6515	Rabbit
α-rat HRP	Jackson Labs	712-035-150	Rat
α-rabbit Alexa488	Invitrogen	A11008	Rabbit
α-rabbit Alexa647	Invitrogen	A21244	Rabbit
α-rat Alexa488	Invitrogen	A11006	Rat
α-rat Alexa647	Invitrogen	A21247	Rat
α-mouse FITC	Jackson Labs	115-095-075	Mouse
α-rabbit Cy3	Jackson Labs	711-165-152	Rabbit
α-mouse Cy3	Jackson Labs	115-165-146	Mouse

Each immunostaining was finalized with 5 minutes staining with 4', 6-Diamidino-2-phenylindole (DAPI, 1:10000 in PBS) in order to visualize the nuclei.

Elvanol: 12 g Mowiol 4 – 88 (Roth, #0713) dissolved in 30 ml 87% glycerol, 60 ml Tris-HCl pH 8.5 and 30 ml H_2O.

DAPI: Sigma, Biochemica, #32670

4.2 Immunohistochemistry (IHC) of sections

To detect intracellular proteins tissue sections were permeabilized with 0.1% Triton X-100 in PBS for 10 minutes at RT prior to blocking in 3% BSA in PBS for 1 hour at RT. After blocking, sections were incubated overnight with indicated primary antibodies (diluted in blocking solution) at 4°C in a humidified chamber. Next day, slides were washed 3 x 10 minutes in PBS and incubated with the indicated secondary antibodies (diluted in blocking solution) for 2 hours at RT in the dark. After three washes with PBS (10 min each, in the dark), the sections were mounted with Elvanol.

4.3 3, 3'-Diaminobenzidine (DAB) staining of sections

3, 3'-Diaminobenzidine is a substrate for peroxidase. A brown precipitate is formed when the two react with each other. Therefore, when peroxidase-conjugated antibodies are bound to epitopes they can be specifically stained by application of DAB. It is necessary to block the endogenous peroxidase activity by a H_2O_2 treatment prior to the DAB staining. To perform a DAB staining, slides were prepared as in the H&E staining protocol and then incubated for 10 minutes in a 0.3% H_2O_2 / methanol solution. After a 5 minute wash in PBS, they were blocked in 5% goat serum in PBS-T for 1 hour at RT. Then sections were incubated with the indicated primary antibody (diluted in blocking solution) overnight at 4°C in a humidified chamber. The following day, they were washed 3 x 10 minutes with PBS-T before the incubation with the indicated (peroxidase-conjugated) secondary antibody (diluted in blocking solution) for 1 hour at RT. Subsequently, they were washed 3 x 10 minute with PBS. Then the staining reaction was initiated via the addition of DAB solution containing 0.03% H_2O_2. When the staining was intense enough, the reaction was stopped by washes under tap water. Lastly, a Hematoxylin stain was performed for 30 seconds to obtain a better contrast of the sample. Then the slides were subjected to dehydration and mounting with Entellan.

4.4 Electron microscopy

Electron microscopy analyses were performed by Dr. Wilhelm Bloch at the Department of Molecular and Cellular Sport Medicine, German Sport University Cologne, Germany. Small pieces of back skin were cut into fragments of about 1mm^3 fixed overnight in 2% paraformaldehyde/2% glutaraldehyde in 0.1 M cacodylate buffer pH 7.2, washed in 0.1 M cacodylate buffer and stained in 1% uranyl acetate. Subsequently, they were incubated in 70% ethanol for 8 hours, and then exposed to an ethanol series for dehydration. Finally, they were embedded in araldite resin. Semi-thin sections (1 µm) were cut with a glass knife using an ultramicrotome (Reichert, Bensheim, Germany) and stained with Methylene Blue. Ultra-thin sections (30-60 nm) for electron microscopy observation were cut on the same microtome with a diamond knife and placed on copper grids. The transmission electron microscopy was performed with a Zeiss 902A electron microscope (Zeiss, Oberkochem, Germany) (Grose et al., 2002).

4.5 Immunofluorescence (IF) of adherent cells

All immunostainings of adherent cells were performed on glass coverslips (Menzel-Gläser). Coverslips were coated with coating medium either overnight at 4°C or 1 hour at 37°C. 5 - 10 x 10^4 cells were allowed adhere and spread overnight. After indicated times of culture in the cell incubator and indicated treatments, cells were washed once with PBS, fixed with ice cold PFA for 15 min at RT, rinsed in PBS 3 x 5 minutes and permeabilized in permeabilization solution (0,05% Triton X-100 in PBS). Subsequently, they were blocked for 1 hour in blocking solution at 37°C, incubated with indicated primary antibodies (diluted in blocking solution) for 1 hour at 37°C, washed with PBS for 3 x 10 minutes and then incubated with the appropriate secondary antibodies (diluted in blocking solution) for 45 minutes at 37°C. Finally, coverslips were washed in PBS for 3 x 10 minutes and incubated in a DAPI-containing solution for 5 minutes before being washed and mounted in Elvanol.

Coating medium:

25ml MEM(sigma #M8167)

2.5ml BSA (Fratction V, 1mg/ml Stock)

0.5ml Hepes pH7.3

0.25ml Vitrogen 100 collagen (Cohesion FXP-019)

0.25ml Fibronectin (1 mg/ml Stock, Invitrogen #33016-015)

Blocking solution:

3% BSA and 5% goat serum in PBS

4.6 TUNEL staining of adherent cells

The hallmark of apoptosis is DNA fragmentation. When the DNA is cleaved, single- or double-stranded DNA is produced with nick ends. The fragmented DNA can be visualized by labeling the free 3'-OH ends with fluorescent-dUTP. This labeling reaction occurs via terminal deoxnucleotidyl transferase (TdT). Therefore this method is called TdT-mediated dUTP nick end labeling (TUNEL).

For TUNEL staining, adherent cells were seeded on glass coverslips, grown at indicated time points in an incubator, then fixed with ice cold 4% PFA in PBS for 15 minutes, rinsed with PBS for 3 x 5 minutes and blocked with 3% H_2O_2 in methanol for 10 minutes at RT followed by rinsing with PBS for 3 x 5 minutes. Subsequently, cells were permeabilized in 0,1% sodium citrate containing 0,1% Triton X-100 for 2 minutes on ice, rinsed with PBS for 5 minutes and treated with TUNEL solution from *In situ* Cell Death Detection Kit (Roche Diagnostics, #11 684 817 910). Manufacturer's instructions were followed.

5. Cell culture methods

5.1 Cell culture material

5, 10, 25 ml pipettes: Corning, Costar Stripette, #4487, #4488, #4489

Multi-well plates (Corning): 96 well: #3799, 24 well: #3524, 6 well: #3046

15, 50 ml conical tubes: Corning, CentriStar, #430791, #430829

Cryogenic vial: Corning, #430489

60, 100 mm dishes: Falcon, Easy Grip, #353004, #353003

140 mm dish: NUNC, #168381

P/S: PAA, Penicillin / Streptomycin (x 100), #P11-010

Trypsin: Trypsin / EDTA (10x), Gibco, 15400-054

5.2 Keratinocyte culture

5.2.1 Keratinocyte isolation from mice

Mice were sacrificed, shaved and washed in an ethanol solution, distilled water and PBS (~1 minute in each), respectively. After cutting off limbs, the skin was peeled off and placed in a sterile Petri dish. The subcutaneous fat layer was scraped off with a scalpel. Then skin was cut into long, narrow strips and placed (epidermis down) in a Petri dish that containing a solution with antibiotics for 5-10 minutes. Subsequently, the skin was transferred (epidermis up) to a new Petri dish containing 25 ml of 0.8% trypsin in PBS (Trypsin 1:250; Invitrogen #27250-018) and incubated for 50 min at 37°C. Following the incubation, skin was transferred into a bacteriological plate containing keratinocyte growth medium (KGM), the epidermis was separated from the dermis, mechanically disassembled by a forceps and the resulting suspension was then filtered through a 70 µm cell strainer (BD Biosciences) to collect the cells. Then cells were centrifuged and washed once in KGM (5 minutes, 500g). Finally, cells were counted and plated on 10 cm dishes coated with FN and collagen I-containing coating medium (4.5) at the density of 6×10^6.

Antibiotic solution:

PBS	500 ml
Penicillin/streptomycin (100x)	10 ml (PAA Laboratories #P11-010)
Nystatin (10000 U/ml)	10 ml (Sigma #N1638)
Fungizone (250 µg /ml)	10 ml (Gibco # 15290-026)

5.2.2 Culture of keratinocytes

Primary keratinocytes were seeded on a plastic or glass surface, coated with coating medium, and cultured in a special medium at 37°C. The medium was changed every 2-3 days. Keratinocytes were grown without splitting until control cells became fully confluent (1 week).

Keratinocyte Growth Medium (KGM):

MEM	500 ml (Sigma #M8167)
Chelated FCS	40 ml (8%)
Insulin (5 mg/ml in 4 mM HCl)	500 µl (5 µg/ml) (Sigma #I5500)
EGF (200 µg/ml)	5 µl (10 ng/ml) (Sigma #E9644)
Transferrin (5 mg/ml)	1000 µl (10 µg/ml) (Sigma #T8158)
10 mM Phosphoethanolamine	500 µl (10 µM) (Sigma #P0503)

10 mM Ethanolamine*	500 µl (10 µM) (Sigma #E0135)
Hydrocortisone (5 mg/ml in EtOH)	36 µl (0.36 µg/ml) [Calbiochem #386698]
200 mM L-Glutamine (100x)	5 ml (Gibco # 25030-024)
Penicillin/streptomycin (100x)	5 ml (PAA Laboratories #P11-010)

The complete medium was sterile filtered (0.22 µm).

FCS (Gibco #10270-106) was chelated to deplete the Ca^{++} ions, which induce differentiation of keratinocytes. To do this, Chelex resin (Biorad #142-2832) was suspended in 5 l ddH2O (40 g/l) and adjusted to pH 7.4. Then the suspension was filtered through a paper filter (Schleicher&Schuell #314856) and the resin was stirred with 500 ml of a heat inactivated FCS, O/N at 4°C. Chelex beads were removed by filtering and subsequent centrifugation (5 min, 8000 rpm). FCS was sterilized with a vacuum filter system (Corning #431097), aliquoted (40 ml) and stored at -20°C.

To store keratinocytes long term, they were frozen by resuspending in freezing medium after trypsinization, at -80°C. They were stored in liquid nitrogen (-196°C) for longer periods. When keratinocytes were thawed, the cryovials were placed in a 37°C water bath and as soon as the freezing medium had thawed, the cells were added into a 10 ml KGM-containing conical tube and centrifuged at 900rpm for 5 minutes. The cell pellet was re-suspended in growth medium and seeded on appropriate plates.

5.2.2 Immortalization and cloning of primary keratinocytes

Keratinocyte immortalization was performed using a spontaneous immortalization. Isolated primary keratinocytes were grown until 100% confluency and then split into two 10 cm dishes at 1:1 ratio. No special treatment was conducted, instead the cells were kept in standard culture conditions and the growth medium was changed every 2-3 days. Besides extensive cell death, small colonies of keratinocytes formed and grew larger. When these colonies reached a certain size, consisting of 1 x 10^5 cells, they were split and further cultured. Thereby, the keratinocytes were spontaneously immortalized.

To isolate single clones, first the feeder cell layer was prepared. Either keratinocytes or NIH3T3 cells were seeded in a 10 cm plate. After reaching a 50-60% confluence, they were treated with mitomycin C (Sigma, #4287) (diluted in KGM, 4µg/ml) for 4 hours. Next, cells were washed with PBS and made ready to be used as feeder cells. To

obtain single clones, cells were seeded in very low densities on 10 cm dishes (100, 200, 400 cells per dish) on mitomycin-treated feeder cells and cultured in KGM for 2-3 weeks until single colonies were visible. Colonies were picked under a microscope by placing a cloning cylinder around to isolate them from the surrounding cells. Then 100µl prewarmed 2 x Trypsin/EDTA was added into the cylinder and the clones were incubated for 15-20 minutes. After the incubation, the colonies were sucked off with a 200µl pipet and transferred into 24-well plates containing 1 ml KGM. Finally, clones were grown for approximately 1 week in 24- wells until they were confluent.

5.2.3 Spreading assay and time-lapse imaging of keratinocytes

Live cell imaging of freshly isolated and immortalized keratinocytes was performed with a Zeiss Axiovert 200 M microscope equipped with a motor-controlled CCD camera (OrcaER, Hamamatsu). Snapshots from the cells were captured every 20 minutes for 20 hours (at 37°C, 5% CO_2). The first snapshot was taken 30 minutes after keratinocytes were seeded on the coated plastic (6-well) dishes. The cell spreading at each indicated time point during the assay was analyzed by measuring the pixel area of 50-60 randomly selected cells. Metamorph software (Universal Imaging Corporation) was used to quantify and process the images.

5.3 Embryonic stem cells (ES cells) culture

ES cells derive from the inner cell mass of the blastocyst and they are pluripotent, meaning that they can give rise to all differentiated cell types. Therefore, they serve as an excellent model to study the molecular and cellular events during differentiation into different cell lineages (Montanez et al., 2007).

ES cells form colonies and any change in the shape or color of the colonies may indicate that they undergo differentiation. Therefore, a special care should be taken to keep ES cells in an undifferentiated state.

5.3.1 ES cell culture material

Cell growth media: Gibco, DMEM (#31966-021),

Non-essential amino acids (NEAA): Gibco, MEM NEAA x 10, #11140

Fetal bovine serum (heat inactivated for 30 minutes at 65°C): Gibco, #10270-106

Trypsin: Gibco, Trypsin / EDTA (x 10), #15400-054

P/S: PAA, Penicillin / Streptomycin (x 100), #P11-010

Leukocyte inhibitory factor (LIF): ESGro, Gibco

5.3.2 ES cell culturing

ES cells were seeded on a subconfluent feeder cell layer consisting of mitotically arrested primary mouse embryonic fibroblasts (MEFs) and grown in ES cell medium. Feeder cells release nutrients and produce LIF important for keeping ES cells in an undifferentiated state. LIF was also supplemented in the medium to secure the concentration. Medium was changed every day.

ES cell medium:

D-MEM	400 ml
FCS	100 ml
NEAA	5 ml
LIF	500 µl

5.4 Embryoid bodies (EBs)

When ES cells are kept in suspension, their aggregates form multicellular 3-dimensional structures called EBs. They recapitulate the peri-implantation stage of mouse embryo development and follow the molecular cues that regulate embryonic implantation. First, the outer layer of EBs differentiates into primitive endoderm cell layer (hypoblast) that forms the first BM. Upon formation of BM, adjacent ES cells different into columnar epithelium (epibast or primitive ectoderm). The rest of the ES cells, which have no contact with BM, undergo apoptosis leading to the formation of a central cavity (Montanez et al., 2007).

5.4.1 Preparation and culturing of EBs

The best moment to start preparing EBs from ES cells is when ES cell colonies reach a 70% confluency of a 10 cm dish. The medium is removed from the dish, cells are rinsed with 2 x 10 ml prewarmed PBS, then 3 ml of 0.25% Trypsin/0.53 mM EDTA is added into the dish for 2 to 3 min at RT to detach the colonies from feeder cells. The trypsinization is stopped by addition of medium once the ES cell aggregate detached from the underlying feeder cells. The cell suspension is collected in a 15 ml conical tube, is allowed to settle by gravity for 10 minutes at RT, the supernatant is discarded and the pellet is resuspended in 1 ml EB growth medium (ES cell medium lacking LIF).

After resuspension, the ES cell aggregates are passed through a 2µM-thick glass Pasteur pipette to separate them and to create EB precursors. This process is repeated until all cell aggregates are separated. Then the EB precursors are plated in a cell culture dish with 8 ml EB medium for 30-40 minutes to remove the feeder cells. Afterwards the EB precursors are plated in a bacterial plate to keep them in suspension. The medium is not changed during the first 3 days, and then it is changed every other day. At the 7th day of EB differentiation, a high percentage of EBs forms an inner layer of columnar epithelial cells and a cavity. They are called cystic EBs.

After 7-8 days of differentiation, EBs were collected in a conical tube, centrifuged at 900rpm for 5 minutes at RT, resuspended in appropriate amounts of EB medium and pipetted up and down several times. Afterwards, they were allowed to stand at RT for 15-20 minutes to let the EBs settle by gravity. The supernatant, containing the isolated endoderm cells was collected and plated on 6-well plates coated with 10µg/ml FN.

5.5 Drug treatments of cells

Keratinocytes were treated with 5nM HGF (Peprotech) for 1 hour, 25µM Y-27632 (Calbiochem) for 1 hour and 25µM blebbistatin for 15 minutes and endoderm cells were treated with 10µM JNK inhibitor (SP600125, Calbiochem) for 45 minutes when necessary.

HGF: Peprotech, #100-39

Y-27632: Calbiochem, #688000

SP600125: Calbiochem, #420119

Blebbistatin: Sigma, #030M1246

6. Biochemical methods

6.1 Materials biochemical methods

Protease inhibitor cocktail: Roche, Complete Mini / EDTA free, #12740900

Phosphatase inhibitor cocktails 1 & 2: Sigma, #P2850, #P5726

Microtip Sonicator: Branson, #B-12

Precision Plus Protein^{TM} Caleidoscope^{TM} Standards: BioRad, #161-0375

Centrifuge: Beckman-Coulter, GS-15R

6.2 Preparation of protein lysates

6.2.1 Preparation of protein lysates from mouse epidermis

Keratinocytes from mice were obtained as described previously (5.2.1) except for the last step, which was modified. After filtering the cells through a 70 µm cell strainer (BD Biosciences) they were collected and washed once with ice cold PBS. Pelleted cells were resuspended in an ice-cold lysis buffer, incubated for 30 minutes on ice, the suspension was then transferred into a microcentrifuge tube and centrifuged at 14000rpm for 15 minutes at 4°C. Cleared lysate was aliquoted and stored at -80°C.

Lysis buffer: 150mM NaCl, 1mM NaF, 1mM Na_3VO_4, 1mM EDTA, 1% Triton X-100 in 50mM Tris-HCl pH 7.6, protease inhibitor cocktail: 1 tablet / 10 ml

6.2.2 Preparation of protein lysates from EBs

EBs were prepared from ES cells as described previously (5.4.1). After 7-8 days of differentiation, EBs were not plated but lysed in appropriate amounts of lysis buffer on ice for 10 minutes, collected in a microcentrifuge tube, sonicated at 4°C (2 x 10 seconds at intensity 4) and centrifuged at 14000rpm for 5 minutes at 4°C. Then the supernatant was collected in a separate microcentrifuge tube and the protein concentration was determined using a BCA protein assay (6.3.1). The lysates were either stored at -80°C, or used directly for SDS-PAGE (6.4).

Cell lysis buffer (RIPA): 150 mM NaCl, 1 mM EDTA, 1% Na-deoxycholate, 0.1% SDS, 1% Triton X-100, 10 mM NaF, 1 mM Na_3VO_4 in 50 mM Tris-HCl pH 7.8, protease inhibitor cocktail: 1 tablet / 10 ml

6.2.3 Preparation of protein lysates from adherent cells

The adherent cells were washed once with ice-cold PBS and then the appropriate amount of cell were incubated with the lysis buffer for 10 minutes on ice. Afterwards, they were scraped off using a rubber cell scraper (Costar), transferred into a microcentrifuge tube, sonicated at 4°C (2 x 10 seconds at intensity 4) and centrifuged at 14000rpm for 5 minutes at 4°C. The supernatant was transferred into a new microcentrifuge tube and the protein concentration was determined using a BCA protein assay (6.3.1). The lysates were either stored at -80°C, or directly used for SDS-PAGE (6.4).

Cell lysis buffer (RIPA): 150 mM NaCl, 1 mM EDTA, 1% Na-deoxycholate, 0.1% SDS, 1% Triton X-100, 10 mM NaF, 1 mM Na_3VO_4 in 50 mM Tris-HCl pH 7.8, protease inhibitor cocktail: 1 tablet / 10 ml

4 x SDS sample buffer (SDS-SB): 16 ml 20% SDS, 0.32 ml 0.5 M EDTA, 16 ml 87% glycerol, 0.001% bromphenol blue in 50 mM Tris-HCl pH 6.8

6.3 Determination of protein concentration

Protein concentration was determined by two methods: 1. BCA assay (6.3.1), and 2. Bradford assay (6.3.2). BCA assay was preferred when a lysis buffer was used containing SDS whereas the Bradford assay was used when the lysis buffer did not contain any SDS.

6.3.1 BCA assay

In alkaline conditions, proteins can reduce Cu^{2+}, which is called Biuret-reaction. Cu^{+} is detected by bicinchoninic acid that is chelated by cuprous ions forming a complex with high spectro-photometric absorbance at 562 nm. The assay was performed according to the manufacturer's instructions.

BCA Protein Assay Kit: Pierce, #23225

6.3.2 Bradford assay

The Bradford assay is a fast and based on the coomassie brilliant blue G-250 dye that binds arginine, tryptophan, tyrosine, histidine and phenylalanine residues. The bound dye gives an absorbance maximum at 595nm. The assay was performed according to the instructions of the manufacturer.

Bradford Reagent: Sigma, #B6916

6.4 SDS-polyacrylamide-gelelectrophoresis (SDS-PAGE)

SDS-PAGE is a commonly used method to separate proteins under denaturizing conditions. Proteins become negatively charged when they are in the SDS containing gel and can be separated by their electrical charge according to the molecular size and shape. Proteins were boiled in the presence of SDS before loading into the gel and when indicated, their disulfide bonds were reduced by addition of 2-mercaptoethanol or di-thiothreitol (DTT). The gel was prepared with two differently buffered layers; the stacking gel and the resolving gel. These two layers also have a different acrylamide

concentration. The stacking gel serves as a concentration layer for proteins, whereas the resolving gel separates proteins according to their molecular size and shape. Proteins were separated in a mini-gel system (73 x 83 x 1.5 mm) using a Mini Protean III System (BioRad, #165-3301). After the polymerization of the gel and assembly of electrophoresis system, samples were mixed with 4 x SDS sample-buffer (4 x SDS-SB), boiled for 5 minutes at 95°C and subsequently kept on ice. After a brief centrifuging the samples were loaded on the stacking gel. The electrophoresis module was filled with 1 x SDS running buffer and the electrophoresis was carried out at 100V (for stacking gel) to 120V (for resolving gel).

separating gel (10ml)	**8%**	**10%**	**12%**	**15%**
H2O	4.6ml	4.0ml	3.3ml	2.3ml
30% ProtoGel	2.7ml	3.3ml	4.0ml	5.9ml
1.5M Tris-HCl pH 8.8	2.5ml	2.5ml	2.5ml	2.5ml
10%SDS	0.1ml	0.1ml	0.1ml	0.1ml
10% APS	0.1ml	0.1ml	0.1ml	0.1ml
TEMED	0.006ml	0.006ml	0.006ml	0.006ml

stacking gel (5ml)	**5%**
H2O	3.4ml
30% ProtoGel	0.83ml
1M Tris-HCl pH 6.8	0.63ml
10%SDS	0.04ml
10% APS	0.04ml
TEMED	0.004ml

N,N,N',N'-Tetramethylethylenediamine (TEMED), Serva #35925

ProtoGel (Ultra Pure), National Diagnostics, #EC-890

6.5 Western blotting and immunodetection

Western blotting is a method to detect and quantify proteins by using antibodies. It is based on separating the proteins on SDS-PAGE, transferring them onto a PVDF membrane and finally detecting them via immunodetection reagents.

After the SDS-PAGE (6.4), the stacking gel was discarded and the separating gel was soaked into transfer buffer. After the gel as well as the methanol-activated PVDF membrane was equilibrated in transfer buffer, transfer was started via assembly of a transfer sandwich.

Proteins were then transferred either overnight with 25V at 4°C or for 1.5 hours with 100V at 4°C. Then the transfer sandwich was disassembled, the membrane was stained with Ponceau S solution for 30 seconds to visualize the protein bands and then washed in H_2O. The membrane was then blocked for 30 minutes at RT in blocking buffer, the membrane was incubated with the primary antibody either overnight at 4°C or for 2 hours at RT, was washed 3 x 15 minutes with TBS-T and then the appropriate secondary antibody was added for 45 minutes at RT. After 3 x 15 minute washes with TBS-T, the membrane was subjected to a chemiluminescence-based detection kit (ECL kit).

Western Blotting transfer buffer (1l)

Tris-HCl	6g
Glycine	28.8g
Methanol	200ml

10x TBS (1l)

Tris-HCl	24.3g
NaCl	80g

TBS-T (1l)

Tween-20	1ml
10x TBS	100ml in H_2O

Blocking buffer

skim milk powder 5% in TBS-T

ECL kit: Millipore, Immobilon™ Western, #WBKLS0500

PVDF membrane: Millipore, Immobilon™ Transfer membranes, #IPVH00010

Ponceau S solution: Sigma, #P3504

6.6 Immunoprecipitation (IP)

Immunoprecipitation is a commonly used biochemical method to detect the interaction between two or more proteins. It works either by pulling down endogenous proteins with the help of a specific antibody coupled to a protein A or G sepharose or by pulling down tagged proteins with a specific antibody recognizing the particular tag. In both methods, cells were washed once with ice-cold PBS before being lysed in IP lysis buffer 10 minutes on ice. Cell lysates were collected via rubber cell scraper, sonicated for 2 x 10 seconds at level 4, centrifuged at 14000rpm for 5 minutes at 4°C and the protein concentration was determined by BCA protein assay (6.3.1).

6.6.1 Endogenous protein pull-down

For immunoprecipitation of endogenous proteins, rabbit serum containing the specific rabbit IgGs was incubated with the cell lysate for 30 minutes at 4°C (1µg antibody per IP) and then this mixture was incubated with 35µl (per sample) prewashed and equilibrated protein G sepharose beads for 2 hours at 4°C. Next, the beads were washed 1 x 800µl 0.05% Na deoxycholate in TBS and 3 x 800µl TBS, resuspended in 35µl 2x SDS sample buffer and boiled for 5min at 95°C.

Protein G sepharose: Fast Flow, Sigma, #3296

6.6.2 GFP pull-down for Western blotting

For immunoprecipitation of GFP-tagged proteins, µMACS GFP isolation kit was used. IP was performed according to manufacturer's instructions. The final eluates were loaded on a SDS gel (6.4) and Western blotting (6.5) was performed.

µMACS GFP isolation kit: Miltenyi Biotech, #130-091-125

6.6.3 GFP pull-down for Mass Spectrometry (MS)

The same kit as in 6.6.1 was used and cell lysis and IP were performed as described (Hubner and Mann, 2011). Briefly, cells were lysed with a buffer containing 150 mM NaCl, 50 mM Tris pH 7.5, 5% Glycerol, 1% IGEPAL-CA-630, 1 mM $MgCl_2$, and protease inhibitors. Lysates were incubated with 50 µl magnetic beads coupled to monoclonal mouse anti-GFP antibody (Miltenyi Biotec GmbH). After appropriate washes, proteins were pre-digested on column with trypsin, eluted from the column with DTT and trypsin and digested overnight. Peptides were purified on C_{18} StageTips before MS analysis.

Trypsin: Promega, #5113

C18 stage tips: Agilent technologies, #12145004

6.7 Liquid chromatography (LC)-MS/MS analysis

MS analysis was performed by Dr. Tamar Geiger from the Department of Signal Transduction of the Max Planck Institute for Biochemistry. Peptides were separated by reverse-phase chromatography coupled to LC-MS/MS analysis using an LTQ-Orbitrap Velos mass spectrometer (Thermo Fisher Scientific). Peptide separation was performed using an EASY-nanoLC system (Thermo Fisher Scientific) with a 180 min gradient from 5% to 35% buffer B (80% acetonitrile, 0.5% acetic acid). In the MS method full scans

were acquired in the Orbitrap with a resolution of 60,000. The top 10 most intense ions were fragmented by CID, and MS/MS spectra were acquired in the LTQ.

6.7.1 Data analysis

Data analysis was also performed by Dr. Tamar Geiger from the Department of Signal Transduction of the Max Planck Institute for Biochemistry. The raw files from the MS were processed with the MaxQuant software version 1.0.13.13 (Cox and Mann, 2008). Data were searched against the forward and decoy database (pi.MOUSE.v3.62.decoy.fasta) using the Mascot search engine. Fixed modifications were carbamidomethylated cysteins and variable modifications were oxidation of methionine, and N-terminal acetylation. Maximum false discovery rates (FDR) were set to 0.01 both on peptide and protein levels. Proteins were quantified using the label-free algorithm in MaxQuant.

To extract significant binders we performed a two-sample t-test between triplicates, with 0.1 FDR.

7. Molecular biological methods

7.1 Material molecular biological methods

Autoclave: KSG, KSG-112

Centrifuge: Eppendorf, 5417C

Centrifuge: Beckman Coulter, Avanti J-25

Centrifuge rotor: Beckman Coulter J 14 / J 25.50

Microwave: Daewoo, KOR 63D7

Thermocycler: Biometra T3

Thermomixer: Eppendorf 5350

7.2 Phenol/chloroform extraction of tail DNA

To isolate mouse genomic DNA, the tail tip was clipped, placed in a microcentrifuge tube and subjected to an overnight lysis reaction in 250 µl lysis buffer containing proteinase K at 55°C on a shaker. The next day, 250µl Phenol/Chloroform (1:1) was added to this mixture, briefly mixed, centrifuged for 5 minutes at 15000xg and then the upper phase was carefully removed and mixed with 1 ml of 100% ethanol and 20 µl of 3

M sodium acetate and centrifuged (2 minutes at 15000xg). The pellet was washed once with 200µl of 70% ethanol, air-dried and dissolved in 50 ddH_2O. It was further used for genotyping PCRs.

DNA lysis buffer

NaCl	20mM
Tris-HCl pH 7.6	100mM
EDTA	5mM
SDS	0.2%
proteinase K	100µg/ml

Phenol / Chloroform / Isoamyl Alcohol (25 : 24 : 1): Calbiochem, #KP31757

7.3 Bacteriological tools

Escherichia coli (E.coli) XL-1 Blue strain was cultured in lysogeny broth (LB) medium. Medium was prepared and autoclaved for 20min at 120°C. Antibiotics were added after the solutions were cooled to RT. LB plates were poured into 100mm Petri dishes and stored at 4°C.

LB medium

NaCl	10g
Trypton	10g
Yeast extract	5g

filled up to 1000ml with H2O, autoclaved and stored at 4°C

LB plates

LB medium	1000ml
Agar	15g

autoclaved, poured into 100mm Petri dishes, stored at 4°C

Antibiotics

Ampicillin	50µg/ml
Kanamycin	25µg/ml
Tetracyclin	12.5µg/ml

7.3.1 Preparation of competent E.coli

XL-1 blue strain of *E.coli* was grown shaking at 180rpm overnight in Tetracyclin containing 10ml LB at 37°C. The next day, 2 ml of the overnight culture was inoculated

into 100ml of Tetracyclin containing LB and shaken until the desired optical density of 0.5 at 550nm was obtained.

The bacterial culture was chilled on ice for 10 minutes, centrifuged for 15 minutes at 4°C at 1000xg and the pellet was resuspended in 10ml TSS and 2.9ml glycerol (87%). The competent cells were aliquoted in 200µl volumes in microcentrifuge tubes, snap-frozen in liquid nitrogenand then stored at -80°C.

TSS (500ml)

polyethylenglycol	50g
Tryptone	5g
Yeast extract	2.5g
NaCl	2.5g
DMSO	25ml
1M MgCl2	25ml

filtered and stored at 4°C

7.3.2 Transformation of competent E.coli

For each transformation, 100µl of competent cells were thawed on ice, incubated with plasmid DNA on ice for 30 minutes, heat shocked at 42°C for 90 seconds and then incubated on ice for 2 minutes. Afterwards, 750µl prewarmed LB medium (no antibiotics) was added and cells were shaken for 1 hour at 37°C at 200rpm. After incubation, cells were pelleted by 30 second centrifugation at 4000xg, resuspended in 100µl LB medium and innoculated on agar plates containing the appropriate antibiotic. Cells were grown overnight at 37°C. Colonies appeared after 12 hours.

7.4 Preparation of plasmid DNA from bacterial cultures

Bacterial colonies were inoculated into 5ml LB medium (with the appropriate antibiotics) overnight at 37°C. Plasmid DNA was isolated from 1ml of this culture by using the Qiagen Plasmid Mini Kit.

When large amounts of plasmid DNA were needed, the same method was applied but with a larger amount of starting culture. In this case, Qiagen Plasmid Maxi Kit was used according to manufacturer's instructions. Plasmid DNA was stored at -20°C.

Qiagen Plasmid Mini Kit: Qiagen, #12125

Qiagen Plasmid Maxi Kit: Qiagen #12162

7.5 Molecular cloning of DNA

To generate DNA constructs, restriction enzymes are used. They bind palindromic DNA recognition sequences and cut them by hydrolyzing the two phosphodiester bonds. The end product of this reaction is a cleaved DNA with a phosphate group in 5' prime and a hydroxyl group in 3' prime. This allows the ligation of two DNA fragments that are cleaved by the same enzyme.

7.5.1 Restriction enzyme digestion of DNA

All restriction enzymes were purchased form New England Biolabs (NEB). Manufacturer's instructions were followed. In principle, the digestion reactions were set in a total volume of 20 µl containing 10 U enzyme per 1 µg DNA dissolved in ddH_2O.

7.5.2 Dephosphorylation of 5'-ends of plasmid DNA

Restriction enzyme digestions expose a 5'-prime phosphate group in the digested plasmid that forms an ester bond with the 3'- hydroxyl group of the same plasmid during ligation reactions. To prevent the self-ligation of digested plasmids, alkaline phosphatases are used to remove the 5'-phosphate group. We used shrimp alkaline phosphatase (sAP). 5µg digested plasmid DNA was treated with 5 U sAP in sAP buffer in a total volume of 30 µl for 60 minutes at 37°C. Afterwards, sAP was heat inactivated for 15 min at 65°C.

Shrimp Alkaline Phosphatase: Roche, #11 758 250 001

7.5.3 Ligation of DNA fragments

In a ligation reaction, a phosphodiester bond is formed between a 3'-hydroxyl group and a 5'-phosphate group. To promote the formation of this bond, the ligation reaction was set as below.

DNA ligation

DNA vector	0.5-1µg (dephosphorylated)
DNA insert	5µg PCR product or digested DNA
ATP (10mM)	1.5µl
Fast link ligase buffer	1.5µl
Fast link ligase	1µl

filled up to 15µl with H2O, incubated for 45 minutes at RT, then heat-inactivated for 10min at 70°C.

7.5.4 Sequencing of DNA

To sequence the cloned DNA, 500 ng DNA was used. It was mixed with 2 µl Big Dye terminator mixture and 1 µl of an appropriate sequencing primer (10 pmol) in a total volume of 10 µl. Then, a PCR reaction (7.6) was performed. The PCR product sequenced at the core-facility of the Max Planck Institute for Biochemistry. The sequence data was processed with the Chromas Lite 2.01 software (www.technelysium.com.au).

7.6 Polymerase chain reaction (PCR)

PCR is a commonly used method to amplify DNA fragments. Typically, a PCR reaction consists of a DNA template, two primers, dNTPs and a DNA polymerase. In a PCR reaction, firstly the DNA is denatured at 95°C, and then the primers are annealed to the DNA template at 55°C – 68°C, and finally the reaction terminates with DNA synthesis at 68°C – 72°C.

7.6.1 Oligonucleotides (primers)

All oligonucleotides were purchased from Metabion International (Martinsried, Germany). siRNA oligonucleotides were purchased from SIGMA.

NAME	5'-3' Sequence	Application
Cre for	AAC ATG CTT CAT CGT CGG	Genotyping
Cre rev	TTC GGA TCA TCA GCT ACA CC	Genotyping
ILK for	GTC TTG CAA ACC CGT CTC TGC G	Genotyping
ILK rev	CAG AGG TGT CAG TGC TGG GAT G	Genotyping
ILK rev (KO)	CCA GGG TGA CGC CTG ACA AAT G	Genotyping
PINCH-1 for	CTA GGC TGG TAA TGC AGG CC	Genotyping
PINCH-1 rev	CCT GCC AAT GAT GAA TTC AC	Genotyping
PINCH-1 rev (KO)	CGC AGT TGG CAC AGT TGA AG	Genotyping
XhoI EPLIN for	TCGA CTC GAG ATG GAA AAC TGT CTG	Cloning EPLIN in pCHERRY and pEGFP (N1)
HindIII EPLIN rev	AGCT AAG CTT TGA TTC TTC ATC CTC GTC	Cloning EPLIN in pCHERRY and pEGFP (N1)
XhoI Bcl-2 for	TCGA CTC GAG ATG GCG CAA GCC GGG AG	Cloning Bcl-2 in pEGFP (N1)
HindIII Bcl-2 rev	AGCT AAG CTT TGA CTT GTG GCC CAG GTA TGC	Cloning Bcl-2 in pEGFP (N1)
EPLIN siRNA1	GAAAUAGGUGCGGGUCAUU	Transfection
EPLIN siRNA2	CUGUAAGCCUCACUUCAAU	Transfection

All PINCH-2 constructs including pCLMFG-PINCH1 and pEGFP-PINCH1 (C1) were cloned as previously described (Braun et al., 2003; Stanchi et al., 2005; Stanchi et al., 2009).

7.6.2 PCR reactions

The following PCR reactions were performed in this study: 1) genotyping PCR using tail DNA and a standard *Taq* polymerase (Metabion) 2) cloning PCR using purified plasmid DNA (7.7.1) and high fidelity polymerase with a proof reading activity (Roche).

Standard *Taq* polymerase: Metabion, #mi-E8001

High Fidelity *Taq* polymerase: Roche, #3300242001

Genotyping PCR (1)

Isolated tail DNA	1 µl
Primer 1 (100 pM)	0.5 µl
Primer 2 (100 pM)	0.5 µl
dNTPs (10 mM)	0.5 µl
10 x PCR buffer	2 µl
Taq polymerase	0.5 µl

Filled up to 20 µl with ddH_2O and subjected to PCR

Cloning PCR (2)

Plasmid DNA (~ 200 ng)	1 µl
Primer 1 (100 pM)	1 µl
Primer 2 (100 pM)	1 µl
dNTPs (10 mM)	1 µl
$MgCl_2$ (50 mM)	1.5 µl
10 x PCR buffer	5 µl
High fidelity polymerase	1 µl

Filled up to 50 µl with ddH_2O and subjected to PCR

7.6.3 PCR programs

Following PCR programmes were used in this study:

Genotyping PINCH-1 and Cre-PCR

step.....time(sec) ....temp(°C)
1.....300 95
2.....30 95
3.....30 63
4.....60 72

Genotyping-ILK-PCR

step..... time(sec) ....temp(°C)
1.....300 95
2.....30 95
3.....30 66
4.....60 72

5.....30 95	5.....30 95
6.....30 55	6.....30 58
7.....60 72	7.....60 72
8.....300 72	8.....300 72
9..... ∞.....4	9.....∞..... 4

PCR reactions were performed for 35 cycles (step 5-7). A touch down program was applied from 63°C-55°C (Cre and PINCH-1) and 66°C-58°C (ILK) in 9 cycles by sequential reduction of the annealing temperature (-1°C / cycle) (step2-4).

Cloning PCR long

step..... time(sec) ....temp(°C)

1.....300 95

2.....30 95

3.....30 66

4.....120 72

5.....30 95

6.....30 58

7.....120 72

8.....300 72

9.....∞..... 4

PCR reactions were performed for 35 cycles (step5-7). A touch down program was applied from 66°C-58°C in 9 cycles by sequential reduction of the annealing temperature (-1°C / cycle) (step2-4).

7.7 Agarose gel electrophoresis

Agarose gel electrophoresis is a widely used method for separation and purification of DNA fragments. To prepare agarose gels an appropriate amount of Ultra pure Agarose was dissolved in 150 ml 1 x TAE buffer, boiled in a microwave, supplemented with 10 µl of ethidium bromide solution after boiling and then poured into a previously-prepared casting tray and allowed to set at RT. When the gel was ready to be loaded it was transferred into an electrophoresis chamber. Before loading onto the agarose gel, the DNA sample was mixed with 6 x DNA loading buffer. Samples were subjected to gel electrophoresis in 1 x TAE buffer at 70 – 120 V at RT. A 1 kb DNA ladder was used as a

size marker. After completing the electrophoresis, DNA samples were visualized under the 366 nm UV-light.

TAE buffer (50x)

Tris-base	242g
EDTA	37.2g
Glacial acetic acid	57.1ml

filled up to 1000ml with H2O

Agarose: Invitrogen, #15510-027

Ethidiumbromid: Roth #2218.1

Agarose: Invitrogen, UltraPureTM Agarose, #15510-027

Ethidium bromide: Roth, #2218.1

1 kb Ladder: Invitrogen, #15615-016

7.7.1 Gel extraction of DNA from agarose gels

DNA bands were excised and extracted from the agarose gels for cloning purposes. The excised DNA band was used to extract the DNA from the agarose gel using a Qiagen Gel Extraction Kit according to the manufacturer's instructions.

Qiagen Gel Extraction Kit, Qiagen, #20021

7.8 Generation of Bcl-2 expression constructs

A Bcl-2 cDNA with HindIII/XhoI restriction sites was amplified from wild type keratinocyte cDNA (kindly provided by Dr Katrin Lorenz-Baath) with the appropriate primers (7.6.1) and inserted in pEGFP (N1) vector (Clontech).

7.9 Generation of EPLIN expression constructs

An EPLINα cDNA with HindIII/XhoI restriction sites was amplified from wild type keratinocyte cDNA (kindly provided by Dr Katrin Lorenz-Baath) with the appropriate primers (7.6.1) and inserted in both pEGFP (N1) vector (Clontech) and pCHERRY (N1) vector. pCHERRY (N1) vector was kindly provided by R.Y. Tsien.

7.10 Plasmids and cDNAs

cDNA	backbone	provided by	reference
RSU-1	pEGFP (N1)	Dr. M. Lou Cutler	(Dougherty et al., 2005b)
PINCH-1	pEGFP (C1)	Dr. R. Fässler	
PINCH-1	pCLMFG	Dr. R. Fässler	

Name	approach	resistance	source
pCLMFG	expression	ampicillin	Dr.Pfeifer (Bonn, Germany)
pEGFP	expression	kanamycine	Clontech
pCherry	expression	kanamycine	Dr. Tsien

7.11 Preparation of retrovirus

All retrovirus preparations were performed in collaboration with Prof. Dr. Alexander Pfeifer (University of Bonn, Germany) and conducted by Hildegard Reiter. To produce VSV-G pseudotyped retroviral vectors, HEK293T were transiently transfected with the pCLMFG vector (7.10), packaging plasmids (encoding HIV *gag*, *pol* and *rev*) and a plasmid encoding for the envelope of the vesicular stomatitis virus G by a calcium phosphate method. The supernatant containing the VSV-G pseudotyped retrovirus was collected, centrifuged and directly used for infection of keratinocytes.

7.12 Lipofectamine transfection of keratinocytes and endoderm cells

Prior to transfection, both cell types were seeded on 6-well plates and grown overnight. When they reached 50-60% confluency, they were transfected with 1 µg (per well) indicated plasmid DNAs by using Lipofectamine™ transfection reagent according to manufacturer's instructions.

Lipofectamine™ transfection reagent: Invitrogen, #11668-019

8. Microscopy

8.1 Confocal microscopy

Confocal images were taken using a confocal microscope (Leica, DMIRE2) with immersion oil objectives HCX PL APO 100 x/1.4-0.70, HCX PL APO 63 x/1.4-0.60 and a HC PL 40 x/0.70 dry objective. Images were acquired, and processed by Leica Confocal Software (version 2.5, Build 1227).

8.2 Light microscopy of living cells

Images of living cells were taken using an inverted light microscope (Zeiss, Axiovert 40 CFL) equipped with a A – PLAN 10 x / 0.25 objective and a LCD camera (Prosilica).

8.3 Light microscopy of histological sections

Images of histological sections were taken by a light microscope (Zeiss, Axioskop) equipped with a 5 x / 0.15 and 10 x / 0.30 objective (Zeiss, Plan-NEOFLUAR) and a LCD camera (Leica, DCC500).

8.4 Total internal reflection fluorescence (TIRF) microscopy

TIRF images were taken with an Axiovert 200M inverted microscope (Zeiss) with a 100× oil objective and a CoolSnap HQ CCD camera (Photometrics). Acquisition was controlled by Metamorph Software (Molecular Devices).

Results

1. Analysis of PINCH-1 function in cell survival

PINCH-1 depletion in mice leads to embryonic lethality shortly after implantation (Li et al., 2005). To elucidate the role of PINCH-1 in early embryonic development, ES cells were kept in suspension to generate EBs. EBs are multicellular three-dimensional structures that closely mimic the peri-implantation stage of development. The outer layer of the ES cell aggregates differentiates into primitive endoderm (PrE) cells that secrete the initial embryonic BM components. Subsequently, the cells adjacent to BM differentiate into columnar epithelium termed epiblast. The ES cells that have no contact with BM undergo apoptosis and form the central cavity (Montanez et al., 2007).

PINCH-1-deficient embryos display an abnormal epiblast polarity, impaired cavitation, detachment of PrE and epiblast cells from the BM, and severe apoptosis of the endoderm cells (Li et al., 2005; Liang et al., 2005). PINCH-1 was also identified as an important survival factor in ES cell-derived EBs (Li et al., 2005). Besides, PINCH-1 was also reported to be a survival factor for tumor cells by enhancing the activities of the pro-survival proteins ERK1/2 and AKT (Chen et al., 2008; Eke et al., 2010; Sandfort et al., 2010). However, it remains elusive how PINCH-1 regulates cell survival in PrE. Therefore, we aimed at understanding the role of PINCH-1 in PrE cell survival.

1.1 PINCH-1 is dispensible for endoderm differentiation

Integrin-mediated signaling is important for the differentiation of PrE (Liu et al., 2009). It is not known whether PINCH-1 acts downstream of integrins to regulate PrE differentiation. To elucidate role of PINCH-1 in regulation of PrE differentiation we generated EBs from wild-type (wt) and PINCH-1-/- ES cells to investigate endoderm differentiation (Montanez et al., 2007). After 7 days wt (*PINCH-1*$^{+/+}$) EBs consisted of an outer layer of endoderm cells, an inner layer of columnar pseudostratified epiblast cells, a thin and continuous BM between epiblast and endoderm, and a central cavity (Fig. 1A). Immunostaining with antibodies against endoderm markers revealed that PrE cells expressed α-fetoprotein (AFP) and disabled homolog 2 (Dab2) in their cytoplasm and the endoderm-specific transcription factor GATA4 in their nuclei (Fig. 1A and data not shown). In line with previous observations, PINCH-1-/- EBs displayed abnormal epiblast

polarity, a discontinuous BM, detached PrE cells and impaired cavitation (Fig. 1A). In addition, DAPI staining showed condensed and fragmented nuclei in PrE cells of all PINCH-1-/- EBs analyzed (Fig. 1B). However, we found no apparent defects in the expression and localization of PrE markers such as AFP, GATA-4 and Dab-2 in PINCH-1-/- endoderm cells (Fig. 1A and data not shown).

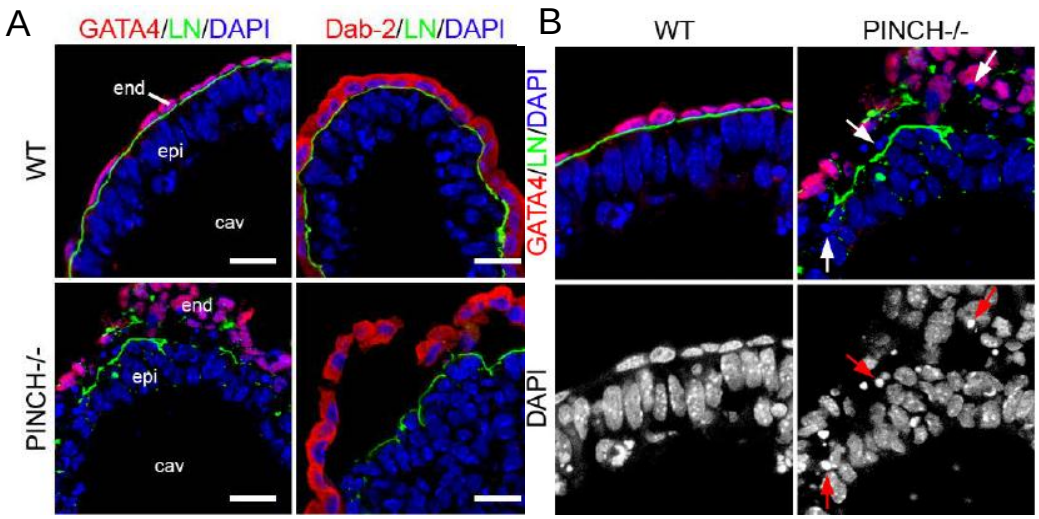

Figure 1: PINCH-1 is dispensible for endoderm differentiation, but necessary for cell survival.

(A) Immunostaining of endoderm markers GATA4 and disabled-2 (Dab-2) of 7 day old wt and PINCH-1-/- EBs. BM was visualized with LN and nucleus with DAPI. Scale bar: 30 µm. (B) PINCH-/- endoderm cells showed condensed and fragmented nuclei (arrows).

It has previously been reported that expression of GATA4 is sufficient for ES cells to differentiate into PrE (Fujikura et al., 2002). We expressed GATA4 in wt and PINCH-1-/- ES cells (Fig. 2A) and monitored the expression of the PrE markers AFP and variant Hepatocyte Nuclear Factor 1 (vHNF1) by RT-PCR. We found similar levels in wt and PINCH-1-/- cells (Fig. 2B). Collectively, these results indicate that PINCH-1 is dispensable for PrE differentiation, but required for its survival.

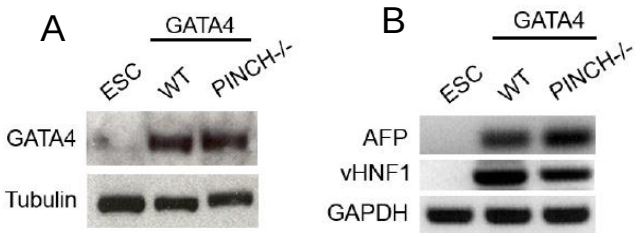

Figure 2: GATA4 expression is sufficient to induce PrE differentiation.

(A) Western blot of the protein level of GATA4 in protein lysates of wt ES cells and GATA4 vector transfected cells. Tubulin serves as a loading control. (B) RT-PCR of the endoderm marker α-fetoprotein (AFP). GAPDH serves as a loading control.

1.2 Loss of PINCH-1 triggers intrinsic apoptosis pathway of PrE cells

The condensed and fragmented nuclei suggests a role for PINCH-1 in PrE cell survival. To test this, we analyzed EBs for apoptosis by TUNEL assay and anti-active caspase-3 immuno-staining. In wt EBs, apoptotic cells were mainly observed at the center of EBs where cells are eliminated to create the pro-amniotic-like cavity and occasionally within the epiblast and very rarely in PrE cells (Fig. 2A). In contrast, PrE cells were undergoing apotosis in PINCH-1-/- EBs (Fig. 2A). Quantification of TUNEL-positive PrE cells showed a 3-fold increase of apoptotic cells in PINCH-1-/- EBs in comparison to wt EBs (Fig. 2B). These results suggest that PINCH-1 depletion leads to caspase-3-dependent apoptosis.

Next we sought the mechanism by which PINCH-1 regulates apoptosis. It was previously reported that the unligated integrins of adherent cells can recruit caspase-8 to the cell membrane that further triggers apoptosis (Fujikura et al., 2002). To test this, we immunostained wt and PINCH-1-/- EBs with an active caspase-8 antibody and demonstrated that both wt and PINCH-1-/- EBs have activated caspase-8 at the central cavity and very rarely at the epiblast or PrE cells (Fig. 3C). To elucidate whether mitochondrial apoptosis pathway is involved in the apoptosis of PINCH-1-/- PrE cells, we immunostained wt and PINCH-1-/- EBs using the 6A7 Bax antibody that recognizes activated Bax. PINCH-1-/- PrE cells displayed a strong and punctate active Bax staining in the cytoplasm (Fig. 2C), which strongly co-localized with the mitochondrial marker Mitotracker (Fig. 2D), suggesting that mitochondrial dysfunction is involved in apoptosis. Interestingly, almost all active Bax-positive PrE cells were still attached to the BM

indicating that apoptosis occurs before cell detachment (Fig. 2C).

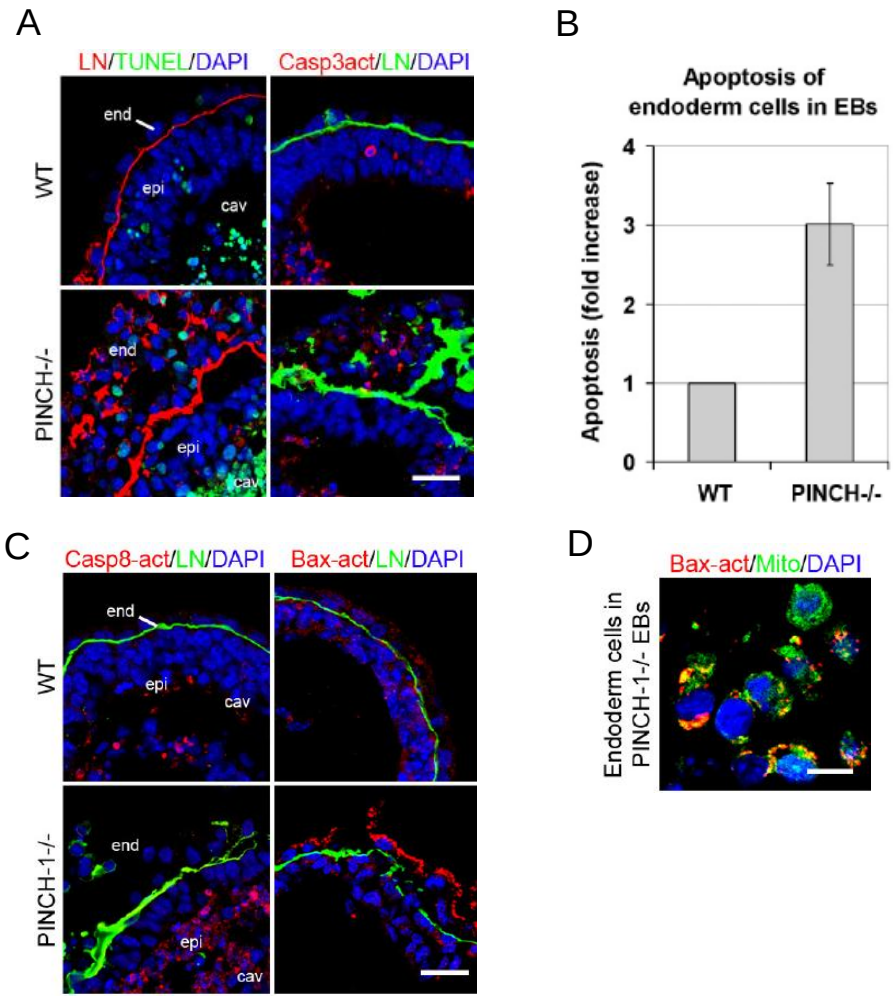

Figure 3: Loss of PINCH-1 leads to the activation of intrinsic apoptotic pathway.

(A) Apoptosis assessed in wt and PINCH-1-/- EBs by TUNEL assay and cleaved-caspase 3 immunostaining. BM was visualized with LN and nucleus with DAPI. Scale bar: 30 µm. (B) Quantification of TUNEL-positive endoderm cells in EBs. Data is presented as mean of number of positive cells/total from PINCH-/- endoderm cells and compared with that of the wt cells (normalized to 1). (C) Immunostaining of active caspase-8 and active-Bax in wt and PINCH-1-/- EBs. BM was visualized with LN and nucleus with DAPI. Scale bar: 30 µm. (D) Colocalization of active-Bax with a mitochondrial marker (Mitotracker) in PINCH-/- endoderm cells. Scale bar: 10 µm.

1.3 Signaling pathways involved in increased apoptosis of endoderm cells

To study which signaling pathways are involved in the regulation of apoptosis in PINCH-1-/- PrE cells, we tested several pathways that were previously shown to be important in cell survival regulation.

1.3.1 PINCH-1 deletion leads to increased JNK activation

PINCH-1 blocks Bax-dependent apoptosis of tumor cells via regulating Bim and ERK1/2 activity (Chen et al., 2008). Furthermore, it was shown that PINCH-1 protects tumor cells from apoptosis through phosphorylation and activation of AKT (Eke et al., 2010). To test whether PINCH-1 also regulates phosphorylation of ERK1/2 and AKT in PrE cells, we measured their phosphorylation levels in lysates of wt and PINCH-1-/- PrE cells cultured on FN. PINCH-1-/- endoderm cells showed similar phosphorylation levels of ERK1/2 and AKT-Ser473 as wt cells, excluding a role for these two signaling molecules in the regulation of Bax levels (Fig. 4A and 4B). To test whether Bim is involved in apoptosis in PINCH-1-/- PrE cells, we checked total and phosphorylated Bim levels with a specific antibody that gives rise to a mobility shift when Bim is phosphorylated. Our results demonstrated that total and phospho-Bim levels were unaltered (Figure 4A). Collectively, these results rule out a role for ERK1/2, AKT and Bim in the regulation of apoptosis in PINCH-1-/- PrE cells.

JNK signaling is important for embryo development. A prolonged activation of JNK can also induce intrinsic apoptotic pathway (Ip and Davis, 1998). To understand whether PINCH-1 loss affects JNK signaling, we checked phosphorylation levels in cell lysates of wt and PINCH-1-/- PrE cells. The phosphorylation levels of JNK in PINCH-1-/- cells remained high in comparison to control cells (Fig. 4A).

To test whether increased JNK activity is responsible for higher active Bax levels, we applied JNK inhibitor (SP600125) on the PINCH-1-/- PrE cells. As anticipated, DMSO (vehicle)-treated cells had high active JNK levels, whereas inhibitor-treated PINCH-1-/- cells displayed decreased activeJNK levels upon inhibition. However, inhibition of JNK phosphorylation did not alter active Bax levels, indicating that blocking JNK signaling is not affecting Bax activity in PINCH-1-/- PrE cells (Fig. 4C).

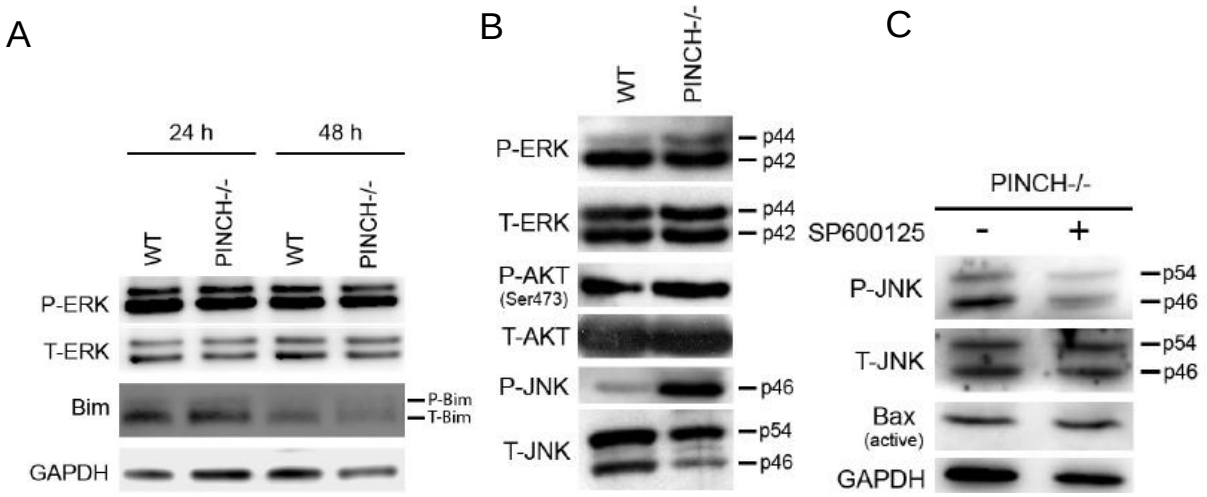

Figure 4: Bim/ERK and AKT pathways are not but JNK pathway is altered upon PINCH-1 loss

(A)Western blot of the protein levels of total and phospho-ERK and Bim in protein lysates of endoderm cells collected from wt and PINCH-1-/- EBs and cultured on FN for 24 and 48 hours. GAPDH serves as a loading control. (B) Western blot of the proteins levels of phospho-ERK, phospho-AKT and phospho-JNK in protein lysates of endoderm cells collected from wt and PINCH-1-/- EBs and cultured on FN for 48 hours. ERK, AKT and JNK total protein levels serves as a loading control. (C) Western blot of the protein levels of total-JNK, phospho-JNK and (active) Bax in protein lysates of endoderm cells collected from PINCH-1-/- EBs, cultured on FN and treated with JNK-inhibitor (SP600125). JNK total protein levels and GAPDH serve as a loading control.

1.3.3 PINCH-1-deficient PrE cells fail to spread on ECM proteins and have decreased Bcl-2 levels

Integrins have been shown to be important for cell survival (Lee and Ruoslahti, 2005). We observed that neither Bim/ ERK pathway nor JNK pathway is responsible for increased active Bax levels in PINCH-1-/- PrE cells. Bax activity can be decreased by Bcl-2 which can be regulated by FN-induced α5β1 integrin signaling. Therefore, we tested integrin-mediated cell signaling. To this end, we isolated PrE cells from wt and PINCH-1-/- EBs (Montanez et al., 2007) and cultured them on fibronectin (FN) and LN-111. After plating, wt endoderm cells spread on FN and LN-111 and formed focal adhesions (FAs) and actin stress fibers, as revealed by phalloidin staining(Fig. 5A). In contrast, PINCH-1-/- PrE cells failed to spread on both substrates and developed very few FAs and stress fibers (Fig. 5A and 5B). Moreover, PINCH-1-/- PrE cells developed multiple membrane blebs associated with apoptosis (Fig. 5B).

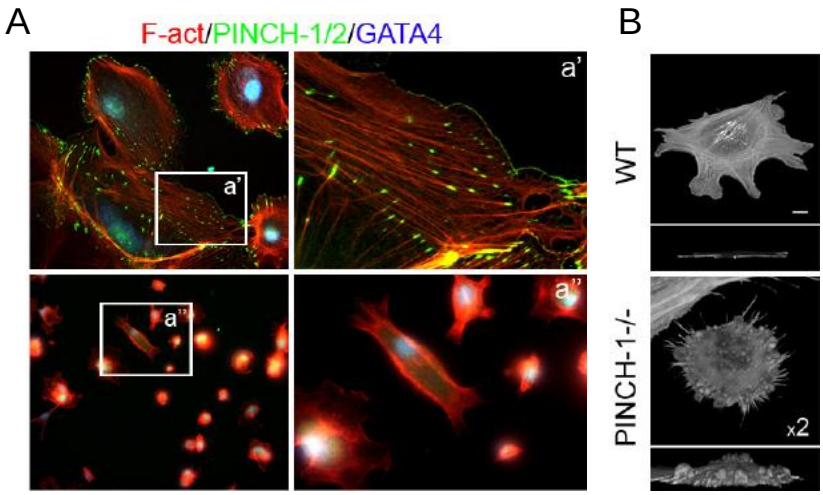

Figure 5: PINCH-1 loss leads to impaired cell spreading and formation of membrane blebs

(A) Phase contrast micrographs of wt (upper panel) and PINCH-1-/- (lower panel) PrE cells cultured on FN for 16 hours. The cells were fixed and immunostained for PINCH-1/2 and GATA4. F-actin was stained with phalloidin-TRITC. Scale bar: 80 µm. (B) 3D reconstruction of wt and PINCH-1-/- PrE cells cultured on FN for 16 hours.

In line with previous reports, we demonstrated that decreased integrin function is responsible for the reduced Bcl-2 levels.To further confirm this, we immunostained wt and PINCH-1-/- EBs with Bcl-2 antibody and observed that Bcl-2 levels were decreased upon PINCH-1 loss (Fig. 6A). We also compared Bcl-2 levels in wt and PINCH-1-/- EB and PrE cell lysates and found that Bcl-2 levels were decreased both in PINCH-1-/- EBs and FN-adhered PrE cells (Fig. 6B and 6C). To test whether reintroducing Bcl-2 in PINCH-1 deficient endoderm cells would rescue cell survival defect, we tried to overexpress a GFP-tagged Bcl-2 cDNA. Although overexpression was successful, our attempts to quantify these cells failed due to the very few number of transfected PrE cells on glass coverslips.

Together these results indicate that PINCH-1 supports integrin binding to FN and Bcl-2 expression in the PrE cells.

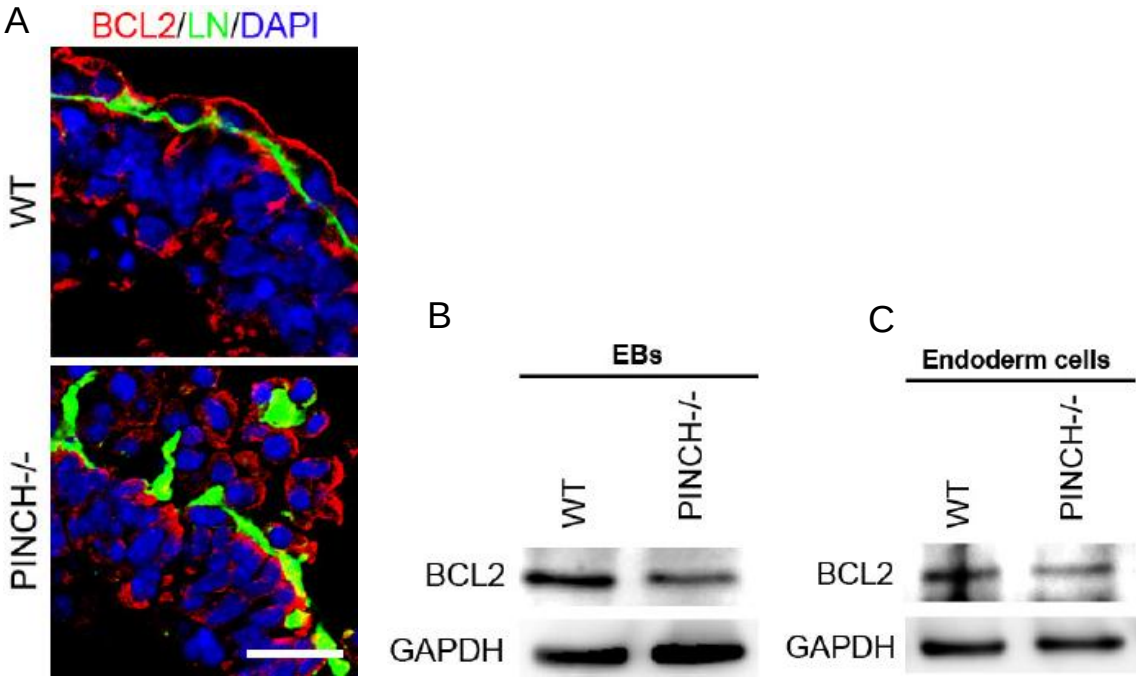

Figure 6: Impaired Bcl-2 signaling in PINCH-1-deficient EBs and endoderm cells

(A) Immunostaining of Bcl-2 in wt and PINCH-1-/- EBs. BM was visualized with LN and nucleus with DAPI. Scale bar: 30 µm. (B) Western blot analysis of the protein levels of Bcl-2 in protein lysates of EBs. (C) Western blot of the protein levels of Bcl-2 in protein lysates of endoderm cells collected from wt and PINCH-/- EBs. GAPDH serves as a loading control.

1.3.4 Loss of PINCH-1 leads to reduced levels of RSU-1

We demonstrated that JNK inhibition does not alter Bax levels (Fig. 4C). To determine whether the sustained JNK activity is involved in the apoptosis of PINCH-1-/- PrE cells, we treated PINCH-1-/- cells with the specific JNK inhibitor SP600125 or DMSO (vehicle) and assayed apoptosis after 48 hours. Blocking JNK reduced the apoptosis rate of PINCH-1-/- PrE cells by around 40-50%, (Fig. 7) indicating that JNK plays a prominent role in PINCH-1-dependent survival of endoderm cells.

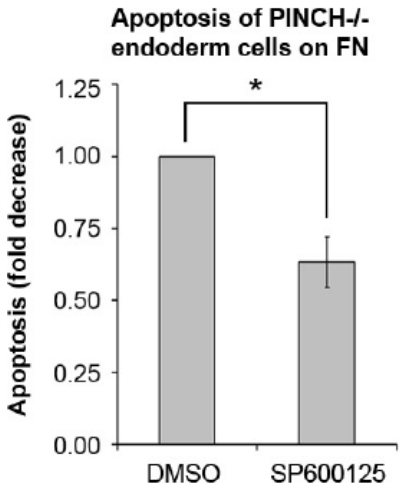

Figure 7: JNK inhibiton partially recues apoptosis of PINCH-1-/- endoderm cells

Quantification of the percentage of TUNEL-positive cells/total in PINCH-/- endoderm cells cultured on FN and treated with the JNK inhibitor SP600125 (10 μM) or DMSO (vehicle).

We next determined the mechanism by which PINCH-1 regulates JNK signaling. PINCH-1 was shown to interact with and regulate the expression of RSU-1, which is a negative regulator of JNK signaling in flies (Kadrmas et al., 2004; Dougherty et al., 2008). To determine the subcellular distribution of RSU-1 during peri-implantation, we performed immunostaining of 7 day-old EBs using a specific antibody against RSU-1. Staining revealed that RSU-1 is highly expressed in PrE, where it partially colocalizes with LN, and absent in the epiblast (Fig. 8A). To determine whether RSU-1 colocalizes with PINCH-1 in PrE cells, we expressed GFP-tagged PINCH-1 cDNA in wt PrE cells and stained them with RSU-1 antibody, and found that PINCH-1 and RSU-1 colocalize at the FA (Fig. 8B). Interestingly, PINCH-1-/- PrE cells displayed a weak RSU-1 staining when compared to wt PrE cells (Fig. 8A). In line with these findings, WB analysis of PrE cells showed that the protein levels of RSU-1 were significantly reduced in PINCH-1-/- PrE cells in comparison to wt cells (Fig. 8C).

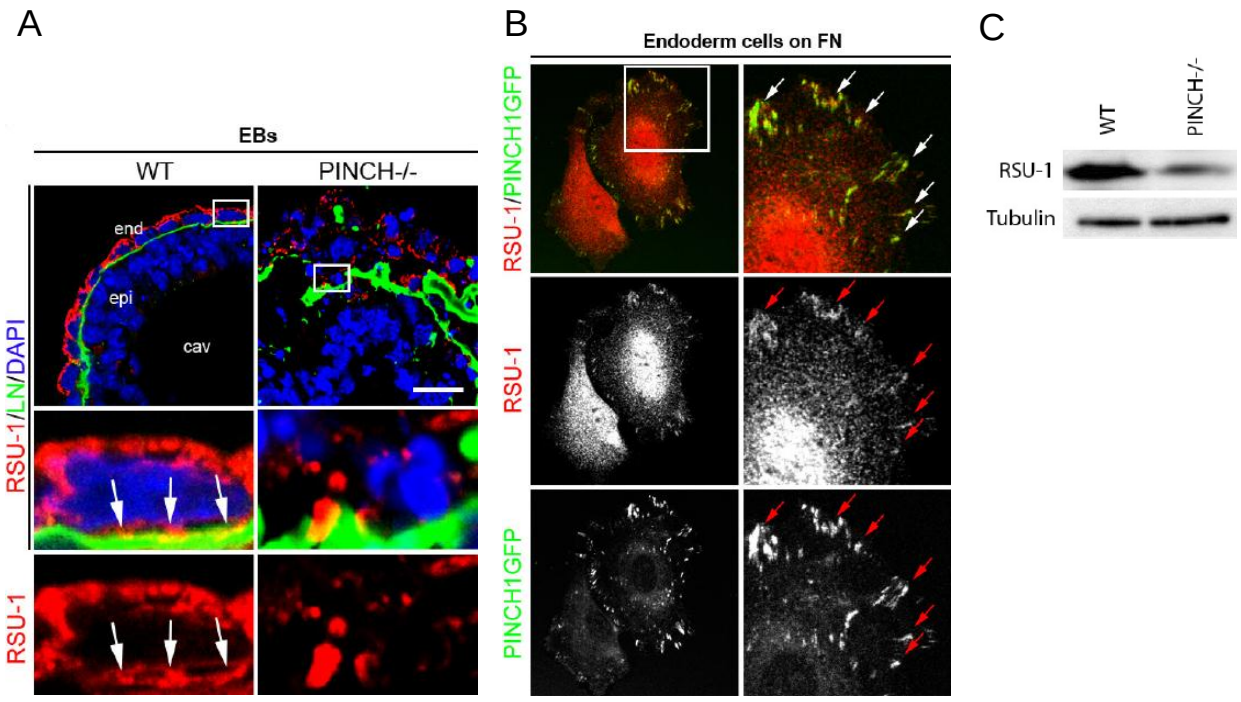

Figure 8: RSU-1 localizes to BM in EBs and to FAs in endoderm cells

(A) Immunostaining of RSU-1 in wt and PINCH-1-/- EBs. Scale bar: 30 µm. BM was visualized with LN and nucleus with DAPI. (C) Immunostaining of RSU-1 in endoderm cells transfected with GFP-tagged PINCH-1 cDNA (D) Western blot of the protein level of RSU-1 in protein lysates of endoderm cells collected from wt and PINCH-1-/- EBs and cultured on FN for 48 hours. Tubulin serves as a loading control.

Next, we overexpressed a GFP-tagged RSU-1 cDNA in PINCH-1-/- cells (Fig. 9A) and monitored JNK phosphorylation. We found that the overexpression of RSU-1 reduced the levels of phosphorylated JNK in PINCH-1-/- PrE cells to wt levels (Fig. 9B).

Together these results indicate that PINCH-1 stabilizes RSU-1 and in turn regulates JNK signaling in PrE cells.

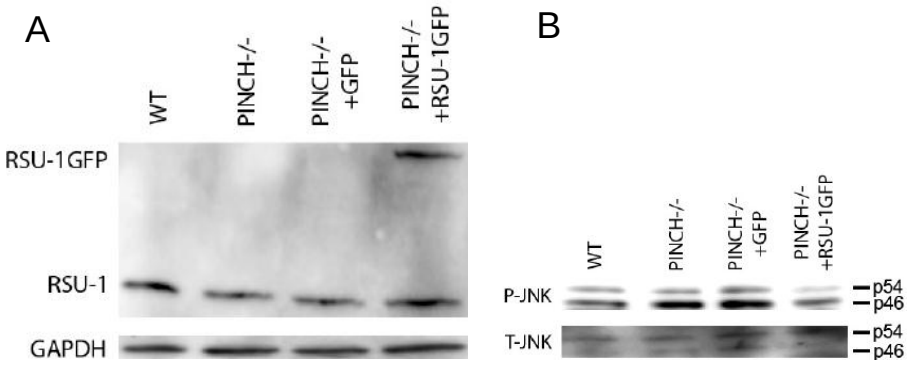

Figure 9: Overexpression of GFP-tagged RSU-1 reduces increased JNK levels

(A) Western blot of RSU-1 in protein lysates of wt, PINCH-/- cells, and PINCH-/- cells transfected either with GFP or with RSU-1GFP. GAPDH serves as a loading control. (B) Western blot of total-JNK and phospho-JNK in protein lysates of endoderm cells.

2. Analysis of PINCH-1 function in cell-cell adhesions of keratinocytes

Mice that lack PINCH-1 die early during pre-implantation stage of development due to abnormal epiblast polarity, impaired cavitation, detachment of endoderm and epiblast cells from the BM and severe apoptosis of the endoderm cells (Li et al., 2005; Liang et al., 2005). Interestingly, PINCH-1 ablation also leads to endoderm survival defects and cell-cell adhesion defects of endoderm and epiblast that are not observed in ILK and β1 integrin knock-out mice (Fassler and Meyer, 1995; Sakai et al., 2003). However PINCH-1 is not known to have a function in cell-cell adhesions thus far. To elucidate the role of PINCH-1 in cell-cell adhesions and to understand the underlying molecular mechanisms, we depleted PINCH-1 specifically in epidermal and HF keratinocytes.

2.1 Loss of PINCH-1 in epidermis leads to impaired cell-ECM and cell-cell adhesions

To study PINCH-1 in the epidermis, we crossed mice with a *loxP*-flanked *PINCH-1* gene (PINCH-1$^{fl/fl}$) (Li et al., 2005) and mice expressing the *Cre* recombinase under control of the *K5* promoter (*K5-Cre*) (Ramirez et al., 2004) to produce PINCH-1^{K5Cre} mice. PINCH-1$^{fl/wt}$ mice were used as a wild type control. Western blotting (WB) of epidermal lysates and immunostaining of back skin confirmed the absence of PINCH-1 in the PINCH-1^{K5Cre} epidermis (Fig. 10B). Since the antibody used in this study recognizes both PINCH-1 and PINCH-2, we conclude that PINCH levels are increased only in the keratinocytes of postnatal day 56 (p56) PINCH-1^{K5Cre} mice (Fig. 10A), which may suggest that PINCH-2 is de novo expressed in p56 PINCH-1^{K5Cre} keratinocytes. However, the mice used for our experiments were never older than p14. On the other hand, loss of PINCH-1 expression was accompanied by a reduction of ILK protein levels (Fig. 10A and 10B).

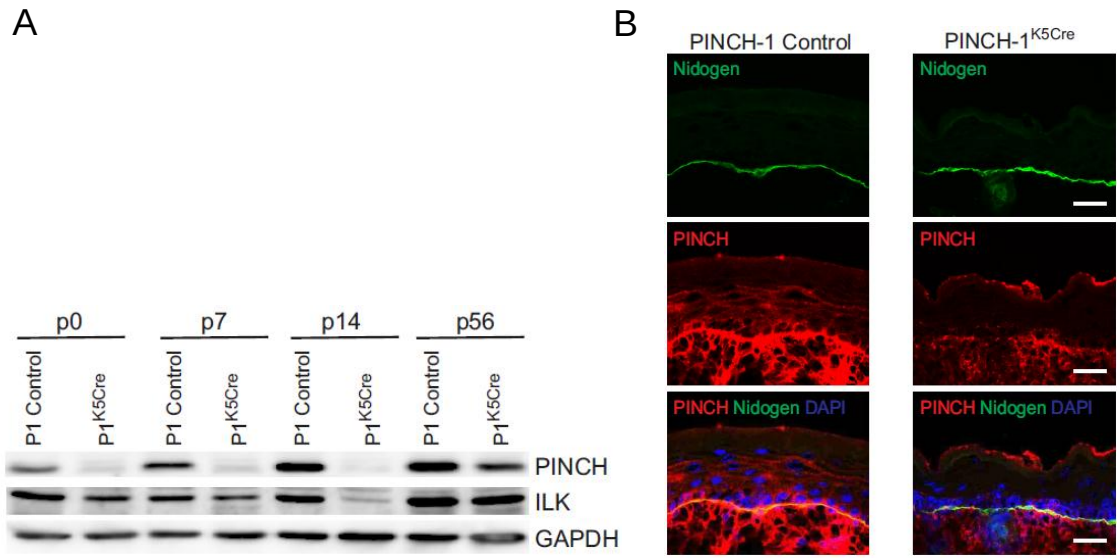

Figure 10: PINCH-1 is efficiently deleted in epidermis

(A) PINCH and ILK protein levels in epidermal lysates of PINCH-1 Co and PINCH-1^{K5CRE} mice at P0, P7, P14 and P56. (B) PINCH and Nidogen immunostaining on skin sections from P0 back skin. Note that PINCH is totally absent in the epidermis of PINCH-1^{K5Cre} mice. Scale bar: 50µm.

PINCH-1^{K5Cre} animals were normal at birth. While control mice developed a smooth hair coat, PINCH-1^{K5Cre} animals had a scattered hair coat with areas of alopecia by p14 (Fig. 11A). At 8 weeks of age, when the first postnatal hair cycle was completed in control mice, PINCH-1^{K5Cre} animals were almost bald. Skin histology revealed that IFE of PINCH-1^{K5Cre} mice was hyperthickened and contained blisters at the dermal-epidermal junctions (DEJ) (arrow in Fig. 11B), suggesting defects in the intact BM and had flattened keratinocytes and aberrant HFs at p14.

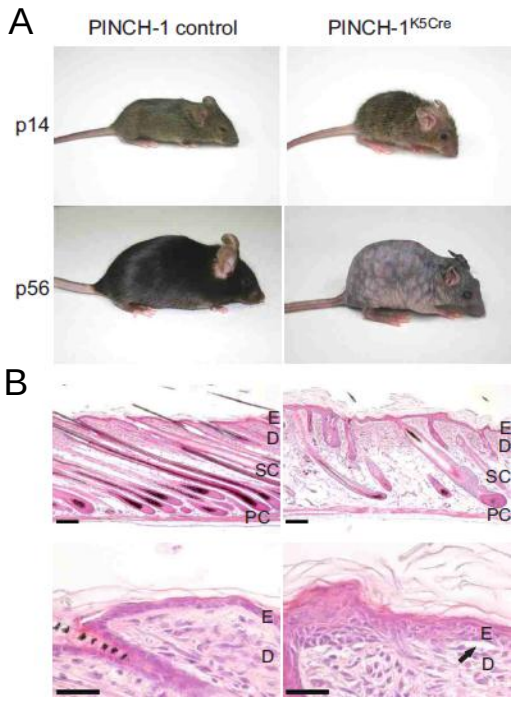

Figure 11: Keratinocyte-specific deletion of PINCH-1 leads to skin abnormalities

(A) Control (PINCH-1 control) and PINCH-1^{K5Cre} animals at 2 and 7 weeks of age. (B) Hematoxylin-eosin staining of back skin sections of 2 week old PINCH-1 control and PINCH-1^{K5Cre} mice. PINCH-1^{K5Cre} skin contains hyperplastic hair follicles that have reached the subcutis or shortened and developmentally arrested hair follicles. PINCH-1^{K5Cre} epidermis is hyperthickened and often detached from the underlying dermis (*arrow*); bar represents 100µm. Epidermis (E); dermis (D); panniculus carnosum (PC); subcutis (SC).

The hyperthickened IFE was not due to increased proliferation of basal keratinocytes; as the number of proliferating cells was similar in control and PINCH-1^{K5Cre} epidermis. While the proliferation was restricted to the basal cell layer in control epidermis, proliferating cells were frequently observed in suprabasal cells of the PINCH-1^{K5Cre} epidermis (Fig. 12B). In control mice, HF morphogenesis was completed at p14 with all HFs residing deep in the subcutis. In contrast, PINCH-1^{K5Cre} animals possessed two types of HFs: fully developed HFs, which reached the subcutis and contained a hyperthickened ORS; and short HFs, which resided in the dermis with an abnormal shape and with either a distorted or no DP (Fig. 12A).

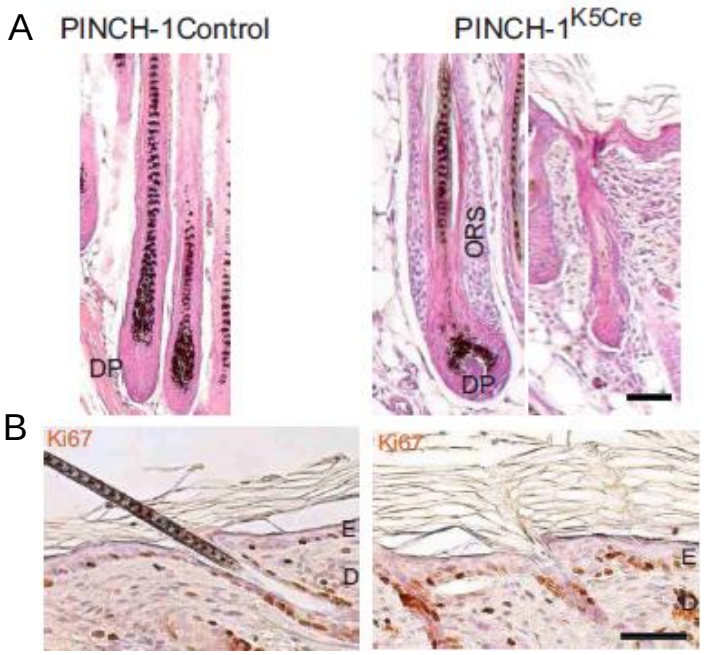

Figure 12: PINCH-1 deletion leads to abnormal hair follicles and suprabasal proliferating cells in skin

(A) High magnification of hematoxylin-eosin stained hair follicles from P14 back skin. PINCH-1^{K5Cre} HFs either have multilayered outer root sheath (ORS) and a condensed dermal papilla (DP) or show premature growth arrest with a malformed or absent DP. (B) Ki67 staining on back skin of P7 mice. Note the presence of suprabasal proliferating cells in PINCH-1^{K5Cre} epidermis. Scale bar represents 50µm.

Ultrastructural analyses revealed that PINCH-1^{K5Cre} epidermis displayed prominent cell-cell adhesion defects with extensive intercellular spaces between cells, whereas control skin had tightly sealed cell-cell adhesions (arrowheads in Fig.13A). Despite these enlarged intercellular spaces, E-cadherin, F-actin, Desmoplakin and Plakoglobin localized to cell-cell junctions (Fig. 13B and data not shown). These findings demonstrate that PINCH-1 stabilizes cell-matrix and cell-cell adhesions in the epidermis.

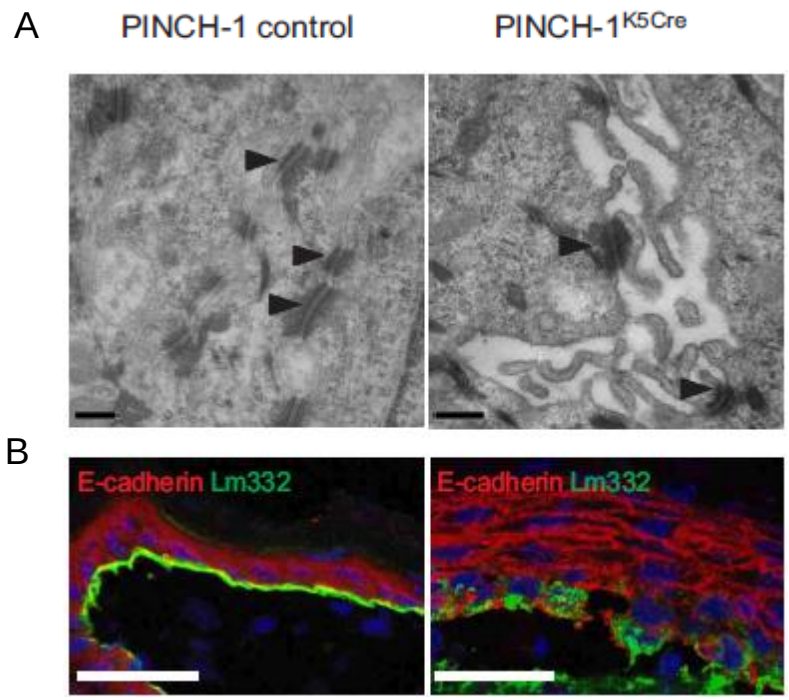

Figure 13: PINCH-1 deletion leads to increased intercellular spacing

(A) Electron microscopic images of back skin from 2 week old mice. Both, PINCH-1 control and PINCH-1^{K5Cre} skin form desmosomal contacts. Intercellular spaces are increased in the PINCH-1^{K5Cre} epidermis (*arrowheads*). Left scale bar represents 0.1 µm and right scale bar represents 0.2 µm. (B) Immunohistochemistry on 2 week-old skin sections of control and PINCH-1^{K5Cre} animals. Localization of E-cadherin is not impaired in the absence of PINCH-1. Scale bar represents 50µm.

2.2 PINCH-1 is required for keratinocyte adhesion and spreading but not for the formation of cell-cell junctions

To test cell-ECM adhesion and spreading we cultured control and PINCH-1-/- primary keratinocytes on fibronectin (FN) and Collagen I (Col-I). Control cells adhered and spread, but PINCH-1-/- primary keratinocytes grew in poorly-spread colonies (Fig. 14A). PINCH-1-/- cells achieved a 4.3-fold smaller spreading area than control cells over a time period of 20 hours (Fig. 14B).

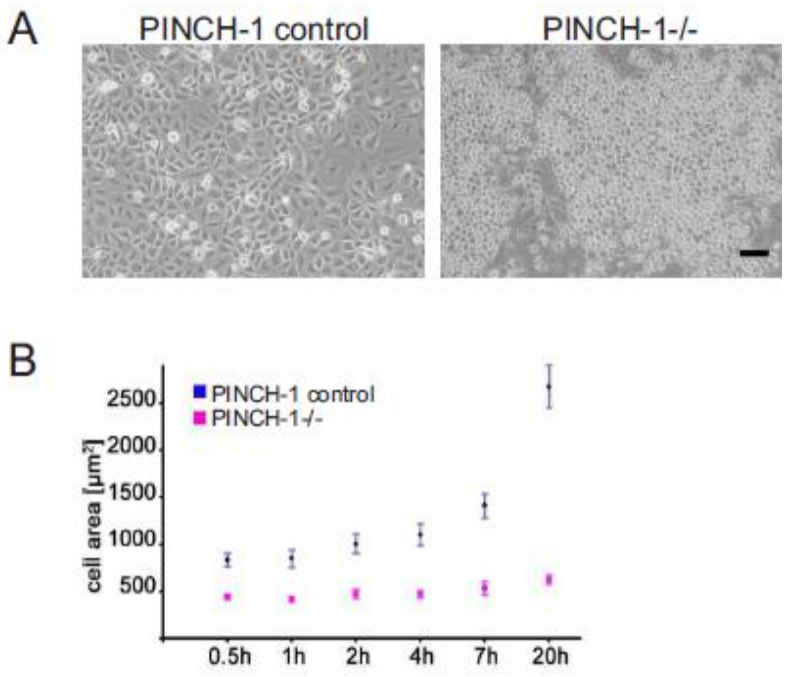

Figure 14: PINCH-1 deletion leads to a spreading defect

(A) Brightfield images of control and PINCH-1-/- primary keratinocytes. Cells were cultured for 6 days. PINCH-1-/- keratinocytes form clusters of small and round cells. Scale bar represents 100µm. (B) Spreading quantifications of primary control and PINCH-1-/- cells plated on a mixture of collagen I and fibronectin. Spreading of more than 100 cells was determined at indicated times (error bars indicate the 95% CI of mean values).

We next immunostained primary cells for ILK, F-actin and Paxillin. Control cells formed stress fibers that attached to FAs containing ILK and Paxillin. In contrast, PINCH-1-/- cells failed to form FAs containing ILK and Paxillin, and no stress fibers were observed (Fig. 15A).

Next, we analyzed cell-cell adhesion formation by differentiating control and PINCH-1-/- primary keratinocytes with Ca^{2+} and immunostaining them for E-cadherin. Although they remained small, round and poorly-spread, PINCH-1-/- keratinocytes were able to assemble cell-cell junctions containing F-actin and E-cadherin, comparable to the control cells (Fig. 15A). Importantly, the architecture of epithelial sheets of PINCH-1-/- cells displayed an increased thickness when compared to control cells, most likely due to the spreading defect (Fig. 15B).

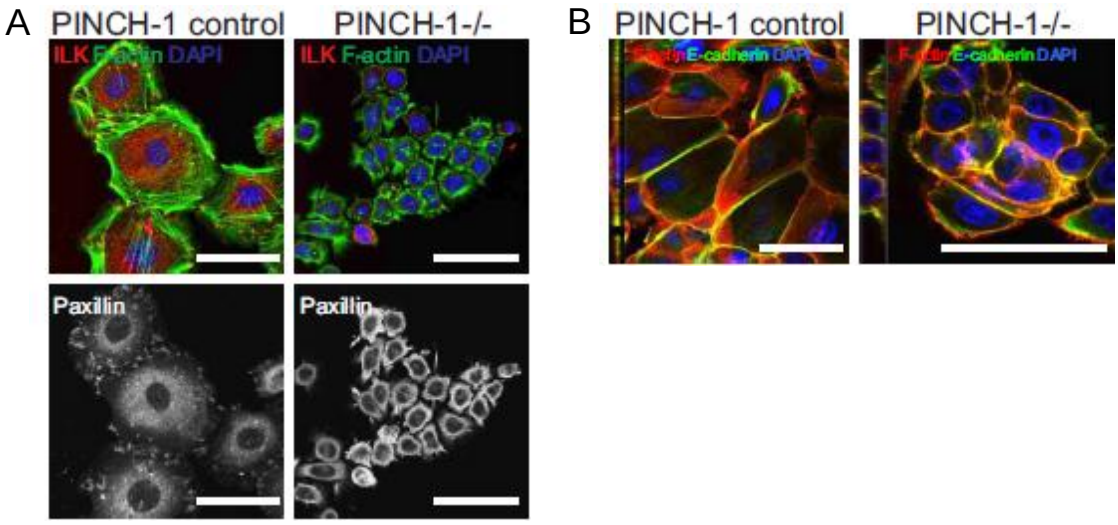

Figure 15: Ablation of PINCH-1 leads to impaired FAs, but does not affect formation of cell-cell junctions

(A) Immunostaining of primary control, PINCH-1-/- keratinocytes for ILK, F-actin and paxillin. PINCH-1-/- cells are poorly spread, displaying only few FAs. Scale bar represents 50µm. (B) Immunostaining of primary control and PINCH-1-/- keratinocytes differentiated with 1mM $CaCl_2$. E-cadherin localizes to cell-cell junctions in differentiated control and PINCH-1-/- keratinocytes. Left panels show a perpendicular view of a confocal Z-stack. Note the increased thickness of PINCH-1-/- keratinocytes. Scale bar represents 50µm.

Taken together, these data indicate that PINCH-1 supports integrin-dependent functions but is not required for the formation of cell-cell adhesions.

2.3 PINCH-1 localizes to cell-cell adhesions in a ROCK-dependent manner

Our findings with TEM analysis as well as previous reports (Li et al., 2005) demonstrate that PINCH-1 is required to maintain cell-cell adhesions. We therefore investigated the localization of PINCH-1 to cell-cell junctions. PINCH-1 localization to cell-cell junctions was enhanced after increasing intracellular tension by HGF treatment (Fig. 16A). Treating cells with the myosin inhibitor blebbistatin dramatically reduced PINCH-1 localization to cell-cell junctions while leaving E-cadherin localization unaltered (Fig. 16B). Consistent with other reports (Yamada and Nelson, 2007), inhibition of ROCK disassembled cortical actin bundles, but the cell-cell contacts remained intact and it also abolished the localization of PINCH-1 to cell-cell junctions, suggesting that the tension required for PINCH-1 localization to cell-cell junctions originated in a ROCK/myosin-II-

dependent manner (Fig. 16B). Expression levels of PINCH-1 and E-cadherin were not altered upon HGF treatment (Fig. 16C).

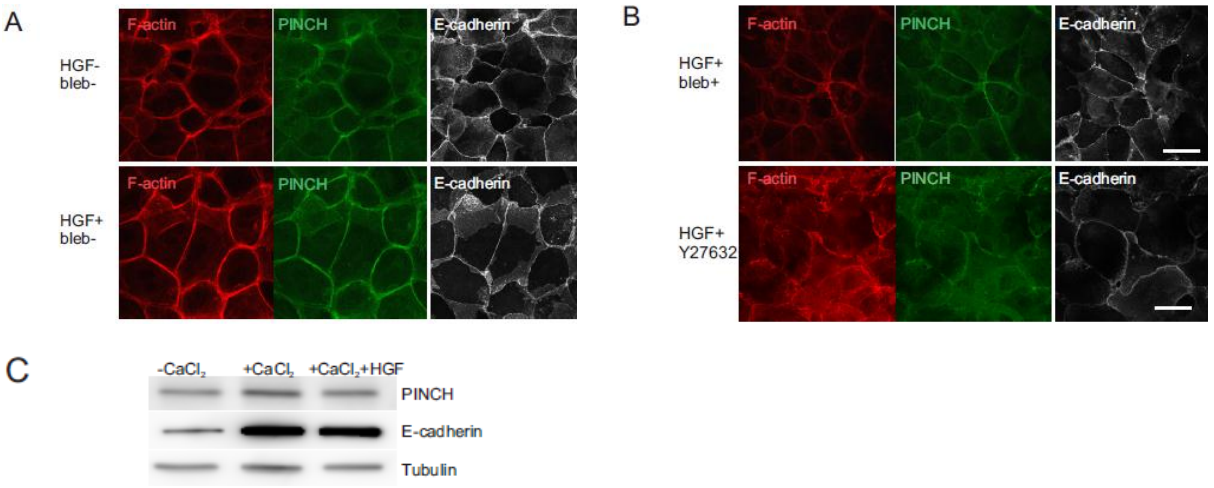

Figure 16: PINCH-1 localizes to cell-cell junctions in a tension-dependent manner

(A) Immunostaining of EGFP-tagged PINCH-1 rescued keratinocytes for PINCH-1, E-cadherin and F-actin. Cells were differentiated overnight and tension was then induced by 50ng/ml HGF treatment for 1 hour. (B) PINCH-1 localizes to cell-cell junctions after HGF treatment, and either with 25µM blebbistatin treatment for 15 minutes or 10µM Y-27632 for 1 hour removes PINCH-1 from cell-cell junctions. Scale bar represents 50µm. (C) WB analysis of EPLIN, F-actin and E-cadherin after HGF treatment. Scale bar represents 50µm.

These results indicate that PINCH-1 localization to cell-cell junctions is controlled by force which is established by ROCK-mediated myosin-II phosphorylation.

2.4 PINCH-1 interacts with a novel partner, EPLIN

To understand how PINCH-1 regulates cell-cell adhesion maintenance in the epidermis, we screened for novel interaction partners for PINCH-1 by performing label free pull-down experiments with EGFP-tagged PINCH-1 expressed in immortalized PINCH-1-/- (PINCH-1 Rescue) keratinocytes followed by mass-spectrometric analyses. WB of cell lysates from PINCH-1-/- cells showed that they are totally devoid of PINCH and that the expression levels of ILK and parvins decrease upon PINCH-1 loss and are restored by reconstitution of GFP-tagged PINCH-1 (Fig. 17A). Primary and immortalized PINCH-1-/- keratinocytes share the same spreading, adhesion and actin distribution defects; which

were fully rescued upon re-expression of EGFP-PINCH-1 (Fig. 17B and 17C and data not shown).

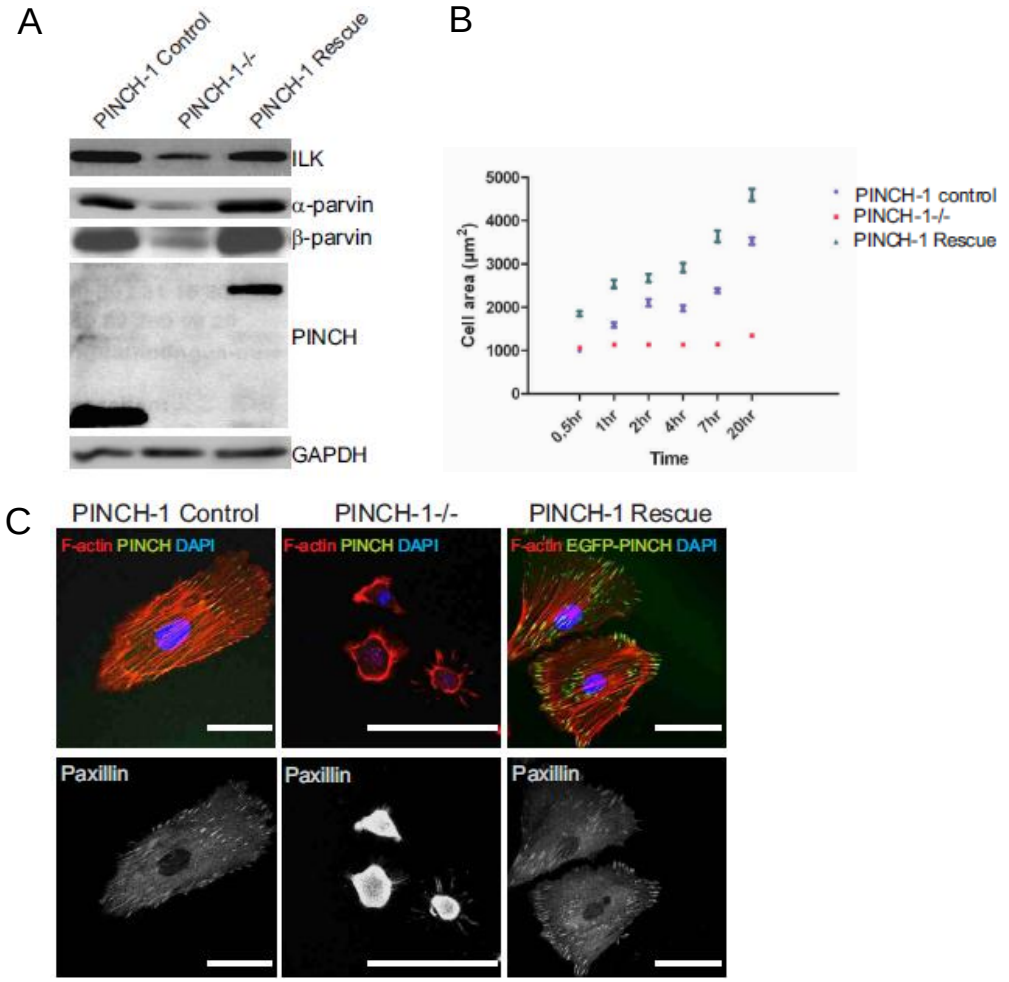

Figure 17: Generation of immortalized PINCH-1 control, PINCH-1-/- and PINCH-1 rescue cells

(A) Western blot analysis of protein lysates from PINCH-1 Co, PINCH-1-/- and EGFP-tagged PINCH-1 rescued keratinocytes. PINCH-1-/- keratinocytes express lower levels of ILK and parvins. (B) Spreading quantification of PINCH-1 control, PINCH-1-/- and EGFP-tagged PINCH-1 rescued cells. Reintroducing EGFP-tagged PINCH-1 rescues the spreading defect. (C) Immunostaining of immortalized and cloned control, PINCH-1-/- and EGFP-tagged PINCH-1 rescued keratinocytes. EGFP-tagged PINCH-1 localizes to FAs and rescues the spreading defect of PINCH-1-/- cells.

Among the binding partners, there were known PINCH interacting proteins such as ILK, and novel PINCH binding partners such as EPLIN (Fig. 18A). Consistent with the

proteomics data, EPLIN was readily detected in GFP-PINCH-1 immunoprecipitates of PINCH-1 Rescue keratinocyte lysates (Fig. 18B) and PINCH-1 was detected in GFP-EPLIN immunoprecipitates of GFP-EPLIN expressing but not of only GFP expressing keratinocyte lysates (Figure 18B).

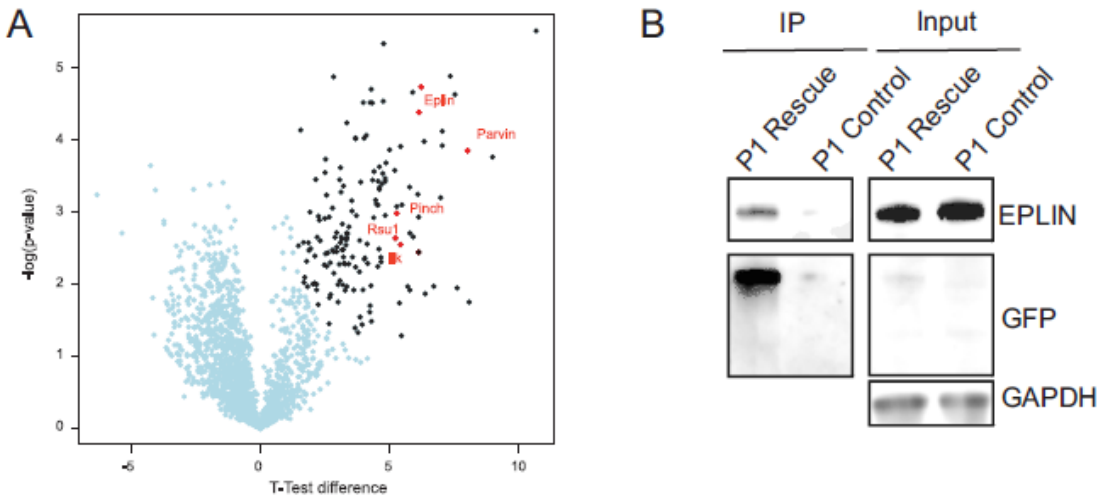

Figure 18: EPLIN is a novel PINCH-1 interacting protein

(A) Volcano plot of label-free mass spectrometry performed with control and PINCH-1-/- cells rescued with EGFP-tagged PINCH-1 following GFP-IP. EPLIN is identified as a new interacting protein of PINCH-1. (B) GFP-IP of EGFP-tagged PINCH-1 and control cells. Note that EPLIN can only be co-IPed when GFP-tagged PINCH-1 is present.

In addition, α-catenin, which has previously been shown to directly associate with EPLIN (Abe and Takeichi, 2008), was detected in the EPLIN immunoprecipitates of PINCH-1 expressing keratinocyte and PINCH-1-/- keratinocyte lysates (Fig. 19A) indicating that the interaction between EPLIN and α-catenin occurs independent of PINCH-1. Moreover, EPLIN can also be detected in endogenous PINCH-1 immunoprecipitates of PINCH-1 control cell lysates (Fig. 19B).

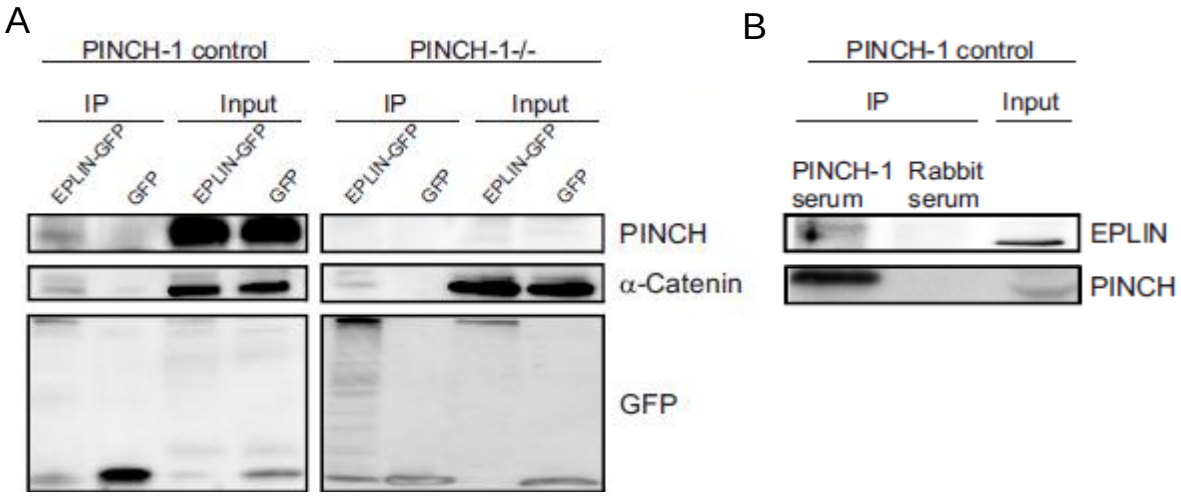

Figure 19: Confirmation of the interaction between PINCH-1 and EPLIN

(A) GFP-IP with immortalized PINCH-1 Co and PINCH-1-/- cells, transfected either with EPLIN-GFP or GFP alone. Note that the interaction between EPLIN and PINCH-1 can only be observed when cells express PINCH-1 and GFP-tagged EPLIN. (D) PINCH-1 immunoprecipitation of control cells, blotted for EPLIN and PINCH. Note that rabbit serum is used as a control and co-IP of EPLIN is only observed when PINCH-1 serum is used.

Immunostainings revealed that EPLIN and PINCH-1 co-localized with vinculin at FAs (Figure 20). However, in PINCH-1-/- keratinocytes EPLIN failed localize to FAs, indicating that PINCH-1 is necessary to recruit EPLIN to FAs.

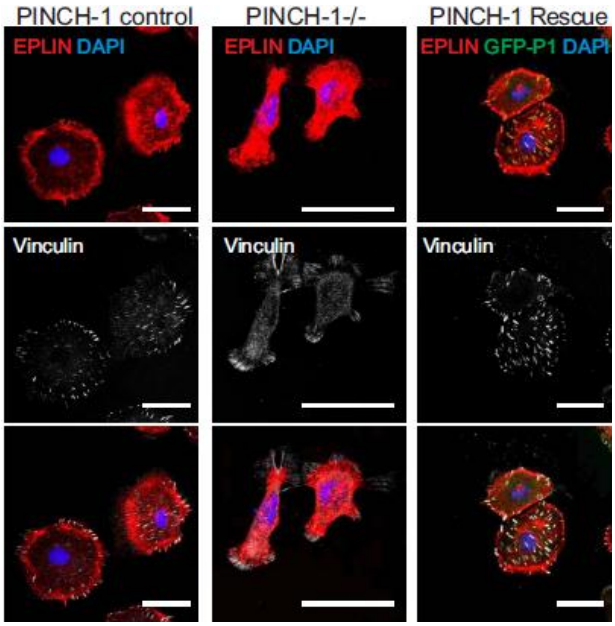

Figure 20: EPLIN localizes to FAs

Immunostaining of control, PINCH-1-/- and EGFP-tagged PINCH-1 rescued cells for EPLIN and vinculin. EPLIN colocalizes with vinculin in control and EGFP-tagged PINCH-1 rescued keratinocytes. In PINCH-1-/- keratinocytes EPLIN fails to colocalize with PINCH-1 in FAs. Scale bar represents 50µm.

2.5 PINCH-1 and EPLIN cooperation is essential both for cell-ECM and cell-cell adhesion maintenance

Having found that EPLIN localization is altered upon loss of PINCH-1, we investigated total expression levels of EPLIN in control, PINCH-1-/- and PINCH-1 Rescue keratinocytes and found that EPLIN expression is decreased in the PINCH-1-/- cells (Fig. 21A). To determine whether ectopic EPLIN expression would rescue the spreading failure, we overexpressed Cherry-tagged EPLIN in PINCH-1 Rescue and PINCH-1-/- keratinocytes and found that overexpression of EPLIN in PINCH-1-/- cells was not sufficient to rescue the spreading failure (Fig. 21B), suggesting that both PINCH-1 and EPLIN should be present at FAs to mediate cell spreading.

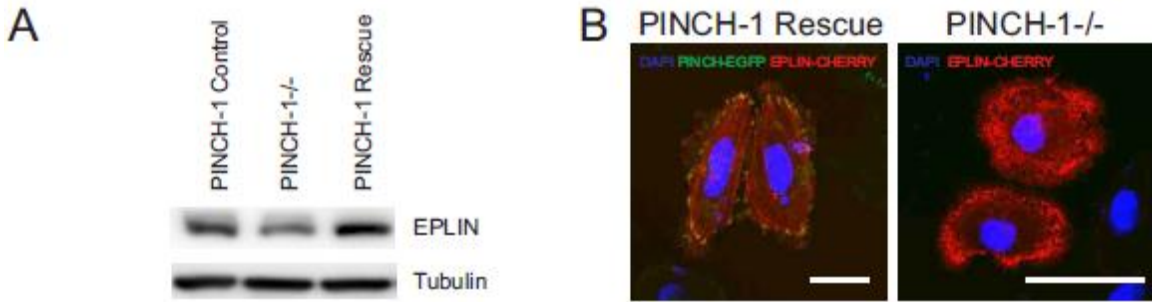

Figure 21: Overexpression of EPLIN is not sufficient to rescue the spreading defect of PINCH-1-/- cells

(A) Western Blot analysis of EPLIN in undifferentiated control, PINCH-1-/- and PINCH-1 Rescue cells. Tubulin shows equal amounts of loading. (B) Overexpression of Cherry tagged EPLIN on PINCH-1 Rescue and PINCH-1-/- cells. Note that EPLIN overexpression is not sufficient to rescue spreading defect of PINCH-1-/- cells. Scale bar represents 50µm.

EPLIN was also detected in AJs, mediating the linkage of the cadherin-catenin complex to F-actin (Abe and Takeichi, 2008). We confirmed that EPLIN colocalized with E-cadherin at AJs of differentiated control keratinocytes (Fig. 22A). Interestingly, in the absence of PINCH-1, although E-cadherin localization was not altered, EPLIN was no longer detected in AJs (Fig. 22A). To further support the hypothesis that PINCH-1 is necessary for EPLIN localization to AJs, we analyzed PINCH-1 control and PINCH-1^{K5Cre} back skin sections of p14 animals. We found that EPLIN was localized to cell-cell junctions in control skin whereas it was distributed in a more diffused manner in the cytoplasm of the keratinocytes of PINCH-1^{K5Cre} mice (Fig. 22B).

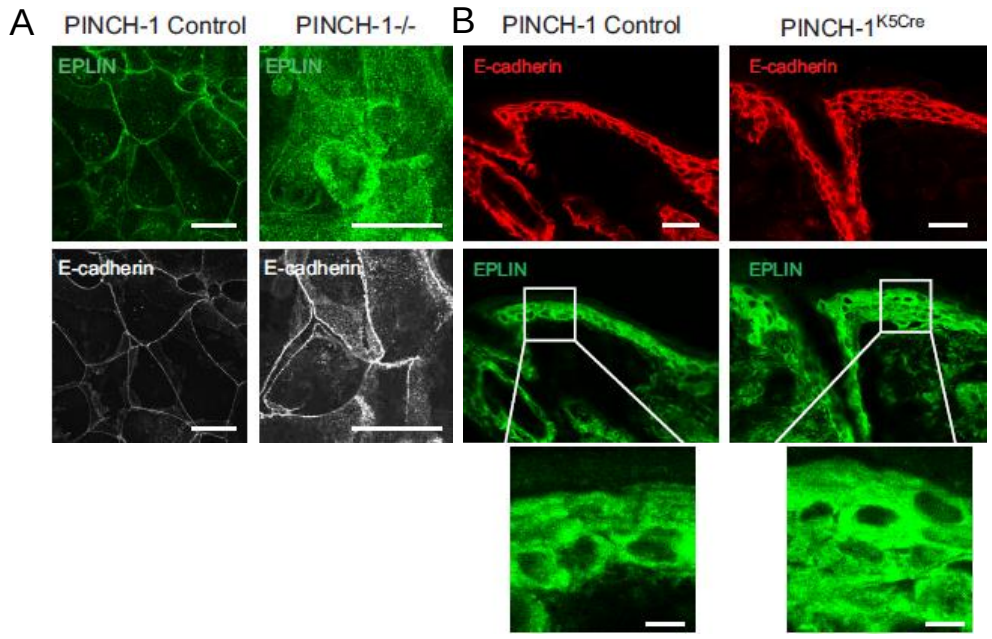

Figure 22: EPLIN localizes to AJs in a PINCH-1 dependent manner

(A) Immunostaining of immortalized control and PINCH-1-/- keratinocytes after differentiation. E-cadherin localizes to cell-cell junctions in control keratinocytes. EPLIN localization is impaired in PINCH-1-/- keratinocytes. (B) Immunohistochemistry of EPLIN and E-cadherin on control and PINCH-K5 skin. Note that in PINCH-1^{K5Cre} skin, EPLIN is not localizing to cell cell-cell junctions, but rather has a diffused localization pattern. Scale bar represents 50µm; scale bar in the insert represents 25µm.

2.5.1 EPLIN localization to FAs and AJs in ILK deficient cells is not impaired

As a core component of the IPP complex, the lower ILK expression levels in PINCH-1-/- cells may be responsible for absence of EPLIN in the FAs. Therefore, we tested whether EPLIN localization would be altered upon ILK loss. EPLIN localized to FAs in both control and ILK^{K5Cre} cells. These results demonstrated that ILK is not necessary to recruit EPLIN to FA sites (Fig. 23A).

We further investigated whether ILK depletion would lead to absence of EPLIN from the AJs. EPLIN immunostaining on control and ILK^{K5Cre} primary keratinocytes revealed that loss of ILK did not alter localization of EPLIN to AJs, suggesting that EPLIN cooperates specifically with PINCH-1 to maintain stable AJs (Fig. 23B).

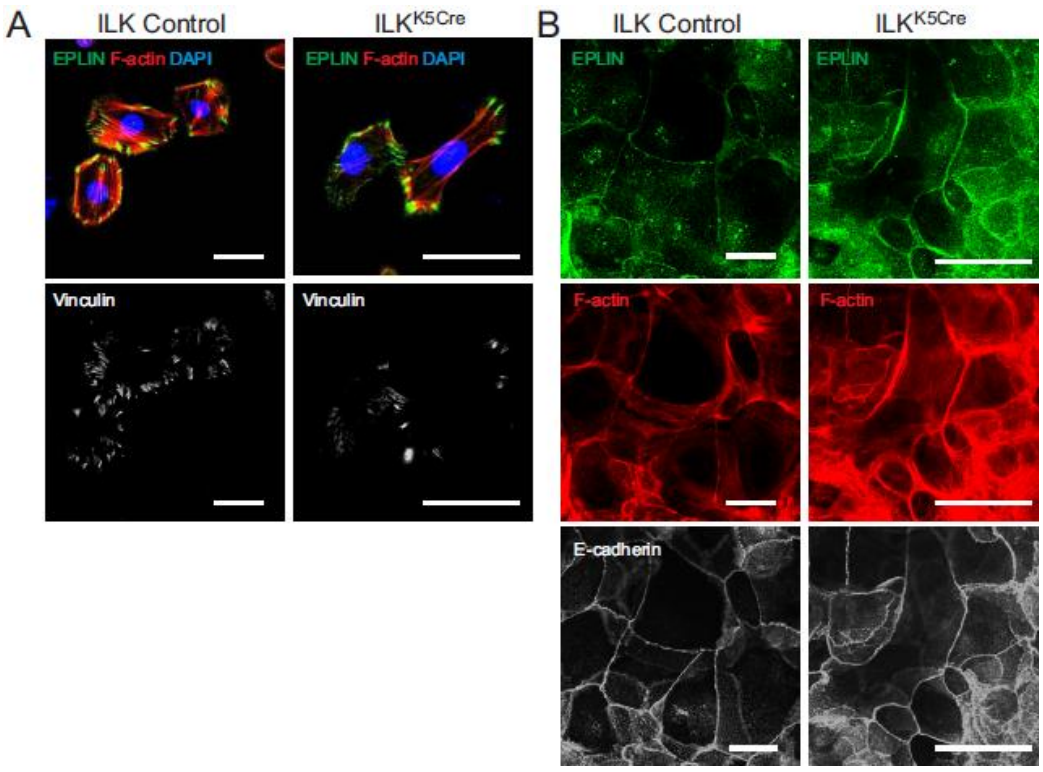

Figure 23: ILK depletion does not alter EPLIN localization to FAs and AJs

(A) Immunostaining for EPLIN on undifferentiated ILK control and ILK-/- primary cells. Note that EPLIN can localize to FAs in ILK control cells. Vinculin staining shows the FAs. Absence of ILK does not disturb EPLIN localization. (B) Immunostaining for EPLIN on differentiated ILK control and ILK^{K5Cre} primary cells. Note that EPLIN is observed at the adhesion junctions. E-cadherin staining clearly points out the cell-cell junctions. In the ILK^{K5Cre} cells, EPLIN is still present at cell-cell junctions.

Our results as well as others' (Legate et al., 2006) have confirmed that protein levels of PINCH are decreased in the absence of ILK. However, it remains elusive if PINCH is able to localize to FA sites when ILK is depleted. To investigate this, we overexpressed GFP-tagged PINCH-1 as well as Cherry-tagged Paxillin and performed total-internal reflection fluorescence microscopy (TIRF). When ILK is depleted, GFP-tagged PINCH-1 can localize to FAs which are marked by paxillin (Fig. 24), indicating that in the absence of ILK, the remaining amounts of PINCH-1 is not only sufficient to for self-recruitment but for EPLIN recruitment to FA sites.

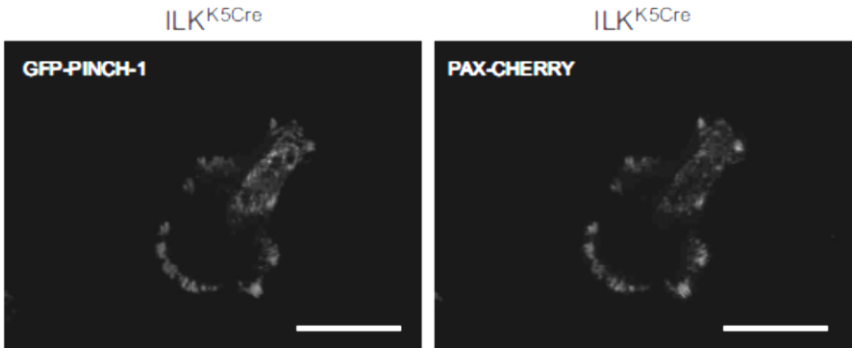

Figure 24: PINCH-1 is able to localize to FAs in the absence of ILK

Snaphots of live ILK^{K5Cre} cells overexpressing GFP-PINCH-1 and Paxillin-Cherry taken by TIRF microscope. Scale bar represents 50µm.

2.5.2 ILK can go to cell-cell junctions of PINCH-1 deficient keratinocytes

ILK was reported to localize to AJs in differentiating keratinocytes (Vespa et al., 2003). We next studied ILK localization by overexpressing GFP-tagged ILK in control and PINCH-1-/- cells. Our results showed that GFP-tagged ILK can be recruited to AJs even in the absence of PINCH-1 (Fig. 25A and 25B).

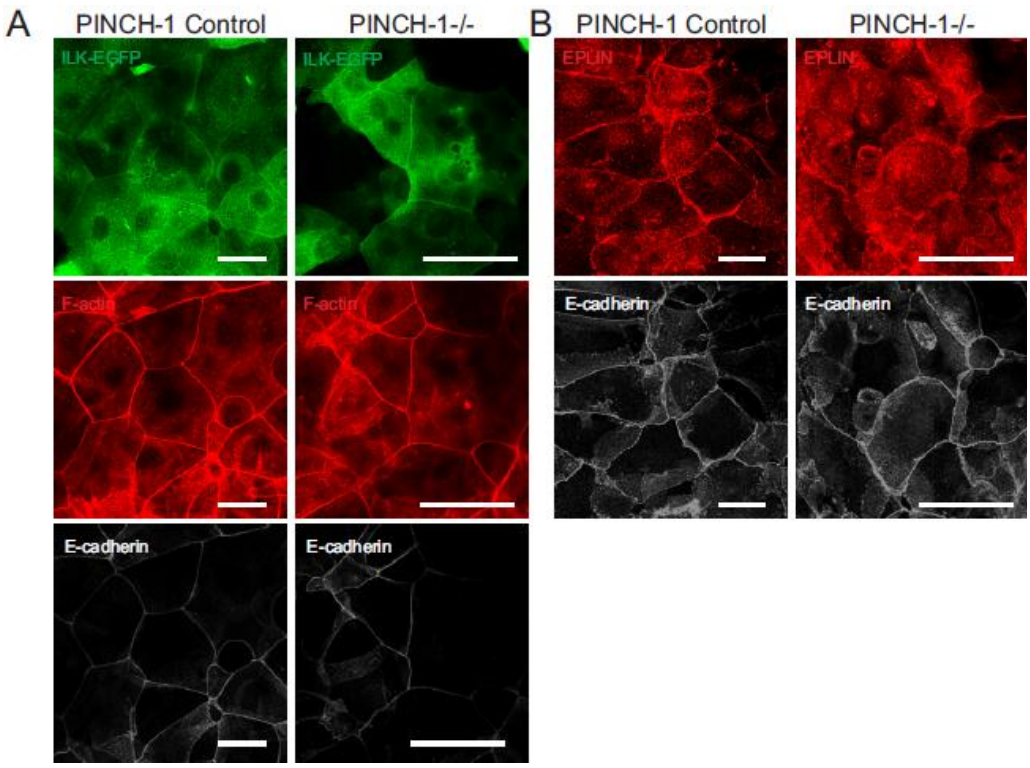

Figure 25: ILK is able to localize to cell-cell junctions, but not sufficient to recruit EPLIN in the absence of PINCH-1

(A) Immunostaining for ILK-GFP, F-actin and E-cadherin on differentiated PINCH-1 control and PINCH-1-/- cells. E-cadherin marks the AJs. (B) Immunostaining for EPLIN and E-cadherin on differentiated PINCH-1 control and PINCH-1-/- cells. Note that EPLIN is not able to localize to AJs when ILK is overexpressed (bar represents 50µM).

Taken together, our data indicate that in the absence of PINCH-1, EPLIN overexpression is not sufficient to rescue the spreading defect of PINCH-1-/- keratinocytes and that PINCH-1, but not ILK, is essential for the recruitment of EPLIN both to cell-matrix interfaces and AJs.

2.6 PINCH-1 localization to cell-cell junctions is not dependent on EPLIN

To understand whether EPLIN is required for the localization of PINCH-1 to cell-cell junctions, we transiently silenced EPLIN in control cells with two different siRNA oligonucleotides. EPLIN knockdown reduced the presence of PINCH at the FAs without affecting PINCH protein levels (Fig. 26A and 26B).

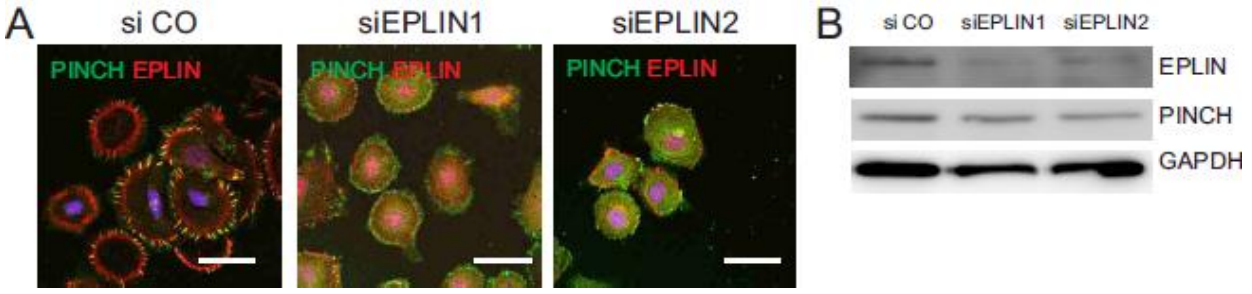

Figure 26: EPLIN depletion leads to less PINCH-1 localizing to FAs

(A) Immunostaining of PINCH and EPLIN. siRNA-mediated knock down of EPLIN was performed by using two different siRNA oligos. In control keratinocytes, EPLIN knock down leads to aberrant cell spreading and impaired localization of PINCH to FAs. (B) Western blot analysis of protein lysates from control keratinocytes transfected with either siControl or siEPLIN oligos. EPLIN knock-down has no effect on protein expression levels, but alters their localization.

EPLIN modulates stability of cell-cell junctions by regulating accumulation of E-cadherin at cell-cell junctions (Abe and Takeichi, 2008). Our data are in line with the previous observations that silencing EPLIN leads to irregular accumulation of E-cadherin at cell-cell contact sites (Fig. 27A and 27B).

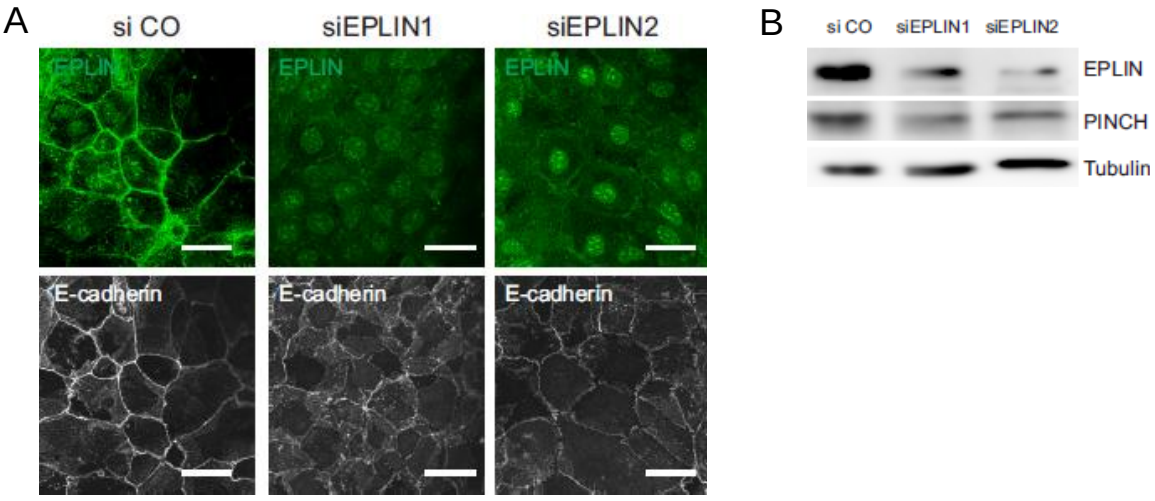

Figure 27: EPLIN depletion leads to irregular AJs

(A) Immunostaining of EPLIN and E-cadherin in differentiated control keratinocytes upon siRNA-mediated EPLIN depletion. E-cadherin localizes to cell-cell junctions in keratinocytes transfected with control siRNA, while EPLIN silencing leads to zipper-like cell-cell junctions. Scale bar represents 50µm. (B) Western blot analysis of protein

lysates from differentiated control keratinocytes transfected with either siControl or siEPLIN oligos.

Since PINCH-1 localization to AJs is a tension-dependent process, we treated cells with HGF following EPLIN silencing and differentiation. Upon tension increase, PINCH-1 expression levels stayed the same and PINCH-1 was observed at AJs. Moreover, PINCH-1 recruitment to AJs appeared to be independent from the presence of EPLIN (Fig. 28A and 28B).

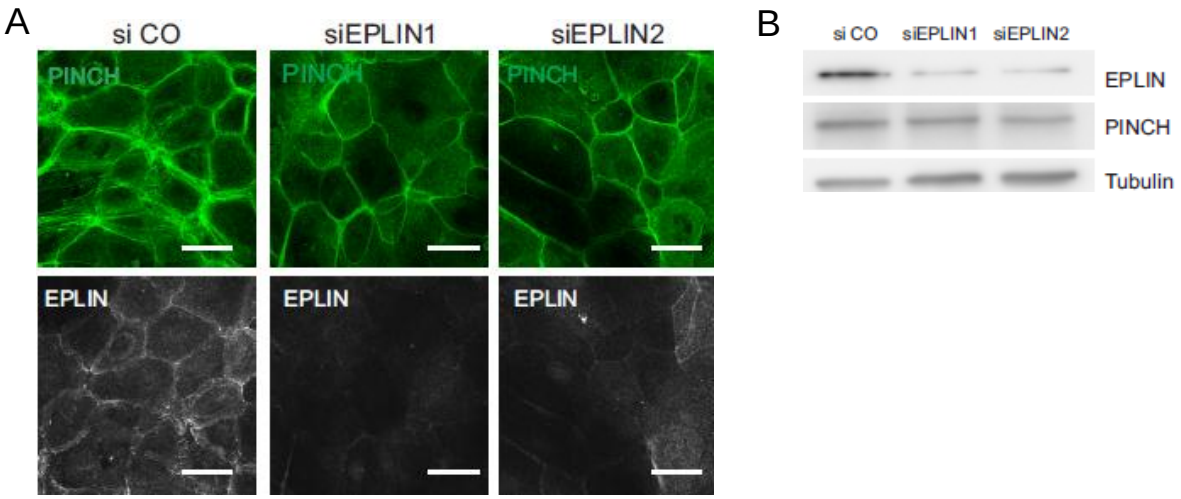

Figure 28: EPLIN depletion does not alter tension-dependent PINCH-1 localization to AJs

(A) Immunostaining of PINCH-1 control cells for PINCH and EPLIN after siRNA-mediated EPLIN depletion. PINCH-1 localizes to cell-cell junctions independent of EPLIN. (B) Western blot analysis of protein lysates from differentiated control keratinocytes transfected with either siControl or siEPLIN oligos after HGF treatment. Scale bars represent 50µm.

Taken together, these data suggest that, although PINCH-1 is required for the localization of EPLIN to FAs and cell-cell junctions in keratinocytes, EPLIN is not crucial for PINCH-1 localization to cell-cell junctions and is only partially important for FA targeting of PINCH-1.

Discussion

1. The role of PINCH-1 in PrE cell survival

Genetic deletion of *PINCH-1* gene in mouse leads early embryonic lethality and embryos display abnormal epiblast polarity, impaired cavitation, and detachment of endoderm and epiblast cells from the BM and severe apoptosis of the endoderm cells. How PINCH-1 is involved in cell survival regulation is not understood.

In this study we demonstrate that PINCH-1 is dispensable for the differentiation of extraembryonic endoderm however it is essential for its survival. We demonstrated that loss of PINCH-1 results in apoptosis of endoderm cells, giving rise to increased active Bax levels, caused by impaired integrin signaling that leads to reduced Bcl-2 levels. We also observed sustained levels of phosphorylated JNK leading to apoptosis via a Bax-independent mechanism. Moreover, we showed that the protein levels of PINCH-interacting protein RSU-1 that is a negative regulator of JNK signaling are reduced in the absence of PINCH-1.

1.1 Bcl-2 family proteins in the regulation of apoptosis in PINCH-1-deficient PrE cells

Apoptosis can occur either following the extrinsic or the intrinsic pathway. In our study, we showed that caspase-8 was not differentially-regulated in PINCH-1-/- PrE cells in comparison to the wt PrE cells, ruling out the possible extrinsic apoptotic pathway as cause for the apoptosis of the PrE. Therefore, we tested the intrinsic apoptotic pathway.

The mitochondrial intrinsic apoptotic pathway is regulated by the balance between anti-apoptotic and pro-apoptotic members of the Bcl-2 family proteins (Tait and Green, 2010). The activity of these proteins is highly regulated at multiple levels such as at transcriptional, post-transcriptional and post-translational levels (Tait and Green, 2010). ERK protects cells from intrinsic apoptosis by phosphorylating and leading to proteasomal degradation of Bim (Ley et al., 2005). Moreover, it was previously shown that PINCH-1 protects cancer cells from Bax-dependent apoptosis by regulating the ERK/Bim pathway (Chen et al., 2008). Furthermore, deletion of PINCH-1 in tumor cells also leads to a reduced phosphorylation of the Ser473 residue from the pro-survival

protein AKT, which increases the apoptosis rate of PINCH-1-deficient tumor cells (Eke et al., 2010; Sandfort et al., 2010). We found that deletion of the *PINCH-1* gene in PrE cells does not affect ERK or AKT activation. Moreover, we also found normal total Bim expression and phosphorylation levels in PINCH-1-deficient PrE cells.

These results indicate that increased active Bax levels in the PINCH-1 null PrE cells are regulated neither by Bim/ERK nor by AKT pathway. These data underline that regulation of cell survival by PINCH-1 acts via a different mechanism in PrE cells in comparison to tumor cells.

1.2 Integrin signaling and its role in apoptosis

β1 integrins are highly expressed in the early mouse embryo and are essential for PrE differentiation (Fassler and Meyer, 1995; Fassler et al., 1995; Liu et al., 2009). β1 integrins induce the nuclear translocation of the PrE-specific transcription factor GATA4, that in turn triggers the expression of BM proteins and regulates endoderm maturation. β1 integrins are also essential for the stable adhesion and spreading of PrE cells on the BM (Liu et al., 2009).

Deletion of *β1 integrin* gene arrests mouse development at the peri-implantation stage (Fassler and Meyer, 1995). On the other hand, deletion of the *PINCH-1* gene also leads to embryonic lethality at peri-implantation stage associated with impaired cell adhesion just as β1 integrin (Li et al., 2005; Liang et al., 2005). We observed that cell spreading is impaired in PINCH-1-/- PrE cells, indicating that PINCH-1 acts downstream of integrins to mediate spreading of PrE cells. In addition to the cell spreading defect, PINCH-1 deletion also gives rise to increased apoptosis in PrE cells (Li et al., 2005). Since our results indicated unaltered active caspase-8 levels in PINCH-1-/- PrE cells, we tested intrinsic apoptotic pathway. We found that loss of PINCH-1 selectively activates the intrinsic apoptotic pathway in PrE cells via increased Bax levels. We excluded that the increased Bax levels are controlled by ERK or AKT pathways.

The anti-apoptotic protein Bcl-2 inhibits intrinsic apoptotic pathway either by directly blocking Bax activation or by sequestering BH3-only proteins from Bax (Tait and Green, 2010). The α5β1 integrin is highly expressed in PrE (Liu et al., 2009) and it regulates

cell survival by up-regulating Bcl-2 expression (Zhang et al., 1995). In line with this report we observed reduced Bcl-2 protein levels in PINCH-1-/- PrE cells indicating that PINCH-1 acts downstream of α5β1 integrin to regulate Bcl-2 expression. How PINCH-1 exactly regulates Bcl-2 expression needs to be further addressed.

FA localization and the function of PINCH-1 require the interaction with ILK and parvin (Fukuda et al., 2003; Zhang et al., 2002b). ILK-deficient mice also die at peri-implantation stage of development (Sakai et al., 2003). Furthermore, ILK-deficient PrE cells have reduced PINCH-1 levels and are unable to spread on FN (Liu et al., 2009); (Montanez and Fässler, unpublished observation). However, deletion of ILK in EBs or PrE cells, does not give rise to apoptosis. The remaining protein levels of PINCH-1 are apparently sufficient to prevent apoptosis of ILK-/- PrE cells, suggesting a role for PINCH-1 in cell survival regulation that is independent of the IPP complex. On the other hand, deletion of the *α-parvin* gene leads to embryonic lethality between E11.5 and E14.5 and mice lacking β- or γ-parvin show no obvious embryonic phenotypes (Chu et al., 2006; Montanez et al., 2009); (Thievessen and Fässler, unpublished observation), suggesting that the parvin isoforms can compensate each other during peri-implantation development.

1.3 JNK signaling in apoptosis of PINCH-1 null endoderm cells

JNK signaling is important to regulate cell survival during embryo development (Davis, 2000). A transient JNK activation leads to cell survival, whereas a sustained activation gives rise to apoptosis (Ip and Davis, 1998). In agreement with this, we found that PINCH-1 loss leads to a sustained activation of JNK in PrE cells. When JNK signaling was blocked, the number of apoptotic PINCH-1-/- PrE cells was reduced, suggesting that the JNK pathway is important in the regulation of apoptosis in PINCH-1-/- PrE cells. This observation is also in line with previous data reporting that PINCH modulates JNK activity by binding and recruiting RSU-1, which is known to negatively regulate JNK (Kadrmas et al., 2004). Interestingly, we found high expression of RSU-1 specifically in the PrE cell layer of EBs and in isolated PrE cells where it co-localizes with PINCH-1 at the FAs. Moreover, RSU-1 levels were reduced when PINCH-1 is absent in PrE cells. A similar co-dependence of RSU-1 and PINCH-1 protein levels has also been reported for

human embryonic kidney cells (Dougherty et al., 2005). How the two proteins stabilize each other needs to be addressed in future studies.

Taken together, our results show that PINCH-1 regulates JNK activity and Bcl-2 levels downstream of integrin signaling. These two pathways are important in the regulation of PrE cell survival. This cell survival mechanism of PrE cells is different than the previously-reported mechanism in tumor cells.

2. The role of PINCH-1 cell-cell adhesions

PINCH-1 ablation in mice leads to lethality in early embryonic development. PINCH-1-deficient embryos display an abnormal epiblast polarity, impaired cavitation, detachment of endoderm and epiblast cells from the BM (Li et al., 2005; Liang et al., 2005) all which resemble the phenotypes observed in ILK and β1 integrin knock-out mice (Fassler and Meyer, 1995; Fassler et al., 1995; Sakai et al., 2003). Surprisingly, deletion of PINCH-1 also leads to cell-cell adhesion defects of PrE and epiblast that are neither observed in the ILK- nor β1-null mice. How PINCH-1 regulates maintenance and stability of cell-cell junctions is not understood. To elucidate how PINCH-1 is involved in this process, we used skin as a model and to this end disrupted *PINCH-1* gene specifically in epidermal and hair follicle keratinocytes.

In this part of the study, we show that deletion of *PINCH-1* gene in keratinocytes of mouse epidermis and hair follicles gives rise to several phenotypes including epidermal hyperplasia, detachment of epidermis from the underlying dermis and abnormal HF formation. These phenotypes are also observed upon deletion of *ILK* or *β1 integrin* genes in epidermis, suggesting that PINCH-1 acts downstream of integrins and has IPP complex-dependent functions in skin (Brakebusch et al., 2000; Lorenz et al., 2007; Vespa et al., 2005). Interestingly, deletion of PINCH-1 in epidermal and hair follicle keratinocytes also leads to increased intercellular spaces between neighboring cells in epidermis. This defect was not present in ILK- or β1 integrin-null epidermis, suggesting that PINCH-1 also plays IPP complex-independent role to regulate cell-cell adhesions.

It has been reported previously that conditional deletion of the AJ molecule α-catenin in keratinocytes leads to intercellular gaps observed at ultrastructural level (Vasioukhin et al., 2001). The increased intercellular spaces in epidermis observed upon PINCH-1 loss appear morphologically similar to the α-catenin null epidermis. Besides, a study by Li et al. (2005) reported a cell-cell adhesion defect in primitive endoderm of PINCH-1 null EBs at the ultrastructural level (Li et al., 2005), suggesting a novel role for PINCH-1 at cell-cell junctions. However, cell-cell adhesion defect upon PINCH-1 depletion has never been further addressed. As the formation of cell-cell junctions was not perturbed in the absence of PINCH-1 in epidermis, we suspected that the increased intercellular

spaces may be due to impaired stability and/or maintenance of AJs. Therefore we first studied the molecular composition of cell-cell junctions in PINCH-1-/- keratinocytes by immunstainings of several cell-cell junction markers including both AJ and desmosome proteins such as E-cadherin, Plakoglobin and Desmoplakin. Although, ultrastructural analysis revealed impaired cell-cell junction morphology in PINCH-1 null skin, the localization of markers were unaltered, suggesting that either a novel or a non-studied protein is crucial to regulate the stability and maintenance of cell-cell junctions together with PINCH-1.

2.1 PINCH-1 localization to cell-cell adhesions

It remains elusive until now whether PINCH-1 *per se* can localize to cell-cell adhesions. Since the attempts to show PINCH-1 at cell-cell adhesions by immunostainings with available antibodies failed, we used GFP-tagged PINCH-1 rescued cells that express wild type levels of GFP-PINCH-1. This allowed us to demonstrate that a small fraction of GFP-tagged PINCH-1 is targeted to cell-cell junctions. When cells are treated with hepatocyte growth factor (HGF) the level of PINCH-1 increased at cell-cell junctions. HGF is a cell scattering agent and is used to apply force on cell-cell junctions without decreasing the function of E-cadherin. This treatment therefore increases the tension on cell-cell junctions as reported by (de Rooij et al., 2005; le Duc et al., 2010). We could demonstrate for the first time that PINCH-1 is a component of cell-cell junctions whose recruitment is mainly mediated by tension.

Stability of cell-cell junctions is crucial for normal embryonic development as well as for avoiding cancer formation (Costa et al., 1998; Larue et al., 1994; Tepass et al., 1996; Thiery, 2002). Recently, cell-cell junction molecules have been reported to sense the force that is applied to the cell. For instance, it has been shown that vinculin is essential for the cell-cell junction integrity by regulating the cytoskeletal response to E-cadherin mechanosensing when it is recruited to cell-cell junctions in a force-dependent manner (de Rooij et al., 2005; le Duc et al., 2010; Peng et al., 2010). Here, we report that in addition to vinculin, also the localization of another FA protein, namely PINCH-1 increases at cell-cell junctions upon force generation.

Recently, LIM domain-containing proteins have been shown to be important for mechanosensory functions at FAs (Kuo et al., 2011; Schiller et al., 2011). A mass-spectrometry approach was used to define the molecular composition of FAs in the presence and absence of the myosin-II inhibitor blebbistatin. Interestingly, recruitment of LIM-domain containing proteins to FAs was highly dependent on myosin-II, suggesting that LIM domains may act as tension sensors. No experimental evidence suggesting a role for LIM domain-containing proteins in tension sensing at cell-cell junctions has been available thus far. Recently, a LIM domain containing protein EPLIN has been identified as a mechanotransducer functioning at AJs (Taguchi et al., 2011). This data may serve as the first evidence that LIM domain proteins are also important members of mechanotransduction machinery at cell-cell junctions. Moreover, we report that PINCH-1 is able to target cell-cell junctions in a tension-dependent manner and therefore we suggest that LIM domain-containing proteins may play a role in tension sensing at cell-cell junctions.

When the myosin-II inhibitor blebbistatin was applied to differentiated keratinocytes treated with HGF to reverse the high HGF-mediated tension at cell-cell junctions, PINCH-1 no longer located to the cell-cell junctions, suggesting that myosin-II-dependent contractility is involved in the mechanosensory role of PINCH-1. Activation of actomyosin contractility requires phosphorylation of Rho-associated protein kinase (ROCK) (Yamada and Nelson, 2007). We therefore inhibited ROCK in HGF-treated keratinocytes with Y-27632. The results of this treatment demonstrated that disruption of myosin phosphorylation also leads to abolishment of PINCH-1 from cell-cell junctions. Thus, we propose that PINCH-1 is recruited to cell-cell junctions in a force-dependent manner, which is mechanistically regulated by ROCK-dependent myosin light chain phosphorylation.

PINCH-1 forms a complex with ILK and parvins that is termed the IPP complex. ILK and parvins have been reported to negatively regulate RhoA-ROCK signaling in vascular smooth muscle cells (Kogata et al., 2009; Montanez et al., 2009). Furthermore, when ILK is depleted in primary fibroblasts it leads to a defect in wound closure that is associated with elevated RhoA levels (Blumbach et al., 2010). Nevertheless, none of

the IPP complex members have been suggested to function as a tension regulator at cell-cell junctions until now. Therefore, our results identify the IPP complex member PINCH-1 as a mechanosensory protein important for cell-cell junction stability and maintenance. Yet, PINCH-1 exerts this role via an IPP complex-independent mechanism. This will be further discussed in the following sections.

2.2 EPLIN, a novel PINCH-1 interacting molecule

To better understand how PINCH-1 is involved in cell-cell junction stability and maintenance, we searched for new binding partners of PINCH-1. To this end, we performed an interaction screen by performing pull-down experiments with GFP-tagged PINCH-1 followed by mass-spectrometry and identified EPLIN as a novel PINCH-1-interacting protein. To validate the proteomics data, we performed pull-down experiments. First, we took the same approach as our mass-spectrometry experiments and confirmed by WB that EPLIN can indeed be detected in GFP-PINCH-1 immunoprecipitates of GFP-PINCH-1 rescued keratinocytes. Second, we overexpressed either only GFP or GFP-tagged EPLIN in control and PINCH-1-/- keratinocytes and validated that PINCH-1 is only co-immunoprecipitated in the lysates of GFP-EPLIN expressing, but not GFP expressing control cells. Finally, we were able to confirm the interaction between EPLIN and PINCH-1 by detecting EPLIN in the endogenous PINCH-1 immunoprecipitates of wild type keratinocytes. Taken together, all our pull-down experiments confirmed that PINCH-1 and EPLIN are interacting with each other. Unfortunately, recombinant expression of PINCH-1 is not feasible. Therefore, we cannot conclude whether the expression is direct or indirect.

To study the subcellular localization of EPLIN we performed immunostainings on undifferentiated and differentiated keratinocytes. The results showed that EPLIN localized to FAs of PINCH-1 control and GFP-PINCH-1 rescued keratinocytes. Interestingly, EPLIN was missing in FAs of PINCH-1-null keratinocytes. Moreover, we found that EPLIN targeting to cell-cell junctions was also abolished in differentiated PINCH-1-null keratinocytes. Similar results were also observed in the epidermis of PINCH-1^{K5Cre} mice.

EPLIN is an adaptor protein consisting of LIM and F-actin binding domains. The F-actin binding domain crosslinks and bundles actin filaments and also maintains the circumferential actin filaments via interacting with α-catenin (Abe and Takeichi, 2008; Maul and Chang, 1999; Maul et al., 2003). Recently, EPLIN was shown to be a mechanosensitive regulator of adherens junction remodeling, by cooperating with vinculin (Taguchi et al., 2011). In our study, the *in vitro* results from immunostainings of wild type and PINCH-1-null keratinocytes showed that EPLIN recruitment to FAs is dependent on PINCH-1. Moreover, the immunostainings of differentiated PINCH-1 control and null keratinocytes as well as the *in vivo* results from the PINCH-1^{K5Cre} mice revealed that PINCH-1 is also required to stabilize EPLIN at cell-cell adhesion structures.

EPLIN has one LIM domain and two actin-binding domains (Han et al., 2007; Maul et al., 2003). The actin binding domains mediate the link between EPLIN and actin and mediate the cytoskeletal rearrangements (Han et al., 2007). Mass-spectrometry approaches identified EPLIN as a component of FAs (Kuo et al., 2011; Schiller et al., 2011). Our study confirms that EPLIN is indeed a bona fide FA protein. The lack of reports showing evidence for EPLIN in FAs may be due to differences in cell culturing conditions. The cells in our study have been cultured on FN and collagen I. The ECM proteins bind to and cluster integrins resulting in robust FA formation.

How EPLIN is recruited to FAs is not clear. Our results showed that FA targeting of EPLIN is dependent on PINCH-1. To address whether the direct interaction between the two proteins is responsible for EPLIN dependency on PINCH-1, we tried to express recombinant proteins. However, we were unable to express a recombinant PINCH-1 due to its cysteine-rich primary structure which in turn leads to formation of disulfide bonds. Whether EPLIN and PINCH-1 interact directly remains an open question. We also show that stress fiber formation is severely impaired in PINCH-1-/- keratinocytes. EPLIN as an actin crosslinking and bundling protein may be abolished from FAs due to the impaired stress fiber formation in PINCH-1-/- cells. However, the exact molecular mechanism regulating EPLIN targeting to FAs and its dependency on PINCH-1 clearly needs to be further investigated.

Since FA targeting of EPLIN has not been demonstrated until now, the role of EPLIN at FAs remains unclear. To understand the role of EPLIN at FAs and to elucidate whether loss of EPLIN results in a PINCH-1-like phenotype, we depleted EPLIN in control keratinocytes using specific siRNAs. Our findings showed that siRNA-mediated EPLIN silencing leads to an impaired spreading of keratinocytes. Moreover, PINCH-1 targeting to FAs is partially perturbed when EPLIN is silenced. These results confirmed that EPLIN knock-down gives rise to a spreading defect in keratinocytes that is reminiscent of PINCH-1-/- cells. Silencing of EPLIN diminished protein levels by 70-80%. The remaining 20-30% of total EPLIN protein level may be responsible for the less-pronounced spreading defect of EPLIN knock-down keratinocytes in comparison to PINCH-1-/- keratinocytes. Taken together, these data demonstrate that EPLIN is a FA protein and its presence is crucial for the regulation of cell spreading. Whether EPLIN also regulates other PINCH-1 properties such as adhesion, migration, proliferation and survival needs further elucidation.

EPLIN has been observed at cell-cell junctions of epithelial and endothelial cells (Abe and Takeichi, 2008; Chervin Petinot et al., 2012; Taguchi et al., 2011). However, EPLIN targeting at cell-cell junctions has not been addressed in keratinocytes until now. We demonstrate that EPLIN is also recruited to the cell-cell junctions of keratinocytes upon Ca^{2+}-induced differentiation. To understand the role of EPLIN at cell-cell junctions, we performed siRNA-mediated EPLIN silencing in control keratinocytes. Our results showed that upon EPLIN loss, cell-cell junctions display irregular accumulation of E-cadherin. We further studied whether EPLIN silencing would alter tension-dependent PINCH-1 recruitment to cell-cell junctions. Our findings demonstrate that silencing EPLIN in HGF-treated differentiated keratinocytes has no effect on PINCH-1 targeting to cell-cell junctions. Altogether, our results indicate that presence of PINCH-1 is crucial for EPLIN recruitment to cell-cell junctions whereas PINCH-1 is not dependent on EPLIN to target cell-cell junctions.

The actin binding domains of EPLIN are responsible for mediating the actin linkage (Han et al., 2007). However, the function of the LIM domain of EPLIN has not been studied so far. EPLIN has recently been demonstrated to play a role in

mechanotransduction. On the other hand, if LIM domain-containing proteins are involved in mechanotransduction machinery at the cell-cell junctions, it is possible to speculate that mechanosensory function of EPLIN is exerted via its LIM domain. Moreover our results indicate that LIM-domain only protein PINCH-1 is also involved in mechanosensing. Therefore it is probable that EPLIN and PINCH-1 collaborate to maintain stable cell-cell junctions.

We observed by TEM studies that mouse skin displays disrupted cell-cell junctions. However, localization of most cell-cell junction markers remains unaltered. This discrepancy may be explained by the different force generation in skin in comparison to cultured keratinocytes. Skin is frequently subjected to external mechanical stimuli and therefore should dynamically respond to them. The higher tension levels present in skin *in vivo*, but not in cultured keratinocytes may be the reason for disruption of cell-cell junctions in PINCH-1 null skin. Given that EPLIN has been reported to be a mechanosensing protein (Taguchi et al., 2011) and that our results reveal PINCH-1 as a force sensor, it is possible that PINCH-1 and EPLIN are collaborating mechanotransducers that respond to force-induced mechanical changes in skin.

Cadherin receptors respond to mechanical stimuli by force-induced changes in protein conformation that can lead to downstream functional responses (Gomez et al., 2011a). It has been shown that α-catenin can recruit vinculin to cell-cell junctions in a force-dependent manner by providing a binding site for vinculin that is exposed only under tension (Yonemura et al., 2010). On the other hand, recent work has demonstrated that EPLIN cooperates with vinculin to maintain AJs (Taguchi et al., 2011). Based on our result that PINCH-1 is also involved in this process, one intriguing possibility to maintain the cell-cell junction stability in a force-dependent manner could be that vinculin, PINCH-1 and EPLIN act in concert.

EPLIN binds the vinculin homology (VH3) domain only, or VH3 domain plus the C-terminal region of α-catenin, whereas vinculin binds the VH2 domain of α-catenin (Abe and Takeichi, 2008; Kobielak and Fuchs, 2004). The vinculin binding site on α-catenin is only exposed when force changes the conformation of α-catenin (Yonemura et al., 2010). It is tempting to speculate that the force, which induces the binding of vinculin to

α-catenin also exposes cryptic binding sites for PINCH-1, and thereby mediates a similar force-dependent localization of PINCH-1 to cell-cell junctions. Another possible way for PINCH-1 to localize to cell-cell junctions in a force-dependent manner might be via interacting with vinculin. Although our results confirmed that EPLIN is capable of binding to α-catenin even in the absence of PINCH-1, yet its recruitment to cell-cell junctions depends on PINCH-1. The PINCH-1 dependent recruitment of EPLIN to cell-cell junctions could indeed be easily explained through an interaction with vinculin or with an unknown protein. Since we did not find vinculin in our PINCH-1 interaction screen we currently favour the interaction with an unknown protein.

2.3 ILK involvement in PINCH-1 and EPLIN cooperation

The stability of IPP-complex members is dependent on the interaction with each constituent. Depletion of one complex member leads to the degradation of the other members (Legate et al., 2006). Consistent with previous studies, we observed that loss of PINCH-1 leads to reduced levels of ILK and parvins (Fukuda et al., 2003; Zhang et al., 2002b) and ILK depletion gives rise to low PINCH-1 expression levels (Lorenz et al., 2007). Interestingly, however, we found that the remaining PINCH-1 levels upon ILK depletion are sufficient to target PINCH-1 to FA sites and are sufficient to localize EPLIN both to FAs and the cell-cell junctions. Furthermore, no major cell adhesion defects were observed in the skin of ILK-deficient mice, suggesting that PINCH-1 plays an IPP complex-independent role in the maintenance and stability of cell-cell junctions. Since small amounts of PINCH-1 are sufficient to recruit EPLIN to FAs and cell-cell junctions, it is possible that a similar cell-cell junction defect is prevented in the skin of ILK-null mice by the remaining low levels of PINCH-1.

ILK was reported to be present on AJs (Vespa et al., 2003). We were unable to immuno-localize ILK in Ca^{2+}-treated control cells with available ILK antibodies. Overexpression of a GFP-tagged ILK in control and PINCH-1 null cells, however, demonstrated that GFP-ILK does indeed localize to cell-cell junctions in both cells. Importantly, GFP-ILK is not able to support EPLIN recruitment to cell-cell junctions in PINCH-1-/- cells, underscoring the importance of the PINCH-1-EPLIN interaction.

In conclusion, we show that conditional PINCH-1 deletion in epidermal and hair follicle keratinocytes leads to epidermal hyperplasia, blister formation at dermal-epidermal junctions, and abnormal hair follicle formation all of which are also observed upon *ILK* and *β1 integrin* gene deletion. This suggests that PINCH-1 functions in an IPP complex-dependent manner in skin. In addition, PINCH-1 ablation also gives rise to impaired cell-cell adhesion morphology in skin that has not been observed in mice conditionally lacking ILK or β1 integrin in skin. This suggests that PINCH-1 exerts this function via an IPP complex-independent mechanism. Our findings suggest that PINCH-1 and EPLIN act together to maintain stable FAs and cell-cell junctions in keratinocytes. Moreover, localization of PINCH-1 to FAs and cell-cell junction is regulated in a tension-dependent manner. Although the main cell-cell junction components remain unaltered, keratinocytes of PINCH-1^{K5Cre} mice lack EPLIN in both adhesion structures, which suggest that the severe cell-matrix and cell-cell adhesion defects of PINCH-1^{K5Cre} mice may in part be explained by an impaired PINCH-1-EPLIN interaction.

References

Abe, K., and M. Takeichi. 2008. EPLIN mediates linkage of the cadherin catenin complex to F-actin and stabilizes the circumferential actin belt. *Proc Natl Acad Sci U S A*. 105:13-19.

Albiges-Rizo, C., O. Destaing, B. Fourcade, E. Planus, and M.R. Block. 2009. Actin machinery and mechanosensitivity in invadopodia, podosomes and focal adhesions. *J Cell Sci*. 122:3037-3049.

Arnaout, M.A., S.L. Goodman, and J.P. Xiong. 2007. Structure and mechanics of integrin-based cell adhesion. *Curr Opin Cell Biol*. 19:495-507.

Arnaout, M.A., B. Mahalingam, and J.P. Xiong. 2005. Integrin structure, allostery, and bidirectional signaling. *Annu Rev Cell Dev Biol*. 21:381-410.

Bajpai, S., J. Correia, Y. Feng, J. Figueiredo, S.X. Sun, G.D. Longmore, G. Suriano, and D. Wirtz. 2008. {alpha}-Catenin mediates initial E-cadherin-dependent cell-cell recognition and subsequent bond strengthening. *Proc Natl Acad Sci U S A*. 105:18331-18336.

Barczyk, M., S. Carracedo, and D. Gullberg. 2010. Integrins. *Cell Tissue Res*. 339:269-280.

Baum, B., and M. Georgiou. 2011. Dynamics of adherens junctions in epithelial establishment, maintenance, and remodeling. *J Cell Biol*. 192:907-917.

Berrier, A.L., and K.M. Yamada. 2007. Cell-matrix adhesion. *J Cell Physiol*. 213:565-573.

Bershadsky, A., M. Kozlov, and B. Geiger. 2006. Adhesion-mediated mechanosensitivity: a time to experiment, and a time to theorize. *Curr Opin Cell Biol*. 18:472-481.

Bhowmick, N.A., M. Ghiassi, A. Bakin, M. Aakre, C.A. Lundquist, M.E. Engel, C.L. Arteaga, and H.L. Moses. 2001. Transforming growth factor-beta1 mediates epithelial to mesenchymal transdifferentiation through a RhoA-dependent mechanism. *Mol Biol Cell*. 12:27-36.

Bierkamp, C., K.J. McLaughlin, H. Schwarz, O. Huber, and R. Kemler. 1996. Embryonic heart and skin defects in mice lacking plakoglobin. *Dev Biol*. 180:780-785.

Bierkamp, C., H. Schwarz, O. Huber, and R. Kemler. 1999. Desmosomal localization of beta-catenin in the skin of plakoglobin null-mutant mice. *Development*. 126:371-381.

Blanpain, C., and E. Fuchs. 2006. Epidermal stem cells of the skin. *Annu Rev Cell Dev Biol*. 22:339-373.

Blanpain, C., and E. Fuchs. 2009. Epidermal homeostasis: a balancing act of stem cells in the skin. *Nat Rev Mol Cell Biol*. 10:207-217.

Blumbach, K., M.C. Zweers, G. Brunner, A.S. Peters, M. Schmitz, J.N. Schulz, A. Schild, C.P. Denton, T. Sakai, R. Fassler, T. Krieg, and B. Eckes. 2010. Defective granulation tissue formation in mice with specific ablation of integrin-linked kinase in fibroblasts - role of TGFbeta1 levels and RhoA activity. *J Cell Sci*. 123:3872-3883.

Bock-Marquette, I., A. Saxena, M.D. White, J.M. Dimaio, and D. Srivastava. 2004. Thymosin beta4 activates integrin-linked kinase and promotes cardiac cell migration, survival and cardiac repair. *Nature*. 432:466-472.

Bonne, S., B. Gilbert, M. Hatzfeld, X. Chen, K.J. Green, and F. van Roy. 2003. Defining desmosomal plakophilin-3 interactions. *J Cell Biol*. 161:403-416.

Bornslaeger, E.A., C.M. Corcoran, T.S. Stappenbeck, and K.J. Green. 1996. Breaking the connection: displacement of the desmosomal plaque protein desmoplakin from cell-cell interfaces disrupts anchorage of intermediate filament bundles and alters intercellular junction assembly. *J Cell Biol*. 134:985-1001.

Brakebusch, C., R. Grose, F. Quondamatteo, A. Ramirez, J.L. Jorcano, A. Pirro, M. Svensson, R. Herken, T. Sasaki, R. Timpl, S. Werner, and R. Fassler. 2000. Skin and hair follicle integrity is crucially dependent on beta 1 integrin expression on keratinocytes. *Embo J*. 19:3990-4003.

Braun, A., R. Bordoy, F. Stanchi, M. Moser, G.G. Kostka, E. Ehler, O. Brandau, and R. Fassler. 2003. PINCH2 is a new five LIM domain protein, homologous to PINCHand localized to focal adhesions. *Exp Cell Res*. 284:239-250.

Brown, N.H., S.L. Gregory, W.L. Rickoll, L.I. Fessler, M. Prout, R.A. White, and J.W. Fristrom. 2002. Talin is essential for integrin function in Drosophila. *Dev Cell*. 3:569-579.

Buday, L., L. Wunderlich, and P. Tamas. 2002. The Nck family of adapter proteins: regulators of actin cytoskeleton. *Cellular signalling*. 14:723-731.

Byron, A., J.D. Humphries, M.D. Bass, D. Knight, and M.J. Humphries. 2011. Proteomic analysis of integrin adhesion complexes. *Sci Signal*. 4:pt2.

Calderwood, D.A., B. Yan, J.M. de Pereda, B.G. Alvarez, Y. Fujioka, R.C. Liddington, and M.H. Ginsberg. 2002. The phosphotyrosine binding-like domain of talin activates integrins. *J Biol Chem*. 277:21749-21758.

Calderwood, D.A., R. Zent, R. Grant, D.J. Rees, R.O. Hynes, and M.H. Ginsberg. 1999. The Talin head domain binds to integrin beta subunit cytoplasmic tails and regulates integrin activation. *J Biol Chem*. 274:28071-28074.

Chang, D.D., N.H. Park, C.T. Denny, S.F. Nelson, and M. Pe. 1998. Characterization of transformation related genes in oral cancer cells. *Oncogene*. 16:1921-1930.

Chen, K., Y. Tu, Y. Zhang, H.C. Blair, L. Zhang, and C. Wu. 2008. PINCH-1 regulates the ERK-Bim pathway and contributes to apoptosis resistance in cancer cells. *J Biol Chem*. 283:2508-2517.

Chen, X., S. Bonne, M. Hatzfeld, F. van Roy, and K.J. Green. 2002. Protein binding and functional characterization of plakophilin 2. Evidence for its diverse roles in desmosomes and beta -catenin signaling. *J Biol Chem*. 277:10512-10522.

Chen, Y.T., D.B. Stewart, and W.J. Nelson. 1999. Coupling assembly of the E-cadherin/beta-catenin complex to efficient endoplasmic reticulum exit and basal-lateral membrane targeting of E-cadherin in polarized MDCK cells. *J Cell Biol*. 144:687-699.

Chervin-Petinot, A., M. Courcon, S. Almagro, A. Nicolas, A. Grichine, D. Grunwald, M.H. Prandini, P. Huber, and D. Gulino-Debrac. 2012. Epithelial Protein Lost In Neoplasm (EPLIN) Interacts with alpha-Catenin and Actin Filaments in Endothelial Cells and Stabilizes Vascular Capillary Network in Vitro. *J Biol Chem*. 287:7556-7572.

Chien, S., S. Li, and Y.J. Shyy. 1998. Effects of mechanical forces on signal transduction and gene expression in endothelial cells. *Hypertension*. 31:162-169.

Chircop, M., V. Oakes, M.E. Graham, M.P. Ma, C.M. Smith, P.J. Robinson, and K.K. Khanna. 2009. The actin-binding and bundling protein, EPLIN, is required for cytokinesis. *Cell Cycle*. 8:757-764.

Chiswell, B.P., R. Zhang, J.W. Murphy, T.J. Boggon, and D.A. Calderwood. 2008. The structural basis of integrin-linked kinase-PINCH interactions. *Proc Natl Acad Sci U S A*. 105:20677-20682.

Choi, C.K., M. Vicente-Manzanares, J. Zareno, L.A. Whitmore, A. Mogilner, and A.R. Horwitz. 2008. Actin and alpha-actinin orchestrate the assembly and maturation of nascent adhesions in a myosin II motor-independent manner. *Nat Cell Biol*. 10:1039-1050.

Chu, H., I. Thievessen, M. Sixt, T. Lammermann, A. Waisman, A. Braun, A.A. Noegel, and R. Fassler. 2006. gamma-Parvin is dispensable for hematopoiesis, leukocyte trafficking, and T-cell-dependent antibody response. *Mol Cell Biol*. 26:1817-1825.

Coller, B.S., and S.J. Shattil. 2008. The GPIIb/IIIa (integrin alphaIIbbeta3) odyssey: a technology-driven saga of a receptor with twists, turns, and even a bend. *Blood*. 112:3011-3025.

Costa, M., W. Raich, C. Agbunag, B. Leung, J. Hardin, and J.R. Priess. 1998. A putative catenin-cadherin system mediates morphogenesis of the Caenorhabditis elegans embryo. *J Cell Biol*. 141:297-308.

Cox, J., and M. Mann. 2008. MaxQuant enables high peptide identification rates, individualized p.p.b.-range mass accuracies and proteome-wide protein quantification. *Nat Biotechnol*. 26:1367-1372.

Critchley, D.R., and A.R. Gingras. 2008. Talin at a glance. *J Cell Sci*. 121:1345-1347.

Davies, P.F., C.F. Dewey, Jr., S.R. Bussolari, E.J. Gordon, and M.A. Gimbrone, Jr. 1984. Influence of hemodynamic forces on vascular endothelial function. In vitro studies of shear stress and pinocytosis in bovine aortic cells. *J Clin Invest*. 73:1121-1129.

de Rooij, J., A. Kerstens, G. Danuser, M.A. Schwartz, and C.M. Waterman-Storer. 2005. Integrin-dependent actomyosin contraction regulates epithelial cell scattering. *J Cell Biol*. 171:153-164.

Degterev, A., M. Boyce, and J. Yuan. 2003. A decade of caspases. *Oncogene*. 22:8543-8567.

del Rio, A., R. Perez-Jimenez, R. Liu, P. Roca-Cusachs, J.M. Fernandez, and M.P. Sheetz. 2009. Stretching single talin rod molecules activates vinculin binding. *Science*. 323:638-641.

Delcommenne, M., C. Tan, V. Gray, L. Rue, J. Woodgett, and S. Dedhar. 1998. Phosphoinositide-3-OH kinase-dependent regulation of glycogen synthase kinase 3 and protein kinase B/AKT by the integrin-linked kinase. *Proc Natl Acad Sci U S A*. 95:11211-11216.

DeMali, K.A., C.A. Barlow, and K. Burridge. 2002. Recruitment of the Arp2/3 complex to vinculin: coupling membrane protrusion to matrix adhesion. *J Cell Biol*. 159:881-891.

Dhanasekaran, D.N., and E.P. Reddy. 2008. JNK signaling in apoptosis. *Oncogene*. 27:6245-6251.

DiPersio, C.M., K.M. Hodivala-Dilke, R. Jaenisch, J.A. Kreidberg, and R.O. Hynes. 1997. alpha3beta1 Integrin is required for normal development of the epidermal basement membrane. *J Cell Biol*. 137:729-742.

Dougherty, G.W., T. Chopp, S.M. Qi, and M.L. Cutler. 2005a. The Ras suppressor Rsu-1 binds to the LIM 5 domain of the adaptor protein PINCH1 and participates in adhesion-related functions. *Experimental cell research*. 306:168-179.

Dougherty, G.W., T. Chopp, S.M. Qi, and M.L. Cutler. 2005b. The Ras suppressor Rsu-1 binds to the LIM 5 domain of the adaptor protein PINCH1 and participates in adhesion-related functions. *Exp Cell Res*. 306:168-179.

Dowling, J., Q.C. Yu, and E. Fuchs. 1996. Beta4 integrin is required for hemidesmosome formation, cell adhesion and cell survival. *J Cell Biol*. 134:559-572.

Drees, F., S. Pokutta, S. Yamada, W.J. Nelson, and W.I. Weis. 2005. Alpha-catenin is a molecular switch that binds E-cadherin-beta-catenin and regulates actin-filament assembly. *Cell*. 123:903-915.

DuFort, C.C., M.J. Paszek, and V.M. Weaver. 2011. Balancing forces: architectural control of mechanotransduction. *Nat Rev Mol Cell Biol*. 12:308-319.

Eke, I., U. Koch, S. Hehlgans, V. Sandfort, F. Stanchi, D. Zips, M. Baumann, A. Shevchenko, C. Pilarsky, M. Haase, G.B. Baretton, V. Calleja, B. Larijani, R. Fassler, and N. Cordes. 2010. PINCH1 regulates Akt1 activation and enhances radioresistance by inhibiting PP1alpha. *J Clin Invest*. 120:2516-2527.

Etienne-Manneville, S., and A. Hall. 2002. Rho GTPases in cell biology. *Nature*. 420:629-635.

Eyckmans, J., T. Boudou, X. Yu, and C.S. Chen. 2011. A hitchhiker's guide to mechanobiology. *Dev Cell*. 21:35-47.

Fassler, R., and M. Meyer. 1995. Consequences of lack of beta 1 integrin gene expression in mice. *Genes Dev*. 9:1896-1908.

Fassler, R., M. Pfaff, J. Murphy, A.A. Noegel, S. Johansson, R. Timpl, and R. Albrecht. 1995. Lack of beta 1 integrin gene in embryonic stem cells affects morphology, adhesion, and migration but not integration into the inner cell mass of blastocysts. *J Cell Biol*. 128:979-988.

Friedland, J.C., M.H. Lee, and D. Boettiger. 2009. Mechanically activated integrin switch controls alpha5beta1 function. *Science*. 323:642-644.

Frisch, S.M., and R.A. Screaton. 2001. Anoikis mechanisms. *Curr Opin Cell Biol*. 13:555-562.

Fuchs, E. 2007. Scratching the surface of skin development. *Nature*. 445:834-842.

Fuchs, E., and V. Horsley. 2008. More than one way to skin. *Genes Dev*. 22:976-985.

Fujikura, J., E. Yamato, S. Yonemura, K. Hosoda, S. Masui, K. Nakao, J. Miyazaki Ji, and H. Niwa. 2002. Differentiation of embryonic stem cells is induced by GATA factors. *Genes Dev*. 16:784-789.

Fukuda, T., K. Chen, X. Shi, and C. Wu. 2003. PINCH-1 is an obligate partner of integrin-linked kinase (ILK) functioning in cell shape modulation, motility, and survival. *The Journal of biological chemistry*. 278:51324-51333.

Furuse, M., K. Fujita, T. Hiiragi, K. Fujimoto, and S. Tsukita. 1998. Claudin-1 and -2: novel integral membrane proteins localizing at tight junctions with no sequence similarity to occludin. *J Cell Biol*. 141:1539-1550.

Furuse, M., T. Hirase, M. Itoh, A. Nagafuchi, S. Yonemura, and S. Tsukita. 1993. Occludin: a novel integral membrane protein localizing at tight junctions. *J Cell Biol*. 123:1777-1788.

Gallicano, G.I., P. Kouklis, C. Bauer, M. Yin, V. Vasioukhin, L. Degenstein, and E. Fuchs. 1998. Desmoplakin is required early in development for assembly of desmosomes and cytoskeletal linkage. *J Cell Biol*. 143:2009-2022.

Geiger, B., J.P. Spatz, and A.D. Bershadsky. 2009. Environmental sensing through focal adhesions. *Nat Rev Mol Cell Biol*. 10:21-33.

Geiger, C., W. Nagel, T. Boehm, Y. van Kooyk, C.G. Figdor, E. Kremmer, N. Hogg, L. Zeitlmann, H. Dierks, K.S. Weber, and W. Kolanus. 2000. Cytohesin-1 regulates beta-2 integrin-mediated adhesion through both ARF-GEF function and interaction with LFA-1. *Embo J*. 19:2525-2536.

Georges-Labouesse, E., N. Messaddeq, G. Yehia, L. Cadalbert, A. Dierich, and M. Le Meur. 1996. Absence of integrin alpha 6 leads to epidermolysis bullosa and neonatal death in mice. *Nat Genet*. 13:370-373.

Getsios, S., A.C. Huen, and K.J. Green. 2004. Working out the strength and flexibility of desmosomes. *Nat Rev Mol Cell Biol*. 5:271-281.

Gilmore, A.P., T.W. Owens, F.M. Foster, and J. Lindsay. 2009. How adhesion signals reach a mitochondrial conclusion--ECM regulation of apoptosis. *Curr Opin Cell Biol*. 21:654-661.

Gimona, M., R. Buccione, S.A. Courtneidge, and S. Linder. 2008. Assembly and biological role of podosomes and invadopodia. *Curr Opin Cell Biol*. 20:235-241.

Gomez, G.A., R.W. McLachlan, and A.S. Yap. 2011a. Productive tension: force-sensing and homeostasis of cell-cell junctions. *Trends Cell Biol*.

Gomez, G.A., R.W. McLachlan, and A.S. Yap. 2011b. Productive tension: force-sensing and homeostasis of cell-cell junctions. *Trends Cell Biol*. 21:499-505.

Grashoff, C., I. Thievessen, K. Lorenz, S. Ussar, and R. Fassler. 2004. Integrin-linked kinase: integrin's mysterious partner. *Curr Opin Cell Biol*. 16:565-571.

Grose, R., C. Hutter, W. Bloch, I. Thorey, F.M. Watt, R. Fassler, C. Brakebusch, and S. Werner. 2002. A crucial role of beta 1 integrins for keratinocyte migration in vitro and during cutaneous wound repair. *Development*. 129:2303-2315.

Guillou, H., A. Depraz-Depland, E. Planus, B. Vianay, J. Chaussy, A. Grichine, C. Albiges-Rizo, and M.R. Block. 2008. Lamellipodia nucleation by filopodia depends on integrin occupancy and downstream Rac1 signaling. *Exp Cell Res*. 314:478-488.

Han, J., C.J. Lim, N. Watanabe, A. Soriani, B. Ratnikov, D.A. Calderwood, W. Puzon-McLaughlin, E.M. Lafuente, V.A. Boussiotis, S.J. Shattil, and M.H. Ginsberg. 2006. Reconstructing and deconstructing agonist-induced activation of integrin alphaIIbbeta3. *Curr Biol*. 16:1796-1806.

Han, M.Y., H. Kosako, T. Watanabe, and S. Hattori. 2007. Extracellular signal-regulated kinase/mitogen-activated protein kinase regulates actin organization and cell motility by phosphorylating the actin cross-linking protein EPLIN. *Mol Cell Biol*. 27:8190-8204.

Hannigan, G.E., C. Leung-Hagesteijn, L. Fitz-Gibbon, M.G. Coppolino, G. Radeva, J. Filmus, J.C. Bell, and S. Dedhar. 1996. Regulation of cell adhesion and anchorage-dependent growth by a new beta 1-integrin-linked protein kinase. *Nature*. 379:91-96.

Harris, T.J., and U. Tepass. 2010. Adherens junctions: from molecules to morphogenesis. *Nat Rev Mol Cell Biol*. 11:502-514.

Hartsock, A., and W.J. Nelson. 2008. Adherens and tight junctions: structure, function and connections to the actin cytoskeleton. *Biochim Biophys Acta*. 1778:660-669.
Hatzfeld, M., K.J. Green, and H. Sauter. 2003. Targeting of p0071 to desmosomes and adherens junctions is mediated by different protein domains. *J Cell Sci*. 116:1219-1233.
Hobert, O., D.G. Moerman, K.A. Clark, M.C. Beckerle, and G. Ruvkun. 1999. A conserved LIM protein that affects muscular adherens junction integrity and mechanosensory function in Caenorhabditis elegans. *J Cell Biol*. 144:45-57.
Huber, A.H., D.B. Stewart, D.V. Laurents, W.J. Nelson, and W.I. Weis. 2001. The cadherin cytoplasmic domain is unstructured in the absence of beta-catenin. A possible mechanism for regulating cadherin turnover. *J Biol Chem*. 276:12301-12309.
Hubner, N.C., and M. Mann. 2011. Extracting gene function from protein-protein interactions using Quantitative BAC InteraCtomics (QUBIC). *Methods*. 53:453-459.
Humphries, J.D., A. Byron, and M.J. Humphries. 2006. Integrin ligands at a glance. *J Cell Sci*. 119:3901-3903.
Humphries, M.J., E.J. Symonds, and A.P. Mould. 2003. Mapping functional residues onto integrin crystal structures. *Curr Opin Struct Biol*. 13:236-243.
Hynes, R.O. 2002. Integrins: bidirectional, allosteric signaling machines. *Cell*. 110:673-687.
Hynes, R.O., and Q. Zhao. 2000. The evolution of cell adhesion. *J Cell Biol*. 150:F89-96.
Ip, Y.T., and R.J. Davis. 1998. Signal transduction by the c-Jun N-terminal kinase (JNK)--from inflammation to development. *Curr Opin Cell Biol*. 10:205-219.
Ishiyama, N., S.H. Lee, S. Liu, G.Y. Li, M.J. Smith, L.F. Reichardt, and M. Ikura. 2010. Dynamic and static interactions between p120 catenin and E-cadherin regulate the stability of cell-cell adhesion. *Cell*. 141:117-128.
Itoh, M., K. Morita, and S. Tsukita. 1999. Characterization of ZO-2 as a MAGUK family member associated with tight as well as adherens junctions with a binding affinity to occludin and alpha catenin. *J Biol Chem*. 274:5981-5986.
Itoh, M., A. Nagafuchi, S. Moroi, and S. Tsukita. 1997. Involvement of ZO-1 in cadherin-based cell adhesion through its direct binding to alpha catenin and actin filaments. *J Cell Biol*. 138:181-192.
Jaalouk, D.E., and J. Lammerding. 2009. Mechanotransduction gone awry. *Nat Rev Mol Cell Biol*. 10:63-73.
Jaffe, A.B., and A. Hall. 2005. Rho GTPases: biochemistry and biology. *Annu Rev Cell Dev Biol*. 21:247-269.
Johnson, M.S., N. Lu, K. Denessiouk, J. Heino, and D. Gullberg. 2009. Integrins during evolution: evolutionary trees and model organisms. *Biochim Biophys Acta*. 1788:779-789.
Kadrmas, J.L., M.A. Smith, K.A. Clark, S.M. Pronovost, N. Muster, J.R. Yates, 3rd, and M.C. Beckerle. 2004. The integrin effector PINCH regulates JNK activity and epithelial migration in concert with Ras suppressor 1. *The Journal of cell biology*. 167:1019-1024.
Kametani, Y., and M. Takeichi. 2007. Basal-to-apical cadherin flow at cell junctions. *Nat Cell Biol*. 9:92-98.
Katsumi, A., A.W. Orr, E. Tzima, and M.A. Schwartz. 2004. Integrins in mechanotransduction. *J Biol Chem*. 279:12001-12004.
Kim, M., C.V. Carman, and T.A. Springer. 2003. Bidirectional transmembrane signaling by cytoplasmic domain separation in integrins. *Science*. 301:1720-1725.
Kirfel, G., A. Rigort, B. Borm, and V. Herzog. 2004. Cell migration: mechanisms of rear detachment and the formation of migration tracks. *Eur J Cell Biol*. 83:717-724.
Knight, C.G., L.F. Morton, D.J. Onley, A.R. Peachey, A.J. Messent, P.A. Smethurst, D.S. Tuckwell, R.W. Farndale, and M.J. Barnes. 1998. Identification in collagen type I of an integrin alpha2 beta1-binding site containing an essential GER sequence. *J Biol Chem*. 273:33287-33294.

Kobielak, A., and E. Fuchs. 2004. Alpha-catenin: at the junction of intercellular adhesion and actin dynamics. *Nat Rev Mol Cell Biol*. 5:614-625.
Kobielak, A., and E. Fuchs. 2006. Links between alpha-catenin, NF-kappaB, and squamous cell carcinoma in skin. *Proc Natl Acad Sci U S A*. 103:2322-2327.
Kobielak, A., H.A. Pasolli, and E. Fuchs. 2004. Mammalian formin-1 participates in adherens junctions and polymerization of linear actin cables. *Nat Cell Biol*. 6:21-30.
Kogata, N., R.M. Tribe, R. Fassler, M. Way, and R.H. Adams. 2009. Integrin-linked kinase controls vascular wall formation by negatively regulating Rho/ROCK-mediated vascular smooth muscle cell contraction. *Genes Dev*. 23:2278-2283.
Kolanus, W. 2007. Guanine nucleotide exchange factors of the cytohesin family and their roles in signal transduction. *Immunol Rev*. 218:102-113.
Kolanus, W., W. Nagel, B. Schiller, L. Zeitlmann, S. Godar, H. Stockinger, and B. Seed. 1996. Alpha L beta 2 integrin/LFA-1 binding to ICAM-1 induced by cytohesin-1, a cytoplasmic regulatory molecule. *Cell*. 86:233-242.
Koster, M.I., and D.R. Roop. 2007. Mechanisms regulating epithelial stratification. *Annu Rev Cell Dev Biol*. 23:93-113.
Kovacs, E.M., M. Goodwin, R.G. Ali, A.D. Paterson, and A.S. Yap. 2002. Cadherin-directed actin assembly: E-cadherin physically associates with the Arp2/3 complex to direct actin assembly in nascent adhesive contacts. *Curr Biol*. 12:379-382.
Kreidberg, J.A., M.J. Donovan, S.L. Goldstein, H. Rennke, K. Shepherd, R.C. Jones, and R. Jaenisch. 1996. Alpha 3 beta 1 integrin has a crucial role in kidney and lung organogenesis. *Development*. 122:3537-3547.
Kumar, S., I.Z. Maxwell, A. Heisterkamp, T.R. Polte, T.P. Lele, M. Salanga, E. Mazur, and D.E. Ingber. 2006. Viscoelastic retraction of single living stress fibers and its impact on cell shape, cytoskeletal organization, and extracellular matrix mechanics. *Biophys J*. 90:3762-3773.
Kuo, J.C., X. Han, C.T. Hsiao, J.R. Yates, 3rd, and C.M. Waterman. 2011. Analysis of the myosin-II-responsive focal adhesion proteome reveals a role for beta-Pix in negative regulation of focal adhesion maturation. *Nat Cell Biol*. 13:383-393.
Ladoux, B., E. Anon, M. Lambert, A. Rabodzey, P. Hersen, A. Buguin, P. Silberzan, and R.M. Mege. 2010. Strength dependence of cadherin-mediated adhesions. *Biophys J*. 98:534-542.
Larue, L., M. Ohsugi, J. Hirchenhain, and R. Kemler. 1994. E-cadherin null mutant embryos fail to form a trophectoderm epithelium. *Proc Natl Acad Sci U S A*. 91:8263-8267.
Laukaitis, C.M., D.J. Webb, K. Donais, and A.F. Horwitz. 2001. Differential dynamics of alpha 5 integrin, paxillin, and alpha-actinin during formation and disassembly of adhesions in migrating cells. *J Cell Biol*. 153:1427-1440.
le Duc, Q., Q. Shi, I. Blonk, A. Sonnenberg, N. Wang, D. Leckband, and J. de Rooij. 2010. Vinculin potentiates E-cadherin mechanosensing and is recruited to actin-anchored sites within adherens junctions in a myosin II-dependent manner. *J Cell Biol*. 189:1107-1115.
Lecuit, T. 2010. alpha-catenin mechanosensing for adherens junctions. *Nat Cell Biol*. 12:522-524.
Lee, B.H., and E. Ruoslahti. 2005. alpha5beta1 integrin stimulates Bcl-2 expression and cell survival through Akt, focal adhesion kinase, and Ca2+/calmodulin-dependent protein kinase IV. *J Cell Biochem*. 95:1214-1223.
Lee, H.S., C.J. Lim, W. Puzon-McLaughlin, S.J. Shattil, and M.H. Ginsberg. 2009. RIAM activates integrins by linking talin to ras GTPase membrane-targeting sequences. *J Biol Chem*. 284:5119-5127.
Lee, S.E., R.D. Kamm, and M.R. Mofrad. 2007. Force-induced activation of talin and its possible role in focal adhesion mechanotransduction. *J Biomech*. 40:2096-2106.
Legate, K.R., and R. Fassler. 2009. Mechanisms that regulate adaptor binding to beta-integrin cytoplasmic tails. *J Cell Sci*. 122:187-198.

Legate, K.R., E. Montanez, O. Kudlacek, and R. Fassler. 2006. ILK, PINCH and parvin: the tIPP of integrin signalling. *Nat Rev Mol Cell Biol*. 7:20-31.

Legate, K.R., S.A. Wickstrom, and R. Fassler. 2009. Genetic and cell biological analysis of integrin outside-in signaling. *Genes Dev*. 23:397-418.

Lei, K., and R.J. Davis. 2003. JNK phosphorylation of Bim-related members of the Bcl2 family induces Bax-dependent apoptosis. *Proc Natl Acad Sci U S A*. 100:2432-2437.

Leung, C.L., K.J. Green, and R.K. Liem. 2002. Plakins: a family of versatile cytolinker proteins. *Trends Cell Biol*. 12:37-45.

Lewis, J.E., J.K. Wahl, 3rd, K.M. Sass, P.J. Jensen, K.R. Johnson, and M.J. Wheelock. 1997. Cross-talk between adherens junctions and desmosomes depends on plakoglobin. *J Cell Biol*. 136:919-934.

Ley, R., K.E. Ewings, K. Hadfield, and S.J. Cook. 2005. Regulatory phosphorylation of Bim: sorting out the ERK from the JNK. *Cell Death Differ*. 12:1008-1014.

Li, F., Y. Zhang, and C. Wu. 1999. Integrin-linked kinase is localized to cell-matrix focal adhesions but not cell-cell adhesion sites and the focal adhesion localization of integrin-linked kinase is regulated by the PINCH-binding ANK repeats. *J Cell Sci*. 112 (Pt 24):4589-4599.

Li, S., R. Bordoy, F. Stanchi, M. Moser, A. Braun, O. Kudlacek, U.M. Wewer, P.D. Yurchenco, and R. Fassler. 2005. PINCH1 regulates cell-matrix and cell-cell adhesions, cell polarity and cell survival during the peri-implantation stage. *J Cell Sci*. 118:2913-2921.

Liang, X., Q. Zhou, X. Li, Y. Sun, M. Lu, N. Dalton, J. Ross, Jr., and J. Chen. 2005. PINCH1 plays an essential role in early murine embryonic development but is dispensable in ventricular cardiomyocytes. *Mol Cell Biol*. 25:3056-3062.

Liu, J., X. He, S.A. Corbett, S.F. Lowry, A.M. Graham, R. Fassler, and S. Li. 2009. Integrins are required for the differentiation of visceral endoderm. *J Cell Sci*. 122:233-242.

Lopez-Rovira, T., V. Silva-Vargas, and F.M. Watt. 2005. Different consequences of beta1 integrin deletion in neonatal and adult mouse epidermis reveal a context-dependent role of integrins in regulating proliferation, differentiation, and intercellular communication. *J Invest Dermatol*. 125:1215-1227.

Lorenz, K., C. Grashoff, R. Torka, T. Sakai, L. Langbein, W. Bloch, M. Aumailley, and R. Fassler. 2007. Integrin-linked kinase is required for epidermal and hair follicle morphogenesis. *The Journal of cell biology*. 177:501-513.

Luo, B.H., C.V. Carman, and T.A. Springer. 2007. Structural basis of integrin regulation and signaling. *Annu Rev Immunol*. 25:619-647.

Ma, Y.Q., J. Qin, C. Wu, and E.F. Plow. 2008. Kindlin-2 (Mig-2): a co-activator of beta3 integrins. *J Cell Biol*. 181:439-446.

Mackinnon, A.C., H. Qadota, K.R. Norman, D.G. Moerman, and B.D. Williams. 2002. C. elegans PAT-4/ILK functions as an adaptor protein within integrin adhesion complexes. *Curr Biol*. 12:787-797.

Martin, S.S., and K. Vuori. 2004. Regulation of Bcl-2 proteins during anoikis and amorphosis. *Biochim Biophys Acta*. 1692:145-157.

Maul, R.S., and D.D. Chang. 1999. EPLIN, epithelial protein lost in neoplasm. *Oncogene*. 18:7838-7841.

Maul, R.S., Y. Song, K.J. Amann, S.C. Gerbin, T.D. Pollard, and D.D. Chang. 2003. EPLIN regulates actin dynamics by cross-linking and stabilizing filaments. *The Journal of cell biology*. 160:399-407.

McKoy, G., N. Protonotarios, A. Crosby, A. Tsatsopoulou, A. Anastasakis, A. Coonar, M. Norman, C. Baboonian, S. Jeffery, and W.J. McKenna. 2000. Identification of a deletion in plakoglobin in arrhythmogenic right ventricular cardiomyopathy with palmoplantar keratoderma and woolly hair (Naxos disease). *Lancet*. 355:2119-2124.

Meier, P., A. Finch, and G. Evan. 2000. Apoptosis in development. *Nature*. 407:796-801.

Meves, A., C. Stremmel, K. Gottschalk, and R. Fassler. 2009. The Kindlin protein family: new members to the club of focal adhesion proteins. *Trends Cell Biol*. 19:504-513.

Monkley, S.J., C.A. Pritchard, and D.R. Critchley. 2001. Analysis of the mammalian talin2 gene TLN2. *Biochem Biophys Res Commun*. 286:880-885.

Monkley, S.J., X.H. Zhou, S.J. Kinston, S.M. Giblett, L. Hemmings, H. Priddle, J.E. Brown, C.A. Pritchard, D.R. Critchley, and R. Fassler. 2000. Disruption of the talin gene arrests mouse development at the gastrulation stage. *Dev Dyn*. 219:560-574.

Montanez, E., A. Piwko-Czuchra, M. Bauer, S. Li, P. Yurchenco, and R. Fassler. 2007. Analysis of integrin functions in peri-implantation embryos, hematopoietic system, and skin. *Methods Enzymol*. 426:239-289.

Montanez, E., S. Ussar, M. Schifferer, M. Bosl, R. Zent, M. Moser, and R. Fassler. 2008. Kindlin-2 controls bidirectional signaling of integrins. *Genes Dev*. 22:1325-1330.

Montanez, E., S.A. Wickstrom, J. Altstatter, H. Chu, and R. Fassler. 2009. Alpha-parvin controls vascular mural cell recruitment to vessel wall by regulating RhoA/ROCK signalling. *Embo J*. 28:3132-3144.

Moser, M., M. Bauer, S. Schmid, R. Ruppert, S. Schmidt, M. Sixt, H.V. Wang, M. Sperandio, and R. Fassler. 2009a. Kindlin-3 is required for beta2 integrin-mediated leukocyte adhesion to endothelial cells. *Nat Med*. 15:300-305.

Moser, M., K.R. Legate, R. Zent, and R. Fassler. 2009b. The tail of integrins, talin, and kindlins. *Science*. 324:895-899.

Moser, M., B. Nieswandt, S. Ussar, M. Pozgajova, and R. Fassler. 2008. Kindlin-3 is essential for integrin activation and platelet aggregation. *Nat Med*. 14:325-330.

Nakrieko, K.A., I. Welch, H. Dupuis, D. Bryce, A. Pajak, R. St Arnaud, S. Dedhar, S.J. D'Souza, and L. Dagnino. 2008. Impaired hair follicle morphogenesis and polarized keratinocyte movement upon conditional inactivation of integrin-linked kinase in the epidermis. *Mol Biol Cell*. 19:1462-1473.

Niessen, C.M. 2007. Tight junctions/adherens junctions: basic structure and function. *J Invest Dermatol*. 127:2525-2532.

Niessen, C.M., D. Leckband, and A.S. Yap. 2011. Tissue organization by cadherin adhesion molecules: dynamic molecular and cellular mechanisms of morphogenetic regulation. *Physiol Rev*. 91:691-731.

Nikolopoulos, S.N., and C.E. Turner. 2000. Actopaxin, a new focal adhesion protein that binds paxillin LD motifs and actin and regulates cell adhesion. *J Cell Biol*. 151:1435-1448.

Nusrat, A., G.T. Brown, J. Tom, A. Drake, T.T. Bui, C. Quan, and R.J. Mrsny. 2005. Multiple protein interactions involving proposed extracellular loop domains of the tight junction protein occludin. *Mol Biol Cell*. 16:1725-1734.

Olski, T.M., A.A. Noegel, and E. Korenbaum. 2001. Parvin, a 42 kDa focal adhesion protein, related to the alpha-actinin superfamily. *J Cell Sci*. 114:525-538.

Pasquet, J.M., M. Noury, and A.T. Nurden. 2002. Evidence that the platelet integrin alphaIIb beta3 is regulated by the integrin-linked kinase, ILK, in a PI3-kinase dependent pathway. *Thromb Haemost*. 88:115-122.

Paszek, M.J., D. Boettiger, V.M. Weaver, and D.A. Hammer. 2009. Integrin clustering is driven by mechanical resistance from the glycocalyx and the substrate. *PLoS Comput Biol*. 5:e1000604.

Paus, R., and G. Cotsarelis. 1999. The biology of hair follicles. *N Engl J Med*. 341:491-497.

Peng, X., L.E. Cuff, C.D. Lawton, and K.A. DeMali. 2010. Vinculin regulates cell-surface E-cadherin expression by binding to beta-catenin. *J Cell Sci*. 123:567-577.

Pereira, J.A., Y. Benninger, R. Baumann, A.F. Goncalves, M. Ozcelik, T. Thurnherr, N. Tricaud, D. Meijer, R. Fassler, U. Suter, and J.B. Relvas. 2009. Integrin-linked kinase is required for radial sorting of axons and Schwann cell remyelination in the peripheral nervous system. *J Cell Biol*. 185:147-161.

Perez-Moreno, M., M.A. Davis, E. Wong, H.A. Pasolli, A.B. Reynolds, and E. Fuchs. 2006. p120-catenin mediates inflammatory responses in the skin. *Cell*. 124:631-644.

Perez-Moreno, M., and E. Fuchs. 2006. Catenins: keeping cells from getting their signals crossed. *Dev Cell*. 11:601-612.

Perez-Moreno, M., C. Jamora, and E. Fuchs. 2003. Sticky business: orchestrating cellular signals at adherens junctions. *Cell*. 112:535-548.

Perez-Moreno, M., W. Song, H.A. Pasolli, S.E. Williams, and E. Fuchs. 2008. Loss of p120 catenin and links to mitotic alterations, inflammation, and skin cancer. *Proc Natl Acad Sci U S A*. 105:15399-15404.

Persad, S., S. Attwell, V. Gray, N. Mawji, J.T. Deng, D. Leung, J. Yan, J. Sanghera, M.P. Walsh, and S. Dedhar. 2001. Regulation of protein kinase B/Akt-serine 473 phosphorylation by integrin-linked kinase: critical roles for kinase activity and amino acids arginine 211 and serine 343. *J Biol Chem*. 276:27462-27469.

Postel, R., P. Vakeel, J. Topczewski, R. Knoll, and J. Bakkers. 2008. Zebrafish integrin-linked kinase is required in skeletal muscles for strengthening the integrin-ECM adhesion complex. *Dev Biol*. 318:92-101.

Raghavan, S., C. Bauer, G. Mundschau, Q. Li, and E. Fuchs. 2000. Conditional ablation of beta1 integrin in skin. Severe defects in epidermal proliferation, basement membrane formation, and hair follicle invagination. *J Cell Biol*. 150:1149-1160.

Ramirez, A., A. Page, A. Gandarillas, J. Zanet, S. Pibre, M. Vidal, L. Tusell, A. Genesca, D.A. Whitaker, D.W. Melton, and J.L. Jorcano. 2004. A keratin K5Cre transgenic line appropriate for tissue-specific or generalized Cre-mediated recombination. *Genesis*. 39:52-57.

Rearden, A. 1994. A new LIM protein containing an autoepitope homologous to "senescent cell antigen". *Biochem Biophys Res Commun*. 201:1124-1131.

Reddig, P.J., and R.L. Juliano. 2005. Clinging to life: cell to matrix adhesion and cell survival. *Cancer Metastasis Rev*. 24:425-439.

Rid, R., N. Schiefermeier, I. Grigoriev, J.V. Small, and I. Kaverina. 2005. The last but not the least: the origin and significance of trailing adhesions in fibroblastic cells. *Cell Motil Cytoskeleton*. 61:161-171.

Ridley, A.J. 2006. Rho GTPases and actin dynamics in membrane protrusions and vesicle trafficking. *Trends Cell Biol*. 16:522-529.

Rimm, D.L., E.R. Koslov, P. Kebriaei, C.D. Cianci, and J.S. Morrow. 1995. Alpha 1(E)-catenin is an actin-binding and -bundling protein mediating the attachment of F-actin to the membrane adhesion complex. *Proc Natl Acad Sci U S A*. 92:8813-8817.

Ruiz, P., V. Brinkmann, B. Ledermann, M. Behrend, C. Grund, C. Thalhammer, F. Vogel, C. Birchmeier, U. Gunthert, W.W. Franke, and W. Birchmeier. 1996. Targeted mutation of plakoglobin in mice reveals essential functions of desmosomes in the embryonic heart. *J Cell Biol*. 135:215-225.

Sahai, E., and C.J. Marshall. 2002. ROCK and Dia have opposing effects on adherens junctions downstream of Rho. *Nat Cell Biol*. 4:408-415.

Sakai, T., S. Li, D. Docheva, C. Grashoff, K. Sakai, G. Kostka, A. Braun, A. Pfeifer, P.D. Yurchenco, and R. Fassler. 2003. Integrin-linked kinase (ILK) is required for polarizing the epiblast, cell adhesion, and controlling actin accumulation. *Genes Dev*. 17:926-940.

Sakakibara, A., M. Furuse, M. Saitou, Y. Ando-Akatsuka, and S. Tsukita. 1997. Possible involvement of phosphorylation of occludin in tight junction formation. *J Cell Biol*. 137:1393-1401.

Sandfort, V., I. Eke, and N. Cordes. 2010. The role of the focal adhesion protein PINCH1 for the radiosensitivity of adhesion and suspension cell cultures. *PLoS One*. 5.

Sawada, Y., M. Tamada, B.J. Dubin-Thaler, O. Cherniavskaya, R. Sakai, S. Tanaka, and M.P. Sheetz. 2006. Force sensing by mechanical extension of the Src family kinase substrate p130Cas. *Cell*. 127:1015-1026.

Sawyer, J.K., N.J. Harris, K.C. Slep, U. Gaul, and M. Peifer. 2009. The Drosophila afadin homologue Canoe regulates linkage of the actin cytoskeleton to adherens junctions during apical constriction. *J Cell Biol*. 186:57-73.

Schiller, H.B., C.C. Friedel, C. Boulegue, and R. Fassler. 2011. Quantitative proteomics of the integrin adhesome show a myosin II-dependent recruitment of LIM domain proteins. *EMBO reports*. 12:259-266.

Schmidt-Ullrich, R., and R. Paus. 2005. Molecular principles of hair follicle induction and morphogenesis. *Bioessays*. 27:247-261.

Schwartz, M.A., and D.W. DeSimone. 2008. Cell adhesion receptors in mechanotransduction. *Curr Opin Cell Biol*. 20:551-556.

Scott, J.A., A.M. Shewan, N.R. den Elzen, J.J. Loureiro, F.B. Gertler, and A.S. Yap. 2006. Ena/VASP proteins can regulate distinct modes of actin organization at cadherin-adhesive contacts. *Mol Biol Cell*. 17:1085-1095.

Senetar, M.A., C.L. Moncman, and R.O. McCann. 2007. Talin2 is induced during striated muscle differentiation and is targeted to stable adhesion complexes in mature muscle. *Cell Motil Cytoskeleton*. 64:157-173.

Serrels, B., A. Serrels, V.G. Brunton, M. Holt, G.W. McLean, C.H. Gray, G.E. Jones, and M.C. Frame. 2007. Focal adhesion kinase controls actin assembly via a FERM-mediated interaction with the Arp2/3 complex. *Nat Cell Biol*. 9:1046-1056.

Shewan, A.M., M. Maddugoda, A. Kraemer, S.J. Stehbens, S. Verma, E.M. Kovacs, and A.S. Yap. 2005. Myosin 2 is a key Rho kinase target necessary for the local concentration of E-cadherin at cell-cell contacts. *Mol Biol Cell*. 16:4531-4542.

Simpson, C.L., D.M. Patel, and K.J. Green. 2011. Deconstructing the skin: cytoarchitectural determinants of epidermal morphogenesis. *Nat Rev Mol Cell Biol*. 12:565-580.

Smutny, M., H.L. Cox, J.M. Leerberg, E.M. Kovacs, M.A. Conti, C. Ferguson, N.A. Hamilton, R.G. Parton, R.S. Adelstein, and A.S. Yap. 2010. Myosin II isoforms identify distinct functional modules that support integrity of the epithelial zonula adherens. *Nat Cell Biol*. 12:696-702.

Stanchi, F., R. Bordoy, O. Kudlacek, A. Braun, A. Pfeifer, M. Moser, and R. Fassler. 2005. Consequences of loss of PINCH2 expression in mice. *J Cell Sci*. 118:5899-5910.

Stanchi, F., C. Grashoff, C.F. Nguemeni Yonga, D. Grall, R. Fassler, and E. Van Obberghen-Schilling. 2009. Molecular dissection of the ILK-PINCH-parvin triad reveals a fundamental role for the ILK kinase domain in the late stages of focal-adhesion maturation. *J Cell Sci*. 122:1800-1811.

Sumpio, B.E., A.J. Banes, L.G. Levin, and G. Johnson, Jr. 1987. Mechanical stress stimulates aortic endothelial cells to proliferate. *J Vasc Surg*. 6:252-256.

Tadokoro, S., S.J. Shattil, K. Eto, V. Tai, R.C. Liddington, J.M. de Pereda, M.H. Ginsberg, and D.A. Calderwood. 2003. Talin binding to integrin beta tails: a final common step in integrin activation. *Science*. 302:103-106.

Taguchi, K., T. Ishiuchi, and M. Takeichi. 2011. Mechanosensitive EPLIN-dependent remodeling of adherens junctions regulates epithelial reshaping. *J Cell Biol*.

Tait, S.W., and D.R. Green. 2010. Mitochondria and cell death: outer membrane permeabilization and beyond. *Nat Rev Mol Cell Biol*. 11:621-632.

Takada, Y., X. Ye, and S. Simon. 2007. The integrins. *Genome Biol*. 8:215.

Tamkun, J.W., D.W. DeSimone, D. Fonda, R.S. Patel, C. Buck, A.F. Horwitz, and R.O. Hynes. 1986. Structure of integrin, a glycoprotein involved in the transmembrane linkage between fibronectin and actin. *Cell*. 46:271-282.

Tanentzapf, G., and N.H. Brown. 2006. An interaction between integrin and the talin FERM domain mediates integrin activation but not linkage to the cytoskeleton. *Nat Cell Biol*. 8:601-606.

Tepass, U., E. Gruszynski-DeFeo, T.A. Haag, L. Omatyar, T. Torok, and V. Hartenstein. 1996. shotgun encodes Drosophila E-cadherin and is preferentially required during cell rearrangement in the neurectoderm and other morphogenetically active epithelia. *Genes Dev*. 10:672-685.

Thiery, J.P. 2002. Epithelial-mesenchymal transitions in tumour progression. *Nat Rev Cancer*. 2:442-454.

Tinkle, C.L., T. Lechler, H.A. Pasolli, and E. Fuchs. 2004. Conditional targeting of E-cadherin in skin: insights into hyperproliferative and degenerative responses. *Proc Natl Acad Sci U S A*. 101:552-557.

Tinkle, C.L., H.A. Pasolli, N. Stokes, and E. Fuchs. 2008. New insights into cadherin function in epidermal sheet formation and maintenance of tissue integrity. *Proc Natl Acad Sci U S A*. 105:15405-15410.

Tu, Y., Y. Huang, Y. Zhang, Y. Hua, and C. Wu. 2001. A new focal adhesion protein that interacts with integrin-linked kinase and regulates cell adhesion and spreading. *J Cell Biol*. 153:585-598.

Tu, Y., F. Li, S. Goicoechea, and C. Wu. 1999. The LIM-only protein PINCH directly interacts with integrin-linked kinase and is recruited to integrin-rich sites in spreading cells. *Mol Cell Biol*. 19:2425-2434.

Tu, Y., F. Li, and C. Wu. 1998. Nck-2, a novel Src homology2/3-containing adaptor protein that interacts with the LIM-only protein PINCH and components of growth factor receptor kinase-signaling pathways. *Mol Biol Cell*. 9:3367-3382.

Tunggal, J.A., I. Helfrich, A. Schmitz, H. Schwarz, D. Gunzel, M. Fromm, R. Kemler, T. Krieg, and C.M. Niessen. 2005. E-cadherin is essential for in vivo epidermal barrier function by regulating tight junctions. *Embo J*. 24:1146-1156.

Tzima, E., M. Irani-Tehrani, W.B. Kiosses, E. Dejana, D.A. Schultz, B. Engelhardt, G. Cao, H. DeLisser, and M.A. Schwartz. 2005. A mechanosensory complex that mediates the endothelial cell response to fluid shear stress. *Nature*. 437:426-431.

Ussar, S., M. Moser, M. Widmaier, E. Rognoni, C. Harrer, O. Genzel-Boroviczeny, and R. Fassler. 2008. Loss of Kindlin-1 causes skin atrophy and lethal neonatal intestinal epithelial dysfunction. *PLoS Genet*. 4:e1000289.

van der Neut, R., P. Krimpenfort, J. Calafat, C.M. Niessen, and A. Sonnenberg. 1996. Epithelial detachment due to absence of hemidesmosomes in integrin beta 4 null mice. *Nat Genet*. 13:366-369.

Vasioukhin, V., C. Bauer, L. Degenstein, B. Wise, and E. Fuchs. 2001. Hyperproliferation and defects in epithelial polarity upon conditional ablation of alpha-catenin in skin. *Cell*. 104:605-617.

Vasioukhin, V., C. Bauer, M. Yin, and E. Fuchs. 2000. Directed actin polymerization is the driving force for epithelial cell-cell adhesion. *Cell*. 100:209-219.

Vasioukhin, V., and E. Fuchs. 2001. Actin dynamics and cell-cell adhesion in epithelia. *Curr Opin Cell Biol*. 13:76-84.

Verma, S., A.M. Shewan, J.A. Scott, F.M. Helwani, N.R. den Elzen, H. Miki, T. Takenawa, and A.S. Yap. 2004. Arp2/3 activity is necessary for efficient formation of E-cadherin adhesive contacts. *J Biol Chem*. 279:34062-34070.

Vespa, A., S.J. D'Souza, and L. Dagnino. 2005. A novel role for integrin-linked kinase in epithelial sheet morphogenesis. *Mol Biol Cell*. 16:4084-4095.

Vespa, A., A.J. Darmon, C.E. Turner, S.J. D'Souza, and L. Dagnino. 2003. Ca2+-dependent localization of integrin-linked kinase to cell junctions in differentiating keratinocytes. *J Biol Chem*. 278:11528-11535.

Wang, N., J.P. Butler, and D.E. Ingber. 1993. Mechanotransduction across the cell surface and through the cytoskeleton. *Science*. 260:1124-1127.

Watabe-Uchida, M., N. Uchida, Y. Imamura, A. Nagafuchi, K. Fujimoto, T. Uemura, S. Vermeulen, F. van Roy, E.D. Adamson, and M. Takeichi. 1998. alpha-Catenin-vinculin interaction functions to organize the apical junctional complex in epithelial cells. *J Cell Biol*. 142:847-857.

Watt, F.M. 2002. Role of integrins in regulating epidermal adhesion, growth and differentiation. *Embo J*. 21:3919-3926.

Wegener, K.L., A.W. Partridge, J. Han, A.R. Pickford, R.C. Liddington, M.H. Ginsberg, and I.D. Campbell. 2007. Structural basis of integrin activation by talin. *Cell*. 128:171-182.

Weiss, E.E., M. Kroemker, A.H. Rudiger, B.M. Jockusch, and M. Rudiger. 1998. Vinculin is part of the cadherin-catenin junctional complex: complex formation between alpha-catenin and vinculin. *J Cell Biol*. 141:755-764.

Wittchen, E.S., J. Haskins, and B.R. Stevenson. 2003. NZO-3 expression causes global changes to actin cytoskeleton in Madin-Darby canine kidney cells: linking a tight junction protein to Rho GTPases. *Mol Biol Cell*. 14:1757-1768.

Yamada, S., and W.J. Nelson. 2007. Localized zones of Rho and Rac activities drive initiation and expansion of epithelial cell-cell adhesion. *J Cell Biol*. 178:517-527.

Yamada, S., S. Pokutta, F. Drees, W.I. Weis, and W.J. Nelson. 2005. Deconstructing the cadherin-catenin-actin complex. *Cell*. 123:889-901.

Yamaji, S., A. Suzuki, Y. Sugiyama, Y. Koide, M. Yoshida, H. Kanamori, H. Mohri, S. Ohno, and Y. Ishigatsubo. 2001. A novel integrin-linked kinase-binding protein, affixin, is involved in the early stage of cell-substrate interaction. *J Cell Biol*. 153:1251-1264.

Yamawaki, H., S. Pan, R.T. Lee, and B.C. Berk. 2005. Fluid shear stress inhibits vascular inflammation by decreasing thioredoxin-interacting protein in endothelial cells. *J Clin Invest*. 115:733-738.

Yonemura, S., M. Itoh, A. Nagafuchi, and S. Tsukita. 1995. Cell-to-cell adherens junction formation and actin filament organization: similarities and differences between non-polarized fibroblasts and polarized epithelial cells. *J Cell Sci*. 108 (Pt 1):127-142.

Yonemura, S., Y. Wada, T. Watanabe, A. Nagafuchi, and M. Shibata. 2010. alpha-Catenin as a tension transducer that induces adherens junction development. *Nat Cell Biol*. 12:533-542.

Young, P., O. Boussadia, H. Halfter, R. Grose, P. Berger, D.P. Leone, H. Robenek, P. Charnay, R. Kemler, and U. Suter. 2003. E-cadherin controls adherens junctions in the epidermis and the renewal of hair follicles. *Embo J*. 22:5723-5733.

Zaidel-Bar, R., S. Itzkovitz, A. Ma'ayan, R. Iyengar, and B. Geiger. 2007. Functional atlas of the integrin adhesome. *Nat Cell Biol*. 9:858-867.

Zervas, C.G., S.L. Gregory, and N.H. Brown. 2001. Drosophila integrin-linked kinase is required at sites of integrin adhesion to link the cytoskeleton to the plasma membrane. *J Cell Biol*. 152:1007-1018.

Zhang, X., G. Jiang, Y. Cai, S.J. Monkley, D.R. Critchley, and M.P. Sheetz. 2008. Talin depletion reveals independence of initial cell spreading from integrin activation and traction. *Nat Cell Biol*. 10:1062-1068.

Zhang, Y., K. Chen, L. Guo, and C. Wu. 2002a. Characterization of PINCH-2, a new focal adhesion protein that regulates the PINCH-1-ILK interaction, cell spreading, and migration. *J Biol Chem*. 277:38328-38338.

Zhang, Y., K. Chen, Y. Tu, A. Velyvis, Y. Yang, J. Qin, and C. Wu. 2002b. Assembly of the PINCH-ILK-CH-ILKBP complex precedes and is essential for localization of each component to cell-matrix adhesion sites. *Journal of cell science*. 115:4777-4786.

Zhang, Y., K. Chen, Y. Tu, and C. Wu. 2004. Distinct roles of two structurally closely related focal adhesion proteins, alpha-parvins and beta-parvins, in regulation of cell morphology and survival. *J Biol Chem*. 279:41695-41705.

Zhang, Z., K. Vuori, J.C. Reed, and E. Ruoslahti. 1995. The alpha 5 beta 1 integrin supports survival of cells on fibronectin and up-regulates Bcl-2 expression. *Proc Natl Acad Sci U S A*. 92:6161-6165.

Zheng, Q., and Y. Zhao. 2007. The diverse biofunctions of LIM domain proteins: determined by subcellular localization and protein-protein interaction. *Biol Cell*. 99:489-502.

Publications

Karaköse E, Schiller HB, Fässler R (2010) „Kindlins et a glance“ J Cell Sci. 2010 Jul 15;123(Pt 14):2353-6.

Acknowledgements

First, I would like to thank Prof. Dr. Reinhard Fässler for giving me the opportunity to carry out my phD thesis work under his supervision. I would like to express my sincere gratitude for the excellent and continuous support and guidance for the past 4.5 years. I am grateful for all the fruitful discussions, fair criticism and encouragements I have received during my time at his lab.

I would also like to thank Prof. Dr. Michael Schleicher, not only for carefully and critically reading my thesis but also for his great help throughout my phD study by being a member of my thesis advisory committee.

I would like to express my deep gratitude to Dr. Tamar Geiger both for her practical and theoretical help during my phD work as a collaborator and also for her guidance by being a member at my thesis advisory committee.

I also thank Prof. Dr. Martin Biel and Prof. Dr. Christian Wahl-Schott for examining this thesis.

I also thank Dr Eloi Montanez for supporting me at each and every step of my phD work by giving his extremely valuable advice and assistance at any time I needed it.

I would like to thank Dr. Katrin Lorenz-Baath for assisting me with the experiments during my first weeks in the lab and also for the intensive discussions throughout my phD time.

I also thank Dr. Armin Lambacher for his assistance with any computer and microscopy-related topic. I also express my gratitude to Dr Walter Göhring and Klaus Weber for all their technical help and to Carmen Schmitz and Ines Lach-Kusevic for their great assistance with any organizational matter.

I would like to thank Dr. Anika Böttcher and Korana Radovanac for never leaving me alone during the coffee breaks at which we had valuable discussions.

I would like to express my deep gratitude to all members of the department of Molecular Medicine at the MPI of Biochemistry for their kind and every-day support.

Last but not least, I would like to thank all my family, but especially my mother Emine Erdogan and my aunt Hanife Erdogan as well as my boyfriend Can Balioglu for being extremely patient, for standing tirelessly by me and giving their love that was essential to succeed in this work.

Curriculum Vitae

Personal details

Name:	Esra Karaköse
Date of birth:	04.08.1981, in Istanbul, Turkey
Nationality:	Turkish
Affiliation:	Max-Planck-Institute of Biochemistry
	Department of Molecular Medicine
Address:	Siebenbürgenerstr. 2, 81377, Munich, Germany

Education

1987-1992:	Primary School, Istanbul, Turkey
1992-1996:	Secondary School, Istanbul, Turkey
1996-2000:	High School, Istanbul, Turkey

Scientific Education

2000-2004:	Study of Biology, Istanbul University, Istanbul, Turkey
2004-2007:	Master of Science, Department of Molecular Biology and Genetics, Bilkent University, Ankara, Turkey
2007-2012:	PhD dissertation, Department of Molecular Medicine, Max-Planck-Institute of Biochemistry, Germany

Honors/Awards

2005-2007:	Research assistantship from The Scientific and Technological Research Council of Turkey (TUBITAK)
2005-2006:	Research fellowship from the Foreign Ministry of Greece

Munich, 30.04.2012